AD-A135 556 CLOUD FORECAST FIELDS COMPARISON TEST(U) AIR FORCE GLOBAL WEATHER CENTRAL OFFUTT AFB NE K E MITCHELL MAY 82 AFGWC/TN-82/003 SBI-AD-E850 383 1/1

UNCLASSIFIED F/G 4/2 NL

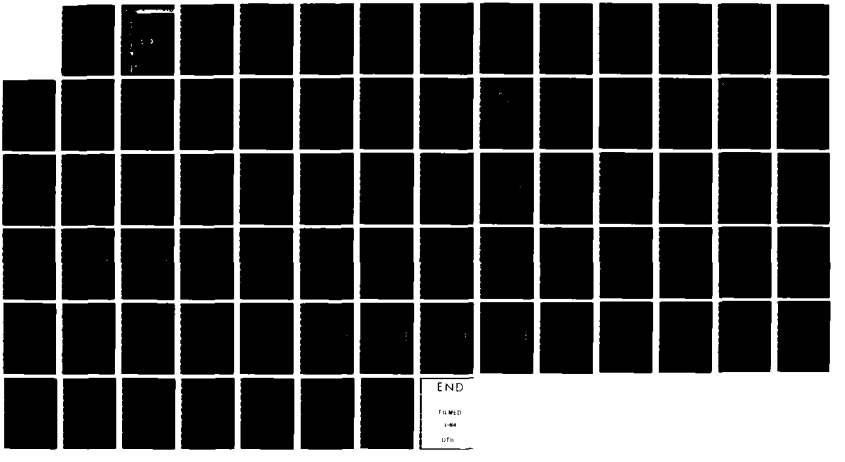

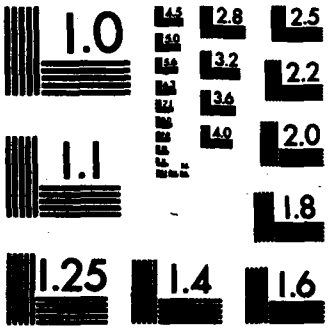

AFGWC/TN-82/003

CLOUD FORECAST FIELDS COMPARISON TEST

By

Capt Kenneth E. Mitchell

APPROVED FOR PUBLIC RELEASE; DISTRIBUTION UNLIMITED

MAY 1982

UNITED STATES AIR FORCE
AIR WEATHER SERVICE (MAC)
AIR FORCE GLOBAL WEATHER CENTRAL
OFFUTT AFB NE 68113

REVIEW AND APPROVAL STATEMENT

This publication approved for public release. There is no objection to unlimited distribution of this document to the public at large, or by the Defense Technical Information Center (DTIC) or to the National Technical Information Service (NTIS)

This technical publication has been reviewed and is approved for publication.

Charles W Cook

CHARLES W. COOK, GM-13, DAFC
Reviewing Official

FOR THE COMMANDER

Kenneth E German

KENNETH E. GERMAN, Colonel, USAF
Chief, Technical Services Division

SECURITY CLASSIFICATION OF THIS PAGE (When Data Entered)

REPORT DOCUMENTATION PAGE

READ INSTRUCTIONS BEFORE COMPLETING FORM

1. REPORT NUMBER: AFGWC/TN-82/003	2. GOVT ACCESSION NO.: AD-A125556
3. RECIPIENT'S CATALOG NUMBER:	
4. TITLE (and Subtitle): Cloud Forecast Fields Comparison Test	5. TYPE OF REPORT & PERIOD COVERED:
	6. PERFORMING ORG. REPORT NUMBER:
7. AUTHOR(s): Kenneth E. Mitchell, Capt, USAF	8. CONTRACT OR GRANT NUMBER(s):
9. PERFORMING ORGANIZATION NAME AND ADDRESS: HQ Air Force Global Weather Central (MAC), Offutt AFB, Nebraska 68113	10. PROGRAM ELEMENT, PROJECT, TASK AREA & WORK UNIT NUMBERS:
11. CONTROLLING OFFICE NAME AND ADDRESS: HQ Air Force Global Weather Central (MAC), Offutt AFB, Nebraska 68113	12. REPORT DATE:
	13. NUMBER OF PAGES: 65 + vi
14. MONITORING AGENCY NAME & ADDRESS(if different from Controlling Office):	15. SECURITY CLASS. (of this report): Unclassified
	15a. DECLASSIFICATION/DOWNGRADING SCHEDULE:

16. DISTRIBUTION STATEMENT (of this Report)
Approved for public release; distribution unlimited.

17. DISTRIBUTION STATEMENT (of the abstract entered in Block 20, if different from Report)
N/A

18. SUPPLEMENTARY NOTES

19. KEY WORDS (Continue on reverse side if necessary and identify by block number)

Automated Objective Cloud Forecasts	Moisture Initialization
Automated Objective Cloud Analysis	Cloud to Moisture Conversions
Objective Cloud Verification	Meteorological Satellite Data
Trajectory Forecast Model	Numerical Weather Analysis
Primitive Equation Forecast Model	Numerical Weather Prediction

20. ABSTRACT (Continue on reverse side if necessary and identify by block number)

This technical note reports a study of the comparative cloud forecast skill of several numerical analysis/forecast systems at the Air Force Global Weather Central (AFGWC) and the National Meteorological Center (NMC). The study compared gridded cloud forecasts derived from AFGWC's trajectory cloud forecast model (5LAYER) and NMC's 7-layer moist primitive equation model (7LHFM) during the period August to September 1979. The study also measured the sensitivity of the 5LAYER model to the accuracy of input forecast winds (used to compute trajectories). The results show that 5LAYER- and 7LHFM-derived cloud forecasts

DD FORM 1 JAN 73 1473 EDITION OF 1 NOV 65 IS OBSOLETE

UNCLASSIFIED

SECURITY CLASSIFICATION OF THIS PAGE (When Data Entered)

Item 20, Cont.

differ appreciably owing to fundamental differences in the methods used by the two centers to initialize their respective model moisture fields. During the first 24-hour forecast period, 5LAYER consistently produces more accurate cloud forecasts than the 7LHFM, because satellite and surface cloud observations are used systematically and globally in the derivation of 5LAYER initial moisture fields.

PREFACE

This Technical Note (TN) describes the results of a study to investigate the comparative cloud forecast skill of several numerical analysis/forecast systems at the Air Force Global Weather Central (AFGWC) and the National Meteorological Center (NMC). The study includes examination of analysis and forecast model databases valid during the period August to September 1979. At times during the course of the study, progress was interrupted by higher priority projects, but the study eventually was completed and reported internally within Air Weather Service (AWS) during April 1981. The results of the study are intended to guide future decisions concerning the evolution and improvement of the automated cloud analysis and forecast system at AFGWC. Owing to subsequent out-of-house requests for the study results, it was decided that the final report should be issued and distributed as a formal AFGWC Technical Note. As such, the report would be available to the public through the Defense Technical Information Center (DTIC) and the National Technical Information Service (NTIS). Aside from inconsequential changes in format, minor wording changes, and redrafting of the figures, this TN is identical to the original study report issued in April 1981.

The author thanks the numerous AFGWC personnel who assisted him in this project. Several persons deserve special mention. They are:

- Lieutenant Colonel William S. Irvine, AFGWC/TSI, for his key expertise in translating the NMC data tapes and his instrumental help in the preparation and editing of the final manuscript.

- Lieutenant Colonel James Kerlin, AFGWC liaison officer to NMC, who coordinated the data archival task at NMC.

- Major Kenneth P. Freeman, AFGWC/TSIT, for his contributions to the writing of the initial project study plan and his overall project coordination.

- Major Arnold L. Friend, AFGWC/TSIT, for the many hours he contributed to the arduous data archival task.

- The following reviewers for their advice and comments:

Colonel Serhij Pilipowskyj	AFGWC/WS
Lieutenant Colonel Lyman L. Kaiser	AFGWC/DOX
Major Terry C. Tarbell	AFGWC/TSIN
Captain Fred P. Lewis	AFGWC/TSIN

- The following members of the AFGWC Word Processing Center for their clerical and administrative support:

Mary Ann Kosmicki
Melissa Hockman
Ruth Drummond

- The staff of the 3902 ABW/OTCG, Graphics Support Section, for their professional drafting support.

Captain Kenneth E. Mitchell
11 May 1982

TABLE OF CONTENTS

		Page
Section 1	INTRODUCTION	1
Section 2	TEST METHODOLOGY	3
2.1	Test Period	3
2.2	Forecast and Analysis Data Sets	3
2.2.1	7LHFM Production Forecasts	3
2.2.2	5LAYER Production Forecasts	4
2.2.3	5LAYER Test Forecasts	7
2.3	Definition of Forecast Cases	7
2.3.1	Forecast Cases for Objective (a) (Cases A-C)	8
2.3.2	Forecast Cases for Objective (b) (Cases D-F)	8
2.3.3	Overview of Case Comparisons	8
2.4	Forecast Verification Procedures	8
2.4.1	Verification Areas	10
2.4.2	Verification Sample Size	10
2.4.3	Verification Parameters	10
Section 3	FORECAST COMPARISON RESULTS	13
3.1	Forecast Comparisons for Objective (b) (Cases A-C)	13
3.1.1	Preliminary Considerations	13
3.1.2	Case A Results	18
3.1.3	Case B-C Results	34
3.2	Forecast Comparisons for Objective (b) (Cases D-F)	40
3.2.1	Preliminary Considerations	40
3.2.2	Case D Results	41
3.2.3	Case E-F Results	54

Section 4 CONCLUSIONS AND RECOMMENDATIONS 60

4.1 Conclusions 60

4.2 Recommendation for Further Study 62

Section 5 APPENDIX - GLOSSARY 63

Section 6 REFERENCES 65

LIST OF TABLES

Table 1 Summary of production and test forecasts used to evaluate test objectives 9

2 Additional statistical information for Case A backhalf and fronthalf areas 27

3 As in Table 2 but for backhalf and fronthalf limited areas 27

4 Additional statistical information for Case B backhalf and fronthalf areas 39

5 As in Table 4 but for Case C 39

6 Additional statistical information for Case D backhalf and fronthalf areas 49

7 As in Table 6 but for backhalf and fronthalf limited areas 49

LIST OF FIGURES

Figure		Page
1	Relationship between condensation pressure spread (CPS) and cloud amount for various levels of the atmosphere	5
2	Schematic example of the total cloud vertical summation problem	6
3	Backhalf (upper) and fronthalf (lower) verification regions for this study	11
4	850 mb root mean square vector error (RMSVE) for 7LHFM, 6LDPE, and station persistence; and 7LHFM percent RMSVE reduction as a function of forecast length for 102 Northern Hemisphere RAOB stations during August - September 1979	15
5	As in Figure 4 but for 500 mb	16
6	As in Figure 4 but for 200 mb	17
7	25/25 score as a function of forecast length for AFGWC production 5LAYER (GP5), the AFGWC test 5LAYER (GT5), and persistence in Case A (Table 1) for the backhalf (BH) area, 14-day set	19
8	As in Figure 7 but for the latter 7-day set	20
9	As in Figure 7 but for the backhalf limited (BHL) area	21
10	25/25 score as a function of forecast length for the AFGWC production 5LAYER (GP5), the AFGWC test 5LAYER (GT5), and persistence in Case A (Table 1) for the fronthalf (FH) area, 14-day set	22
11	As in Figure 10 but for the latter 7-day set	23
12	As in Figure 10 but for the fronthalf limited (FHL) area	24
13	25/25 skill score (using the data in Figure 7) as a function of forecast length for the AFGWC production 5LAYER (GP5) and the AFGWC test 5LAYER (GT5) Case A (Table 1) for the backhalf (BH) area, 14-day set. Also shown is the GT5 to GP5 skill-score ratio	25
14	As in Figure 13 but for the fronthalf (FH) area (using the data in Figure 10)	26
15	Total cloud frequency distribution for the AFGWC production 5LAYER (GP5) and the AFGWC test 5LAYER (GT5) 24-hour forecasts and verifying analysis in Case A (Table 1) for the fronthalf (FH) area, 14-day set	30

16 As in Figure 15 but for 48 hours 31

17 As in Figure 15 but for the backhalf (BH) area 32

18 As in Figure 15 but for the backhalf (BH) area and for 48 hours 33

19 25/25 score as a function of forecast length for the AFGWC production 5LAYER (GP5), the AFGWC test 5LAYER (GT5), and persistence in Case B (Table 1) for the backhalf (BH) area, 14-day set 35

20 As in Figure 19 but for the fronthalf (FH) area 36

21 As in Figure 19 but for Case C (Table 1) 37

22 As in Figure 19 but for the fronthalf (FH) area and for Case C (Table 1) 38

23 25/25 score as a function of forecast length for the AFGWC production 5LAYER (GP5), the NMC production 7LHFM (NP7), and persistence in Case D (Table 1) for the backhalf (BH) area, 14-day set 42

24 As in Figure 23 but for the first 7-day set 43

25 As in Figure 24 but for the backhalf limited (BHL) area 44

26 25/25 score as a function of forecast length for the AFGWC production 5LAYER (GP5), the NMC production 7LHFM (NP7), and persistence in Case D (Table 1) for the fronthalf (FH) area, 14-day set 45

27 As in Figure 26 but for the first 7-day set 46

28 As in Figure 26 but for the fronthalf limited (FHL) area 47

29 Total cloud frequency distribution for the AFGWC production 5LAYER (GP5) and the NMC production 7LHFM (NP7) 0-hour analyses in Case D (Table 1) for the fronthalf limited (FHL) area, 14-day set 50

30 As in Figure 29 but for the backhalf limited (BHL) area 51

31 As in Figure 29 but for the 48-hour forecasts and verifying analysis 52

32 As in Figure 29 but for the 48-hour forecasts and verifying analysis in the backhalf limited (BHL) area 53

33 Shaded total cloud display of the AFGWC production 5LAYER (GP5) 0-hour analysis from the 03Z GP5 database on 10 September 1979. Blank areas are cloud-free and heavily darkened areas are overcast. All half-mesh (100 nm) grid points are represented 55

34 Shaded total cloud display of the NMC production 7LHFM (NP7) 3-hour forecast from the 00Z NP7 database on 10 September 1979. The forecast valid time agrees with that of the GP5 analysis in Figure 33. Otherwise as in Figure 33 56

35 As in Figure 33 but for the 24-hour forecast 57

36 As in Figure 34 but for the 27-hour forecast. The forecast valid time agrees with that of the GP5 forecast in Figure 35 58

37 As in Figure 33 but for the GP5 0-hour analysis from the 03Z GP5 database on 11 September 1979. This analysis represents the verifying field for the forecasts in Figure 35 and 36 59

38 25/25 score as a function of forecast length for the AFGWC production 5LAYER (GP5), the AFGWC test 5LAYER (GT5), the NMC production 7LHFM (NP7), and persistence for Cases A and D (Table 1) for the backhalf limited (BHL) area, 14-day set 61

1. INTRODUCTION

Beginning with the January 1979 meeting at AFGWC of the USAF Scientific Advisory Board (SAB), Ad Hoc Committee on Improved Cloud Forecasting, HQ AWS initiated the formulation of a plan for future improvements in the automated cloud forecast support that AWS provides to DOD customers. To obtain further input and guidance for this planning effort, HQ AWS in February 1979 directed AFGWC to undertake a Forecast Fields Comparison Test in which cloud forecast fields derived from several proposed numerical cloud models would be compared. The concern underlying this proposed test was whether a new advanced prediction model at AFGWC would yield sufficiently improved sensible weather forecasts, in particular cloud forecasts, to justify the increased computation costs of an advanced model.

This report presents the results of this test. It uses AFGWC's current production cloud model, known as 5LAYER, as the basis for comparisons. The 5LAYER model produces extratropical hemispheric forecasts of tropospheric temperature and moisture, from which are derived forecasts of layer and total cloud (among other derived parameters such as precipitation and icing). 5LAYER is best described as a quasi-Lagrangian model, because the forecast mechanism in the model is the application of three-dimensional air parcel trajectories. These trajectories, reinitialized at each time step, are computed from input forecast wind velocity components. A more complete description of 5LAYER is given by Friend and Mitchell (1982).

Owing to the trajectory computations, 5LAYER is not a stand-alone forecast model. In addition to initial temperature and moisture fields, 5LAYER also requires forecast wind input from a separate wind forecast model, which currently at AFGWC is the AWS 6LDPE. Clearly, the forecast skill of 5LAYER is substantially dependent on the skill of the input forecast winds, especially for long-range forecasts.

Significantly improved counterparts of the AWS 6LDPE model are executed operationally at other meteorological forecast centers. One such counterpart is the NMC 7LHFM model, the primary hemispheric forecast model at NMC from January 1978 to August 1980, a period which includes the August 1979 to September 1979 period of this study. The 7LHFM and 6LDPE models are closely related, hydrostatic, primitive equation models. The 6LDPE model represents the AFGWC adaption of the PE model of Shuman and Hovermale (1968), first implemented at NMC in 1966. The 7LHFM is the advanced version of the 6LDPE as it has evolved at NMC over the last 15 years. The key differences between the 6LDPE and the 7LHFM are summarized below:

(a) Addition of explicit equations and algorithms to model synoptic and convective moisture, precipitation, and latent heating.

(b) Addition of a seventh active layer to improve stratospheric forecasts.

(c) Improved modeling of radiative heating such as addition of longwave cooling above clouds.

(d) Expansion of model grid domain to cover the entire hemisphere.

(e) Reduction of horizontal grid spacing from whole-mesh (381 km) to half-mesh (190.5 km).

(f) Use of a special form of the governing physical equations known as the vorticity-energy form.

Verification statistics over the operational lifetime of the 7LHFM model show a significant reduction in the RMSVE of the 7LHFM forecast winds versus the 6LDPE forecast winds. We shall provide later a specific example of this error reduction from the data archived for this study. Presumably, if the 7LHFM model replaced the 6LDPE model as the source of 5LAYER driving motion fields, an improved cloud forecast would result. One objective of this study is to test this hypothesis and quantify any changes in forecast accuracy.

Improved numerical forecasts, however, are obtained invariably at increased computational cost. A cost increase is certainly incurred in the case of the 7LHFM versus the 6LDPE. Therefore, we will quantify any change in 5LAYER forecast accuracy in this study in order to provide useable input into cost/benefit ratio determinations. For this reason, we shall perform an objective model comparison based on objective grid-to-grid verification statistics.

The increased cost of an advanced moist dynamic model such as the 7LHFM, could be partially offset at AFGWC by eliminating 5LAYER and replacing it with cloud forecasts derived directly from the 7LHFM moisture forecasts. A second objective in this study is to determine if 7LHFM-derived cloud forecasts are competitive with 5LAYER. The single, moist, high-resolution, hemispheric or global, dynamic model concept was recommended for AFGWC in the final report of the aforementioned SAB. This concept is employed at virtually all other major numerical weather centrals (NMC, FNOC, ECMWF, and CMC) in the western countries. AFGWC however, unlike the other centrals cited above, has a particularly strong requirement for providing automated, gridded, global forecasts of layer and total cloud cover. The requirement initiated the separate development of the 5LAYER trajectory model in the middle 1960's before moist PE models were available. Thus, before eliminating 5LAYER to partially offset the increased cost of executing an advanced PE model, we must demonstrate whether or not a moist PE model can at least maintain and hopefully surpass the skill of 5LAYER, particularly during the first 24 hours.

In summary then, the two objectives of this study are as follows:

(a) Quantify the change in the total cloud forecast accuracy of the 5LAYER cloud model when forecast winds from the AWS 6LDPE model are replaced with forecast winds from the NMC 7LHFM model. If forecast accuracy improves, quantify degradations in this improvement resulting from the delayed availability of the 7LHFM databases relative to current 6LDPE database timeliness.

(b) Compare the accuracy of the respective total cloud forecasts derived from the forecast moisture fields of the NMC 7LHFM model and the AFGWC 5LAYER cloud model. If the 7LHFM-derived forecasts show superior accuracy, quantify degradations in this improvement resulting from the delayed availability of the 7LHFM databases relative to current 6LDPE database timeliness.

2. TEST METHODOLOGY

2.1 Test Period

The test period began at 00Z on 11 August 1979 and continued for 28 days through 00Z on 18 September 1979. During this period, various 7LHFM, 6LDPE, and 5LAYER model initial analyses and forecasts of vertical motion, horizontal wind velocity, temperature, moisture, and cloud amount were archived and later used in forecast comparisons and verifications. This section describes the specific databases that were archived and compared and the verification procedures that were used in this study. The results are then presented in Section 3. Conclusions are given in Section 4.

2.2 Forecast and Analysis Data Sets

2.2.1 7LHFM Production Forecasts

The 7LHFM forecasts projected onto the NMC whole-mesh grid were archived from the 00Z database on the first day and every second day thereafter during the test period. Data collected included horizontal wind components (u, v), vertical motion (omega), temperature (T), and relative humidity (RH) at the standard pressure levels from 850 mb through 300 mb (except 400 mb) and extending out to 48 hours at 3-hour intervals. The resulting 14 sets of 7LHFM forecast data were sent to AFGWC on magnetic tapes. These tapes were translated and reformatted to the database formats of AFGWC. For example, the 65X65 NMC whole-mesh hemispheric grid was truncated to the 47X51 subset grid that bounds the octagon domain of the AWS 6LDPE (Hoke et al., 1979). In addition, the 7LHFM RH and T databases were used to derive corresponding dew-point (T_d) and dew-point depression ($T-T_d$) databases.

Explicit cloud amount forecasts are not provided in the 7LHFM forecast database. Therefore, to accomplish objective (b) we derived cloud amount forecasts from the 7LHFM ($T-T_d$) databases cited above. To do this, we used the ($T-T_d$)/cloud conversion algorithms currently used in 5LAYER. We thereby ensured that the comparisons of 7LHFM and 5LAYER cloud forecasts in objective (b) are in fact comparisons of moisture forecast skill rather than comparisons of two different moisture/cloud conversion algorithms. We next describe in some detail the algorithm used to convert 7LHFM ($T-T_d$) forecasts to cloud amount forecasts.

At each standard pressure level used in 5LAYER (i.e., at 850, 700, 500, and 300 mb), we interpolated the whole-mesh 7LHFM ($T-T_d$) forecasts to the 93x101 half-mesh 5LAYER octagon grid. We then converted the interpolated 7LHFM half-mesh ($T-T_d$) values to Condensation Pressure Spread (CPS). CPS is defined as the amount of dry adiabatic vertical uplift in mb required for an air parcel, having a given T and T_d at pressure P, to reach its LCL. CPS is the active moisture variable carried by the 5LAYER trajectory model. On a thermodynamic chart, CPS is easily derived graphically from given values of P, T, and T_d. Analytically, however, the relation between CPS, P, T, and T_d is given by an impractical, transcendental equation that must be solved iteratively (Irvine, 1981). Alternatively, at AFGWC we use the approximate relation given by

(1) $CPS = (T-T_d)[-4.9 - 0.93(P/1000) - 9.0(P/1000)^2]$.

This relation yields CPS values that are within 13 percent of the rigorous, iteratively derived values over typical tropospheric ranges of T, T_d, and P (Irvine, 1981).

The conversion of CPS to cloud amount is accomplished using the set of empirical curves in Figure 1. The curves have been stratified by standard pressure level and are applied globally. The fact that the CPS curves yield some cloud for nonzero CPS values owes to the nonhomogeneous nature of an atmospheric layer over a large area, in which some fraction of the area may have locally achieved saturation (zero CPS and thus cloud), although the areal average CPS value is nonzero.

Equation (1) together with the curves in Figure 1 permit one to derive cloud amount forecasts at discrete pressure levels from $(T-T_d)$ forecasts at those levels. Finally, a determination of total cloud amount from the cloud amounts at discrete levels is derived. Because total cloud is the most reliably observed and analyzed cloud parameter (as opposed to ceilings, tops, layer cloud amounts, or cloud type), total cloud will be the single cloud parameter verified in this study. The relation used in 5LAYER and also here with the 7LHFM data to obtain the sum, S, of two fractional layer cloud amounts, C_1 and C_2 (where $0 \quad C_2 \quad C_1 \quad 1$) at discrete levels 1 and 2, is given by

(2) $S = C_1 + C_2 \ (1 - C_1)F$,

where F is a variable "unstacking" or randomness factor in the range of $0 \quad F \quad 1$. It can be shown that $C_1 \quad S \quad 1$. The factor F measures the extent of overlap or superposition among cloud layers and it is specified to decrease with increasing vertical separation between levels 1 and 2. Thus F is modeled conceptually after the vertical cloud stacking examples in Figure 2. The vertical cloud summation embodied in equation (2) and Figure 2 is probably least reliable in areas dominated by deep convection. More details on the successive application of equation (2) through several levels and the values of F used operationally to derive total cloud are given in Friend and Mitchell (1982). It suffices here to state that this same vertical cloud summation algorithm was used to obtain both 7LHFM and 5LAYER total cloud forecasts for objective (b). The 7LHFM total cloud forecasts obtained by the techniques described in this section will be denoted henceforth in figures and discussions as NP7 forecasts (NMC Production 7LHFM).

2.2.2 5LAYER Production Forecasts

To understand the 5LAYER cloud forecasts that were archived for this study, we must first briefly review the AFGWC cloud forecast production cycle. A 5LAYER forecast is initialized and executed from each 3DNEPH objective cloud analysis. The 3DNEPH is described by Fye (1978). The basetime (i.e., the 0-hour start time) of each 5LAYER forecast is therefore given by the basetime of the corresponding 3DNEPH analysis. Because of the emphasis at AFGWC on short-range cloud forecasts, the 3DNEPH/5LAYER cloud analysis and forecast system cycles eight times daily starting at 00Z plus

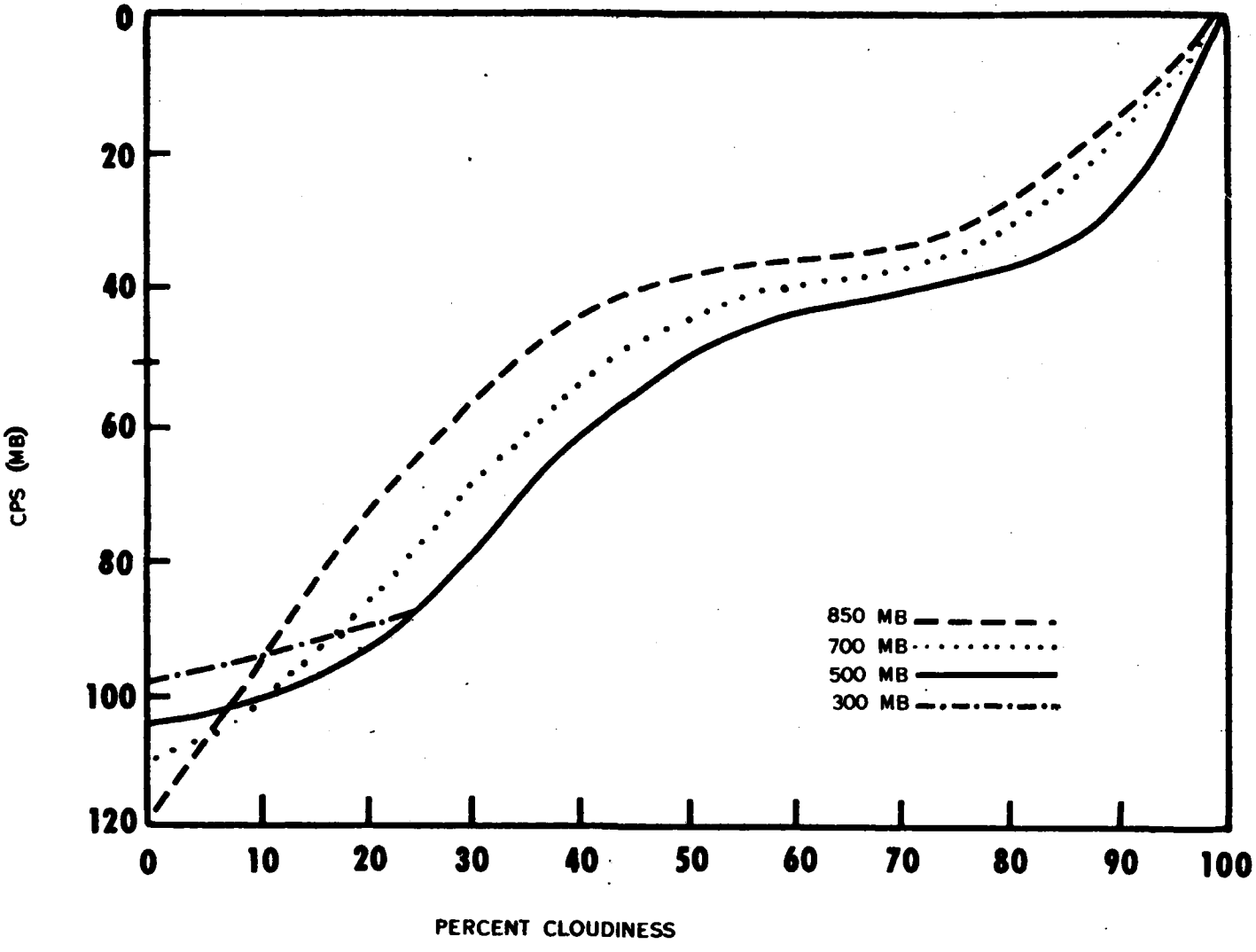

Figure 1. Relationship between condensation pressure spread (CPS) and cloud amount for various levels of the atmosphere.

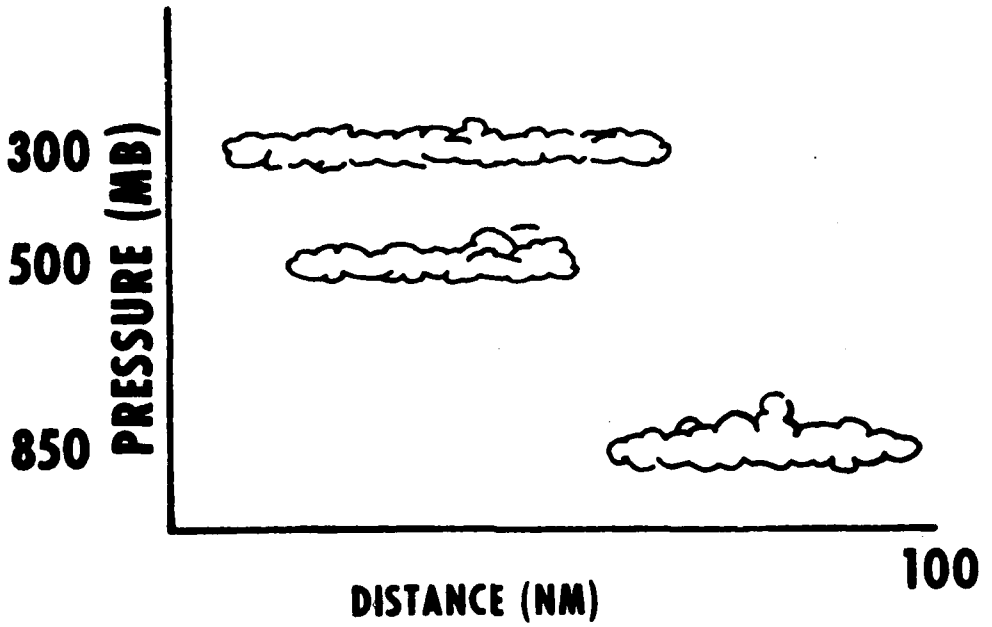

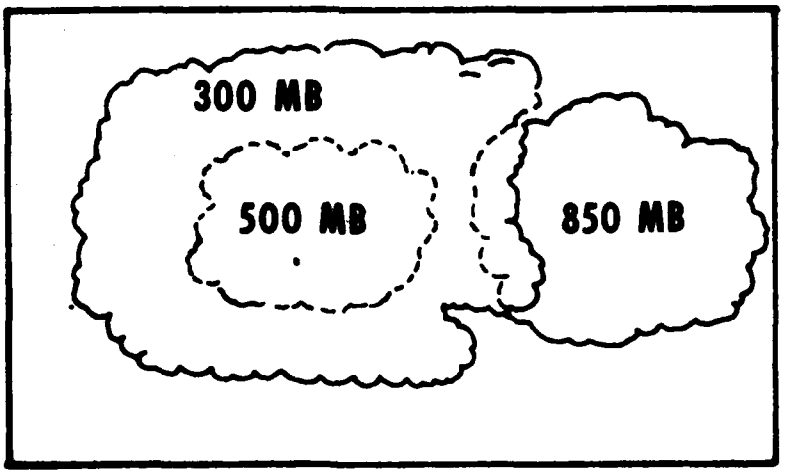

Figure 2. Schematic example of the total cloud vertical summation problem.

every three hours. The main obeservational data set input to the 3DNEPH analysis during each cycle is infrared polar orbiting satellite cloud imagery (from either NOAA or DMSP vehicles). In contrast, the HUFANL/6LDPE wind analysis and forecast system, which drives 5LAYER trajectories, cycles every six hours starting at 00Z, or only four times per day. The crucial point here is that owing to current production 3DNEPH and 6LDPE scheduled completion times and the above differences in cycle frequency, the 6LDPE forecast at basetime TTZ provides the driving motion fields for 5LAYER forecasts at basetimes (TT + 03)Z and (TT + 06)Z. The AFGWC automated cloud analysis and forecast cycling is described in more detail by Tarbell and Hoke (1979).

For this study, the northern hemisphere 03Z, 09Z, and 15Z 5LAYER forecasts, which respectively use the 00Z, 06Z, and 12Z 6LDPE wind forecasts, were archived on the 14 test days corresponding to the 14 archived 00Z 7LHFM forecasts. These production 5LAYER forecasts will be denoted henceforth in figures and discussions as GP5 (AFGWC Production 5LAYER).

2.2.3 5LAYER Test Forecasts

The NP7 cloud forecasts that we derived as described in Section 2.2.1 were needed to answer objective (b). To answer objective (a), the 03Z, 09Z, and 15Z 5LAYER model runs were executed again, using in each case the 00Z 7LHFM wind forecasts as input. The same production 03Z, 09Z, and 15Z 3DNEPH cloud analyses, respectively, were used to derive the 5LAYER initial moisture fields. These test 5LAYER forecasts using 7LHFM motion fields will be denoted henceforth in figures and discussions as GT5 (AFGWC Test 5LAYER). The 09Z and 15Z GT5 forecasts were limited to a maximum 36-hour range owing to the 00Z 7LHFM forecasts having been archived only out to 48 hours.

2.3 Definition of Forecast Cases

The chosen combinations of production and test forecasts that were used to evaluate objectives (a) and (b) are summarized in Table 1 and described in detail below.

2.3.1 Forecast Cases for Objective (a) (Cases A-C)

Case A: The GP5 and GT5 total cloud forecasts labled A in Table 1 were compared to answer the first part of objective (a), wherein we assume that the 7LHFM and 6LDPE databases for basetime TTZ are available concurrently. These comparisons measure the sensitivity of 5LAYER to the accuracy of the input motion field without regard to the timely availability of the motion field in a given production cycle.

Case B: The GP5 and GT5 total cloud forecasts labled B in Table 1 were compared to answer the second part of objective (a), wherein we seek to measure the impact of a 6-hour later offset in the time availability of the 7LHFM versus the 6LDPE wind databases in a given production cycle. We expect this simulated 7LHFM delay to reduce somewhat, any increase in GT5 versus GP5 accuracy from the previous case.

Case C: Closely analogous to Case B, the GP5 and GT5 total cloud forecasts labeled C in Table 1 also were compared to answer the second part of

objective (a), except, in this case, we measure the impact of a 12-hour later offset in the 7LHFM versus 6LDPE database time of availability for a given production cycle. We regard this case as a worst case situation in which, for example, the AFGWC 06Z and 18Z 6LDPE wind forecast cycles are eliminated in conjunction with the implementation of an advanced model having a significantly later completion time relative to the corresponding analysis data cutoff time.

2.3.2 Forecast Cases for Objective (b) (Cases D-F)

Case D: The GP5 and NP7 total cloud forecasts labeled D in Table 1 were compared to answer the first part of objective (b), wherein we once again assume that the 7LHFM and 6LDPE databases for TTZ are available concurrently. These comparisons measure the skill of 7LHFM-derived total cloud forecasts (see Section 2.2.1) relative to current 5LAYER production cloud forecasts.

Case E: The GP5 and NP7 total cloud forecasts labeled E in Table 1 were compared to answer the second part of objective (b), wherein we seek to measure the effect of a 6-hour offset (delayed availability) in the 7LHFM versus the 6LDPE database time.

Case F: The GP5 and NP7 total cloud forecasts labeled F in Table 1 also were compared to answer the second part of objective (b), but here we seek to measure the impact of a 12-hour offset in the 7LHFM versus the 6LDPE database time of availability.

2.3.3. Overview of Case Comparisons

We emphasize that the following results from Cases A-C, objective (a), and Cases D-F, objective (b), must be interpreted within two different contexts. Cases A-C represent tests of 5LAYER sensitivity to input motion field accuracy. Strictly speaking, Cases A-C do not represent a cloud forecast model comparison, but rather a test of the sensitivity of a single cloud forecast model to inputs from two previously compared wind models having well-known relative RMSVE characteristics. On the other hand, Cases D-E represent a comparison of the ability of two separate, independent analysis/forecast systems (as configured at data archival time) to provide skillful global cloud forecasts. Briefly, the AFGWC system (Tarbell and Hoke, 1979) consists of the HUFANL/6LDPE analysis-forecast subsystem for the winds, temperatures, and heights, which are then used in a separate 3DNEPH/5LAYER subsystem for moisture and clouds. The NMC system (as configured during the test peiod) consists of a single HUFANL/7LHFM analysis-forecast system for winds, temperatures, heights, and moisture (McPherson, 1980).

2.4 Forecast Verification Procedures

Throughout the 28-day test period, the half-mesh (100 nm) 5LAYER initial 0-hour total cloud fields available at 00Z plus every 3 hours were archived and subsequently used to accomplish grid-to-grid verification of all concurrently valid GP5, GT5, and NP7 forecasts in Table 1. 5LAYER half-mesh initial total cloud fields actually represent a horizontal compaction (weighted areal average) of the corresponding eighth-mesh (25 nm) 3DNEPH objective cloud analysis. In this sense then, all verifications were performed against the 3DNEPH.

Table 1. Summary of production and test forecasts used to evaluate stated objectives. See text for details.

Case	Initial Moisture	Forecast Model	Driving Motion Field Input to 5LAYER	Max Fcst Projection	Offset Time	Intended Objective
A (GP5)	3DNEPH (03Z)	5LAYER (03Z)	AFGWC 6LDPE (00Z)	48	N/A	(a)
A (GT5)	3DNEPH (03Z)	5LAYER (03Z)	NMC 7LHFM (00Z)	48	0	(a)
B (GP5)	3DNEPH (09Z)	5LAYER (09Z)	AFGWC 6LDPE (06Z)	36	N/A	(a)
B (GT5)	3DNEPH (09Z)	5LAYER (09Z)	NMC 7LHFM (00Z)	36	6	(a)
C (GP5)	3DNEPH (15Z)	5LAYER (15Z)	AFGWC 6LDPE (12Z)	36	N/A	(a)
C (GT5)	3DNEPH (15Z)	5LAYER (15Z)	NMC 7LHFM (00Z)	36	12	(a)
D (GP5)	3DNEPH (03Z)	5LAYER (03Z)	AFGWC 6LDPE (00Z)	48	N/A	(b)
D (NP7)	HUFANL (00Z)	7LHFM (00Z)	N/A	48	0	(b)
E (GP5)	3DNEPH (09Z)	5LAYER (09Z)	AFGWC 6LDPE (06Z)	36	N/A	(b)
E (NP7)	HUFANL (00Z)	7LHFM (00Z)	N/A	36	6	(b)
F (GP5)	3DNEPH (15Z)	5LAYER (15Z)	AFGWC 6LDPE (12Z)	36	N/A	(b)
F (NP7)	HUFANL (00Z)	7LHFM (00Z)	N/A	36	12	(b)

2.4.1 Verification Areas

Within the 5LAYER octagon domain, two verification areas were defined for this study and are denoted in Figure 3 as the "fronthalf" area (FH) and the "backhalf" area (BH), which respectively encompass the North American and Eurasian land masses. Within each of the FH and BH areas, a corresponding limited area, FHL and BHL respectively, was defined by verifying only extratropical grid points north of about 30°N. The motivation for defining the additional limited areas is discussed in later sections.

2.4.2 Verification Sample Size

The FH and BH areas contained nearly equal numbers of half-mesh grid points (2358 in FH and 2306 in BH). For the limited areas FHL and BHL, the grid-point totals are 62% and 65% of the FH and BH totals respectively. When verifying over any of the four areas defined for this study, we verified all half-mesh grid points within the defined area. Therefore, for each set of 14 separate executions of each model (GP5, GT5, and NP7) for each given basetime in Table 1 (00Z, 09Z, and 15Z for GP5 and GT5 and 00Z for NP7), a total verified sample of 33,012 points (FH) or 32,284 points (BH) was generated for each forecast projection (e.g., a 24-hour forecast). The FHL and BHL totals respectively are obtained from the latter totals using the previously given percentages. Finally, to measure the temporal sampling dependence in the statistics, each 14-day sample was divided into two 7-day samples corresponding to the first and second half of the 14-day test period.

2.4.3 Verification Parameters

At each half-mesh grid point in the 5LAYER octagon domain, each of the GP5, GT5, and NP7 total cloud forecasts consists of a cloud amount value (in whole percent, ranging continuously from 0-100). This value is treated in applications as the percent of the respective 100 nm square half-mesh grid box that is covered by cloud. For verification purposes, the cloud amount percentage is rounded to the nearest multiple of 5 percent.

In the verification procedure used for this study, we paired the gridded forecast cloud amounts, F, point by point with the corresponding 0-hour gridded analysis cloud amounts, A, for the given forecast valid time. From the resulting sample of errors (F-A) (see Section 2.4.2 for sample size), we derived the bias, root mean square error (RMSE), standard deviation of the error (STDE), linear correlation coefficient, and the 25/25 score. This latter score is the primary accuracy measure used in this study and will be defined in the next section. The other statistical parameters are standard. We should emphasize here that although the frequency of occurrence distribution of cloud amount is quasi-binary (dominated by the clear and overcast ends of the range of cloudiness), the distribution of sample errors, E=F-A, is nearly normal. The frequency distribution for E cannot be strictly normal, however, because here $E \leq 100$ and thus the tails of the distribution are truncated.

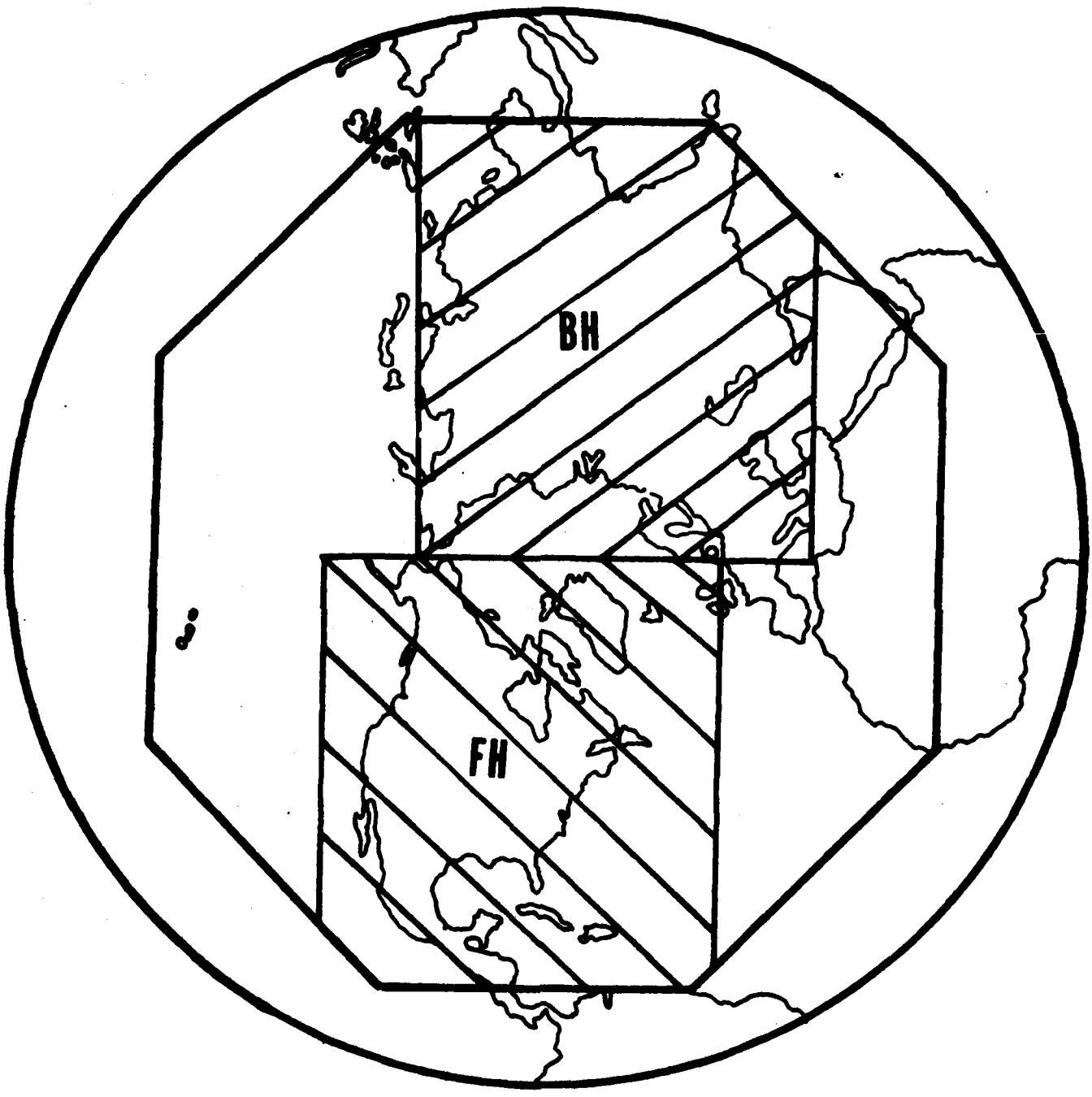

Figure 3. Backhalf (upper) and fronthalf (lower) verification regions for this study.

The 25/25 score is defined as the number, R, of "correct" grid point forecasts divided by the total number, T, of verified grid points in the sample. A forecast total cloud amount, F, for a given grid point is considered "correct" if F is within ± 25 percent of its paired verifying analysis amount, A; that is, if $E \leq 25$. The ratio R/T is multiplied by 100 to yield a final percent correct score. Quantitatively then, we define

$$(3) \quad 25/25 \text{ Score} = (R_{25}/T) \times 100 \quad ,$$

where the subscript on R_{25} denotes the dependence of R on the chosen error tolerance. A perfect 25/25 score of 100 percent indicates that $E \leq 25$ at all grid points in the verified sample. Clearly, we can define scores analogous to equation (3) for other choices of the error tolerance. For larger (smaller) error tolerances, R and the percent correct will increase (decrease). We have chosen a rather liberal error tolerance here for two reasons. First, previous cloud model comparison studies have shown that the 25/25 score is the most sensitive indicator of its type. That is, the greatest spread in percent correct scores among various test forecast cases tends to be in the 25/25 score. Secondly, the objective 0-hour, half-mesh, GP5 gridded total cloud analysis used as the verifying field is not perfectly reliable, because it is derived from the objective 3DNEPH analysis. Like any objective analysis model, the 3DNEPH has certain characteristic errors. The impact of these errors on the statistics obtained here is discussed further in Section 3.1.1.

A familiar skill score can be derived by comparing the 25/25 score of a forecast sample to the 25/25 score of the sample's persistence forecast. Here in this study, we use the skill score, S, given by

$$(4) \quad S_{25} = (R_{25} - P_{25}) \; / \; (T - P_{25}),$$

where P_{25} is the number of persistence forecast points at which $E \leq 25$.

3. FORECAST COMPARISON RESULTS

3.1 Forecast Comparisons for Objective (b) (Cases A-C)

3.1.1 Preliminary Considerations

Before we evaluate the impact of using 7LHFM versus 6LDPE as the source of 5LAYER input forecast winds, we must estimate the upper limit on the improvement in 5LAYER skill that one may expect. We need this limit in order to judge the significance of a given increase in forecast accuracy resulting from improved winds. From the 5LAYER forecast study by Garrison (1974), we estimate that the sources of a typical STDE of 33 percent cloud for a 24-hour 5LAYER total cloud forecast may be given as follows:

Contribution to the 24-hour 5LAYER STDE	Error Source
8	Gridding and interpolation operations
11	Shortcomings in cloud model physics
6	Errors in initial or verifying 3DNEPH objective analysis
8	Input wind forecast inaccuracies
33	Total STDE

The study by Garrison (1974) gives a detailed example of how cloud forecast errors arise from gridding and interpolation operations. Here, we shall discuss briefly the other sources of 5LAYER forecast error given above.

Shortcomings in 5LAYER model physics include, for example, insufficient representation of boundary-layer cloud processes (such as fair-weather cumulus and radiation fog) and a lack of an explicit treatment of liquid cloud water. These and other shortcomings in model physics owe largely to the computational constraint whereby the model execution time must meet daily production deadlines. This computational constraint, which precludes inclusion of the complex algorithms of certain physical processes, is in turn a strong function of the limitations of the computer hardware being utilized.

5LAYER forecast errors also arise from errors in the 3DNEPH cloud analysis, which provides both the initial and verifying cloud fields for 5LAYER. In areas of sparse conventional data, the 3DNEPH is unable to discern low-level cloud underlying a higher level overcast, which in this case will be the only cloud deck represented in the video and infrared satellite data. Also, in conventional data-sparse regions, the 3DNEPH analysis is largely persisted over the several analysis cycles that may occur between successive satellite passes. For the DMSP satellite configuration that existed during the test period, up to 8 hours separated successive satellite passes over any given area during certain periods of the day. The resulting tendency in the 3DNEPH toward persistence during these periods in data-sparse regions somewhat distorts the short-range forecast statistics in this study. We

expect, then, that the 6-hour persistence forecast scores are anomalously inflated, while the 6-hour model forecast scores are anomalously degraded. It is difficult to quantify the statistical impact arising from persisted regions in the 3DMEPH verification fields. However, we suspect it is not large for forecast periods beyond 12-hours.

Our primary interest in objective (a), however, is in the last 5LAYER error source listed above, namely, errors arising from inaccuracies in the input forecast winds. The 8 percent estimate given above in this category was determined from the "perfect prog" 5LAYER study (Garrison, 1974) in which actual objective upper-air wind analyses were used as input to 5LAYER in place of the wind model forecasts. Thus, an 8 percent reduction in STDE is the extreme upper limit in improvement that one can reasonably expect in 5LAYER by using improved forecast winds. In this regard, we note that when the AWS 6LDPE model replaced the quasi-geostrophic 6LVL model in 1975, the 5LAYER monthly STDE values only dropped about 3 percent in the subsequent winter months and only 1.5 percent in the subsequent summer months. Overall then, because the period of the present study was late summer, we estimate that on the order of only a 1-2 percent drop in the 5LAYER 24-hour STDE values will be obtained here when we replace the 6LDPE input with that of the 7LHFM.

To produce a meaningful evaluation of the sensitivity or response of 5LAYER to improved 7LHFM wind output, we must quantify the RMSVE reduction in the 7LHFM over the 6LDPE; that is, we must measure how much better the 7LHFM winds are than 6LDPE winds. Optimally for this purpose, we might have compared the RMSE values obtained from a special verification of the 14 specific 00Z 7LHFM and 6LDPE databases actually used in the Case A (see Table 1). This was not done, however, because of the associated increase in the volume of archived data required. Instead, we give the routine monthly RMSVE values (as derived from a common standard set of 102 Northern Hemisphere RAOB stations) for the 7LHFM, 6LDPE, and station persistence for the combined months of August and September 1979, which include the test period. These RMSVE values are given as a function of forecast length in Figures 4-6 for the 850, 500, and 250 mb levels respectively. The 14 7LHFM and 6LDPE 00Z databases used in Case A represent about 12 percent of the 122$\pm$2 7LHFM and 6LDPE databases from which Figures 4-6 were derived. The availability of comparative statistics determined the choice of pressure levels shown in Figures 4-6. The 5LAYER model specifically utilizes u, v, and omega wind components at the 1000, 850, 700, 500, and 300 mb levels.

Figures 4-6 also give the percent reduction in the 7LHFM versus the 6LDPE RMSVE. Overall, these figures show a 7LHFM RMSVE reduction of around 14 percent when averaged over the given levels and forecast intervals. Alternatively, we may interpret Figures 4-6 as showing that the 7LHFM forecast of length TT + Δt hours has the same RMSVE accuracy as the 6LDPE forecasts of length TT hours. The Δt "forecast extension" here is obtained by translating each point on the 7LHFM RMSVE curves to the right by an interval Δt until coincidence with the 6LDPE RMSVE curve is achieved. Figures 4-6 show a minimum 7LHFM versus 6LDPE Δt value of 12 hours. In the next section we evaluate the comparative verification statistics obtained from Cases A-C in Table 1 and then we establish to what extent this increase in 7LHFM versus 6LDPE skill translates into measured improvements in 5LAYER total cloud forecast accuracy.

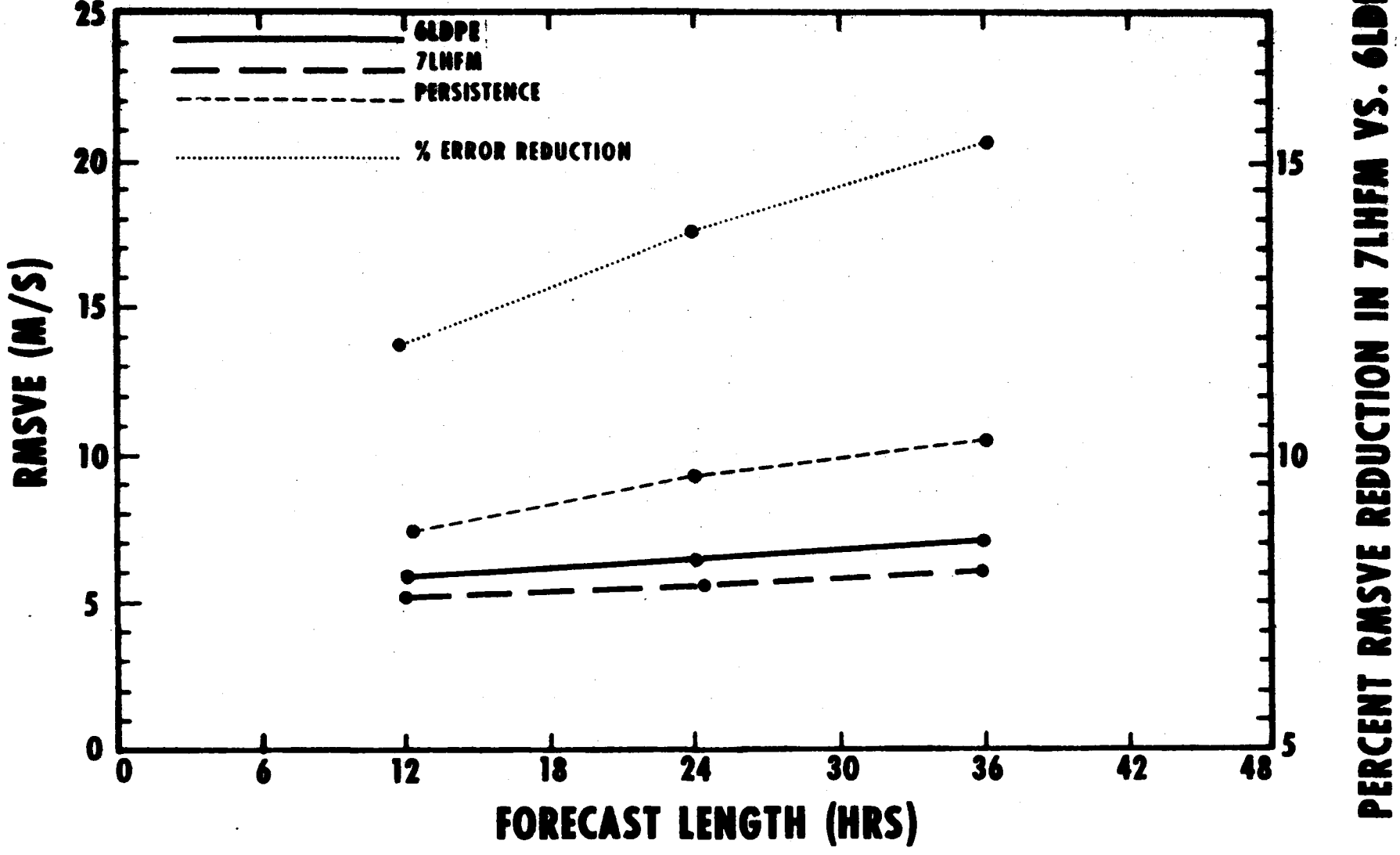

Figure 4. 850 mb root mean square vector error (RMSVE) for 7LHFM, 6LDPE, and station persistence and 7LHFM percent RMSVE reduction as a function of forecast length for 102 Northern Hemisphere RAOB stations during August-September 1979.

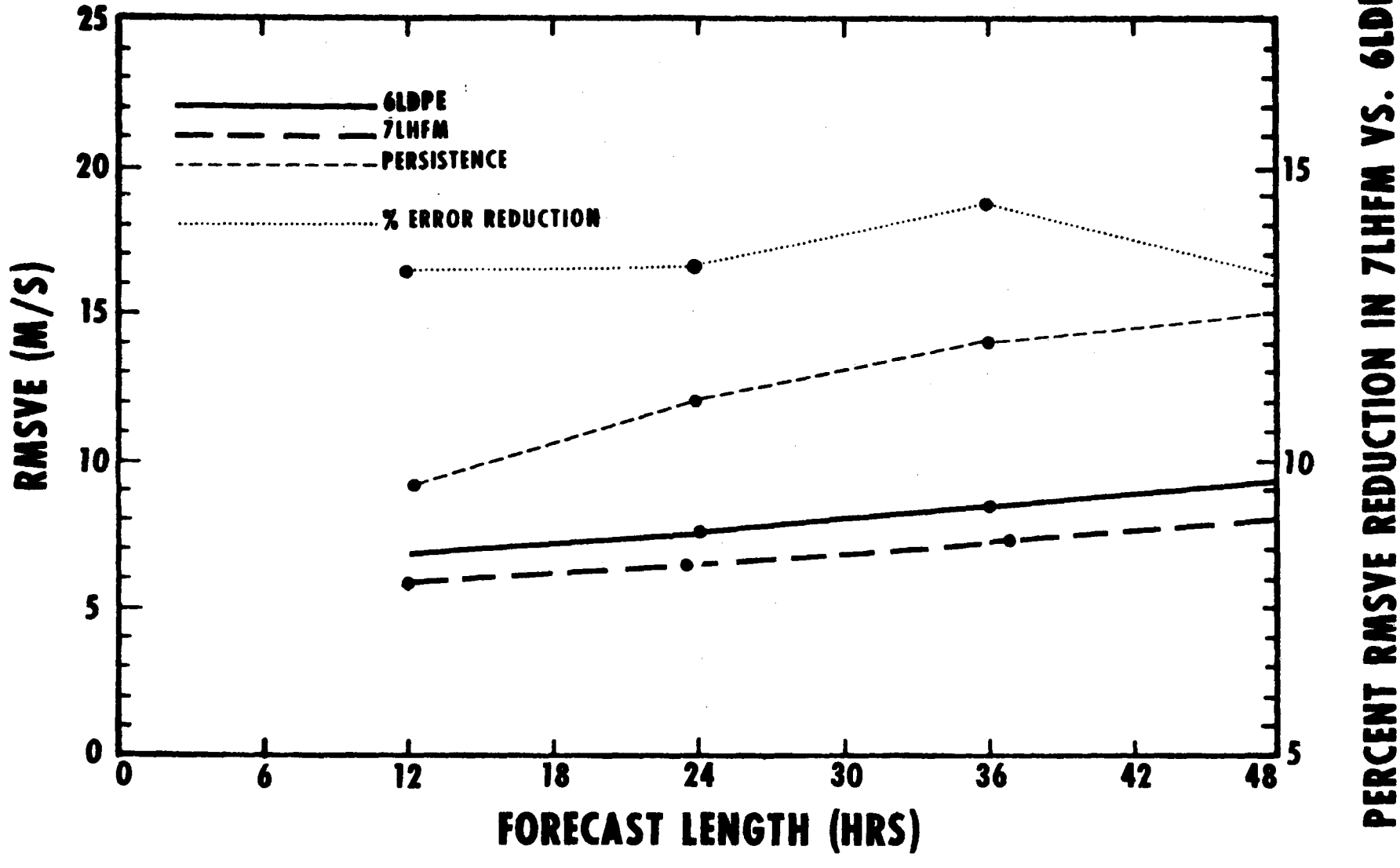

Figure 5. As in Figure 4 but for 500 mb.

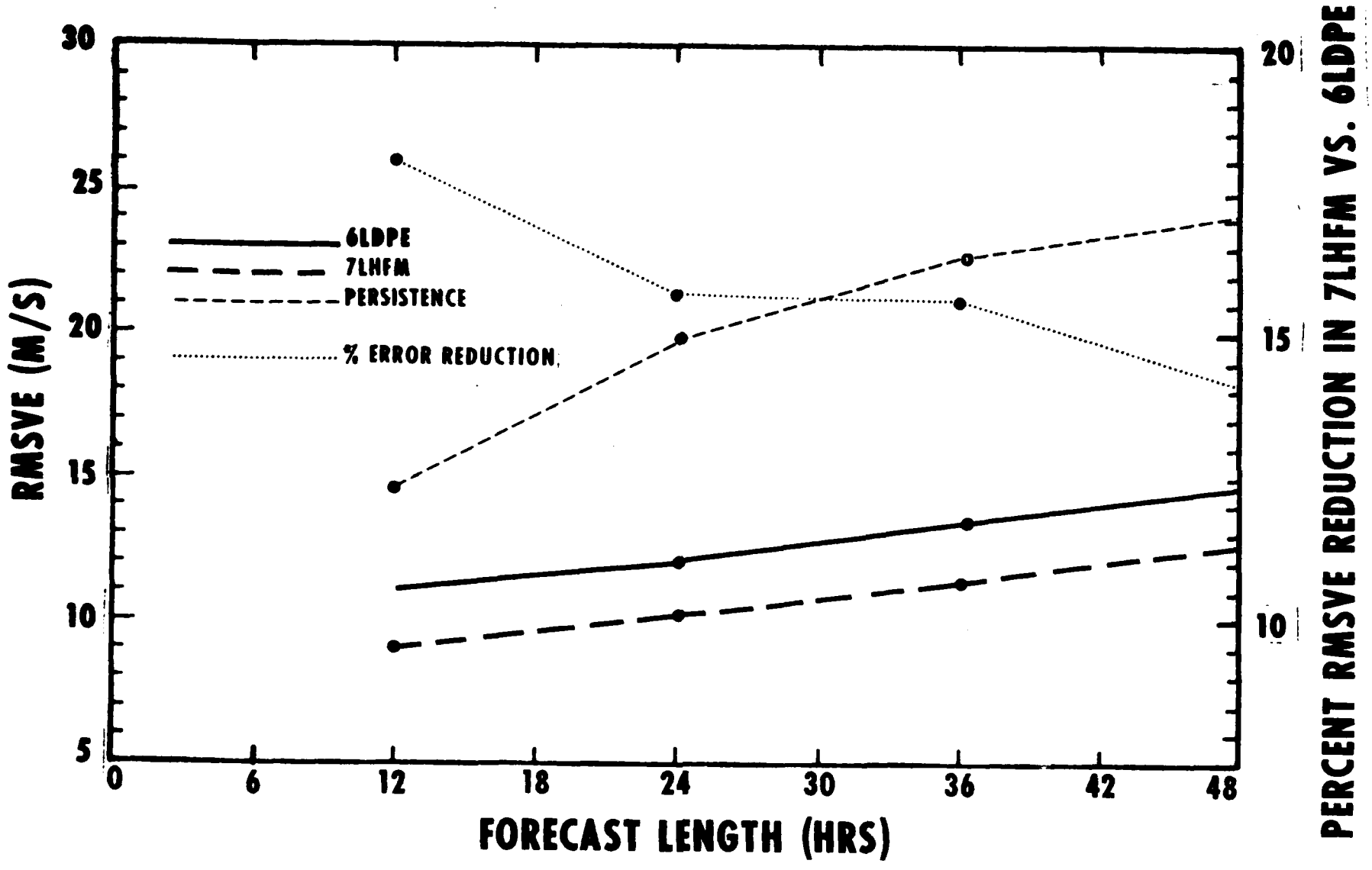

Figure 6. As in Figure 4 but for 250 mb.

3.1.2 Case A Results

The 25/25 scores for the GP5, GT5, and persistence forecasts labeled Case A in Table 1 are given as a function of forecast length in Figures 7, 8, and 9 for the BH region (14-day set), BH region (latter 7-day set), and BHL region (14-day set), respectively. The corresponding Case A results for the FH and FHL regions are given in Figures 10-12.

Before 9 hours, the GP5 and GT5 25/25 scores are nearly equivalent. But beyond 9 hours the GT5 score is superior to the GP5 score throughout Figures 7-12. The absolute improvement in the 25/25 score of GT5 versus GP5 never exceeds about 3 percent in the BH cases or about 1.5 percent in the FH cases. We conclude from the figures that the 14 percent RMSVE reduction in the 7LHFM versus the 6LDPE wind field forecasts has translated roughly into an order of magnitude smaller absolute improvement in the total cloud 25/25 score of the 5LAYER model.

It is important, however, that we also consider the improvment in GT5 versus GP5 25/25 score relative to persistence. In Figure 7, for the overall BH case, we find at 24 hours and beyond at least a doubling of the spread between the model forecast and persistence curves in the GT5 case versus the GP5 case. Inspection of equation (4) shows that the GT5 25/25 skill score is thus twice that of GP5 for the 14-day BH case. This is shown graphically in Figure 13, which is the skill-score plot corresponding to Figure 7. Figure 14 shows the FH skill-score plot corresponding to Figure 10. It is apparent in Figure 14 that the GT5 versus GP5 skill-score improvement in the FH case was substantially less than in the BH case in Figure 13.

We also note in comparing Figures 9 and 12 with Figures 7 and 10 respectively, that both the GP5 and GT5 25/25 scores are larger relative to persistence (thus implying greater skill scores) in the limited versus full verification areas, owing to the lower persistence 25/25 scores in the limited areas. This result agrees with routine monthly 5LAYER statistics, which consistently show lower persistence scores in extratropical versus subtropical regions. The subtropical regions have been eliminated in the FHL and BHL areas. Thus, in the BHL area we would not obtain a GT5 skill score that is twice that of GP5; nevertheless, the absolute 25/25 score improvement in the BHL and BH areas is roughly equivalent. In the FHL area, we find the GT5 absolute 25/25 score improvement to be larger than in the FH area, but still smaller than in the BHL area.

We next consider the Case A comparisons for the remaining statistical verification parameters introduced earlier. The results of these comparisons for the FH and BH areas are presented in Table 2 and for the FHL and BHL areas in Table 3. There is a fairly consistent reduction in the GT5 RMSE and STDE values relative to the corresponding GP5 values, with the exception of the RMSE values for the entire FH area. Thus, the 7LHFM wind input in Case A has also improved the RMSE and STDE statistics in general. It is significant to note that while the FH-area values of GT5 RMSE and STDE actually increased relative to GP5 in three of five forecast periods, the FHL-area values of GT5 RMSE and STDE showed the largest consistent decreases for the 24-hour period and beyond. Thus, it is clear here, and in the previous 25/25 score results, that the GT5 forecasts were the least accurate over the FH subtropics area.

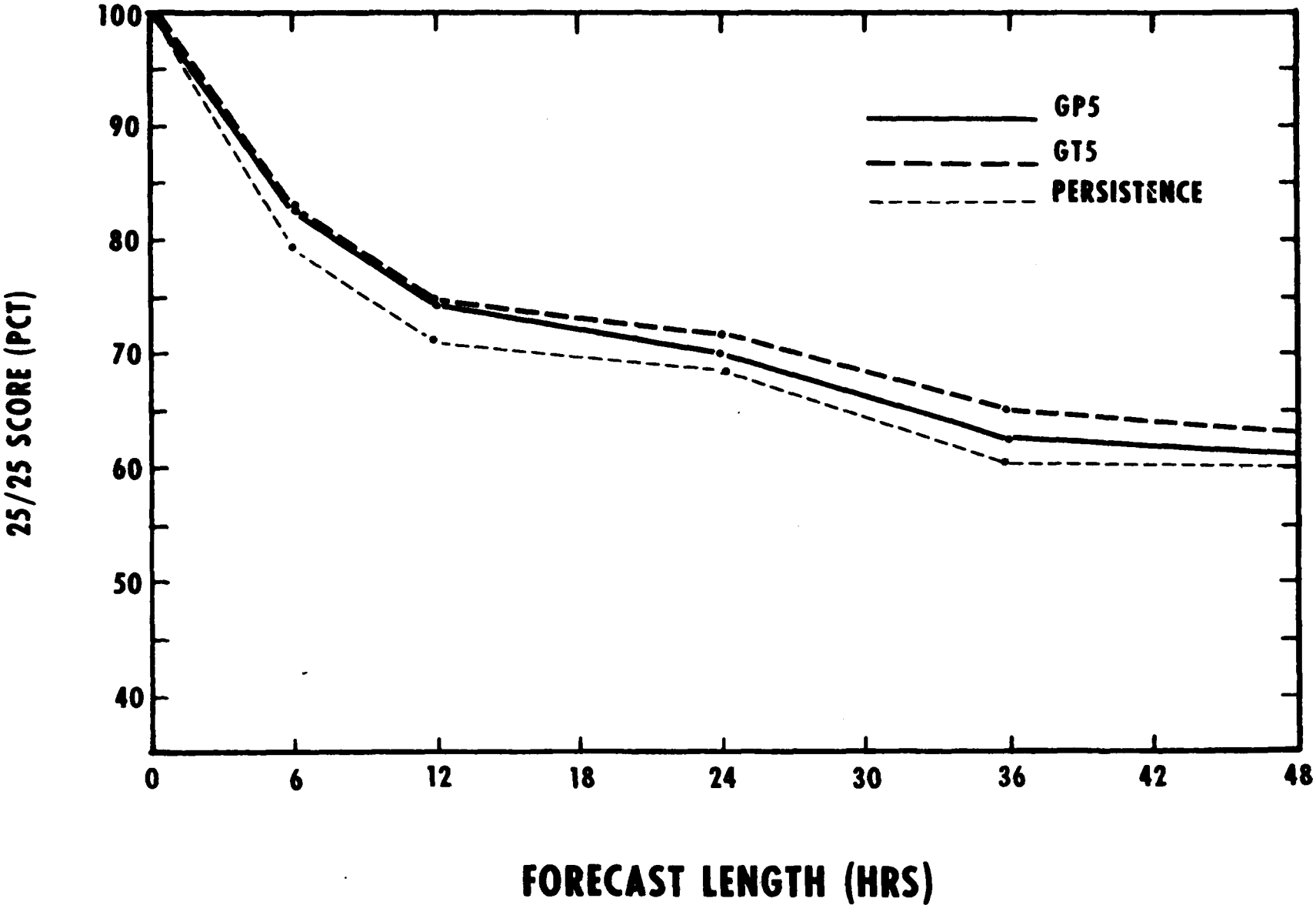

Figure 7. 25/25 score as a function of forecast length for the AFGWC production 5LAYER (GP5), the AFGWC test 5LAYER (GT5), and persistence in Case A (Table 1) for the backhalf (BH) area, 14-day set.

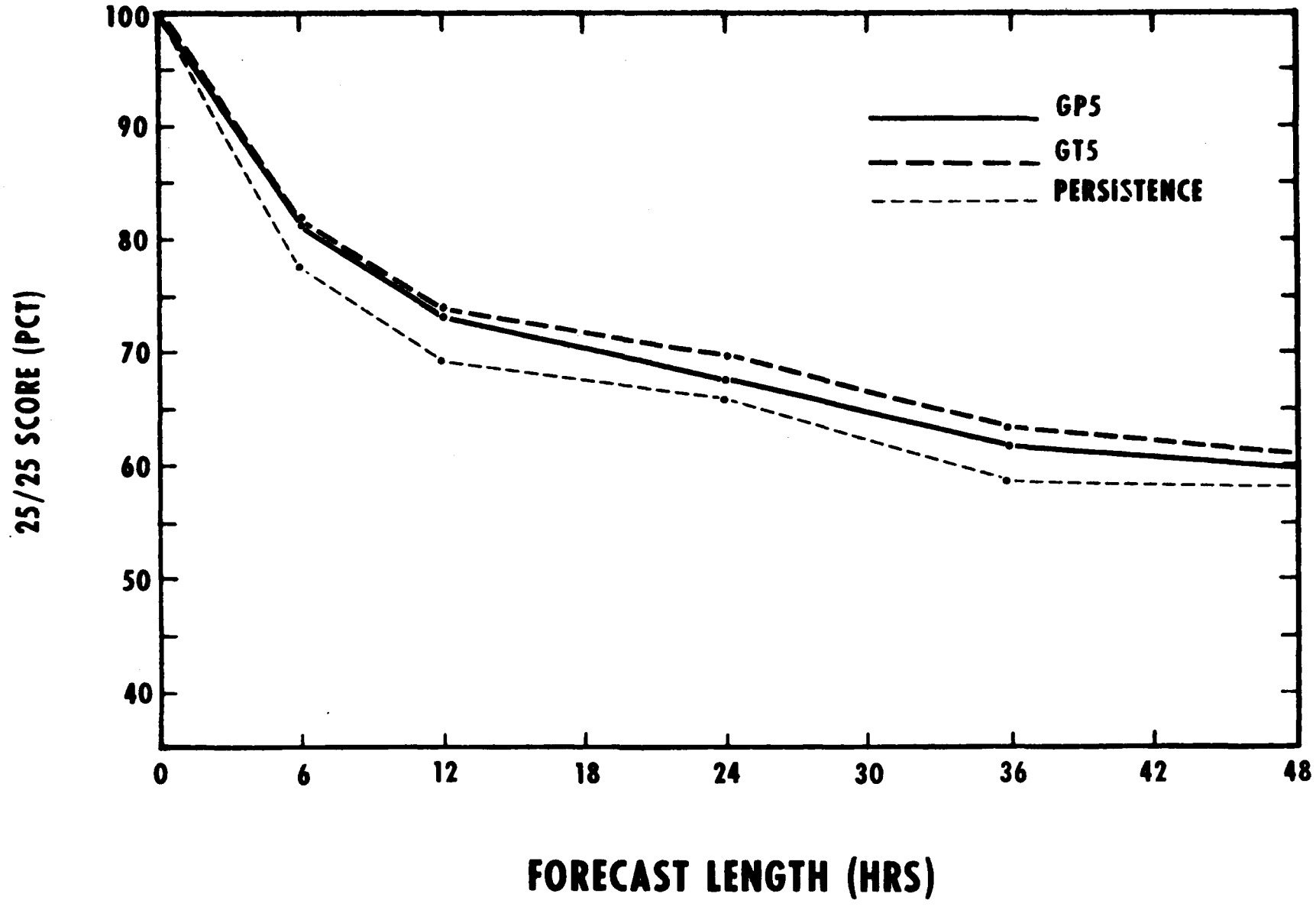

Figure 8. AS in Figure 7 but for the latter 7-day set.

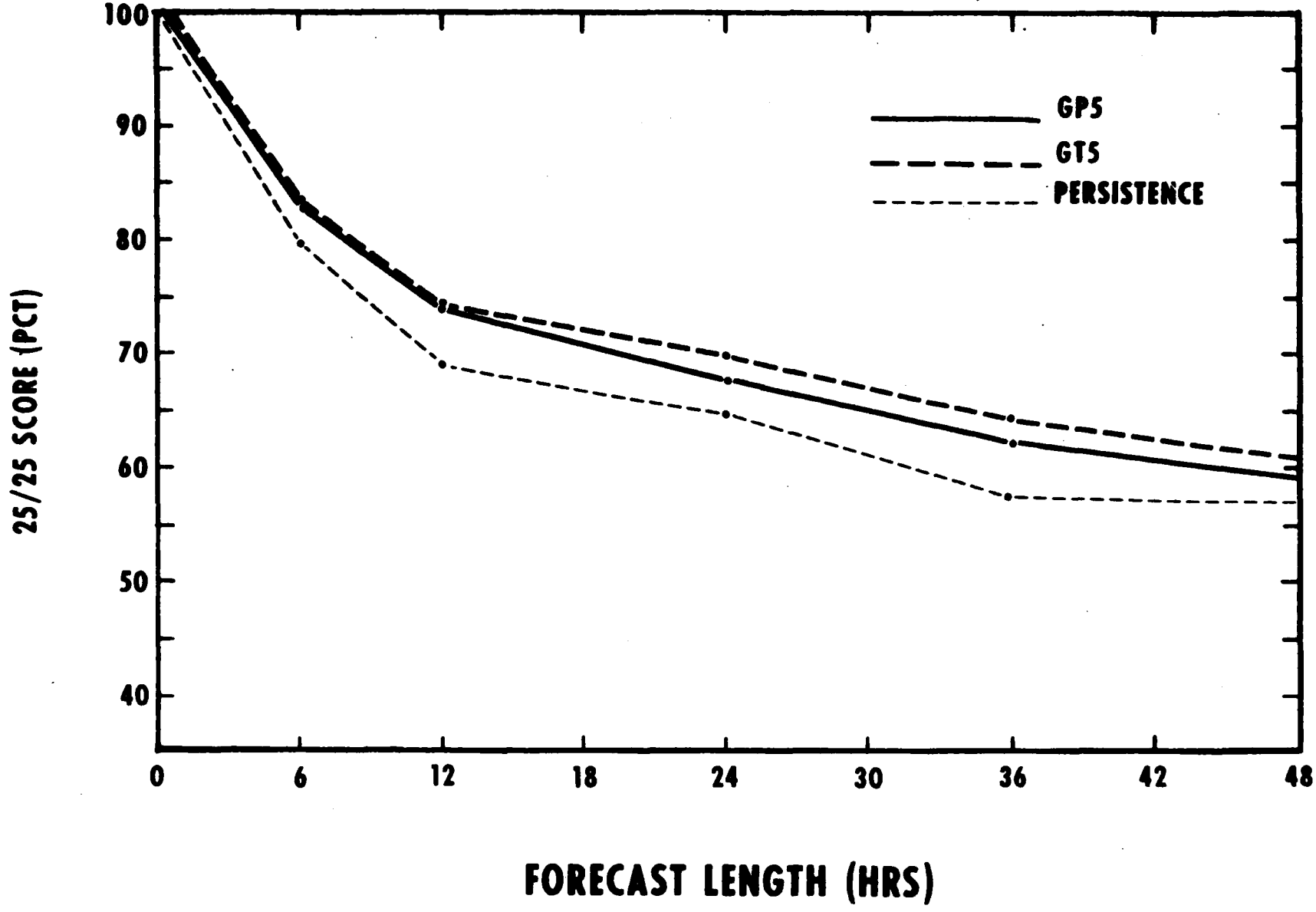

Figure 9. AS in Figure 7 but for the backhalf limited (BHL) area.

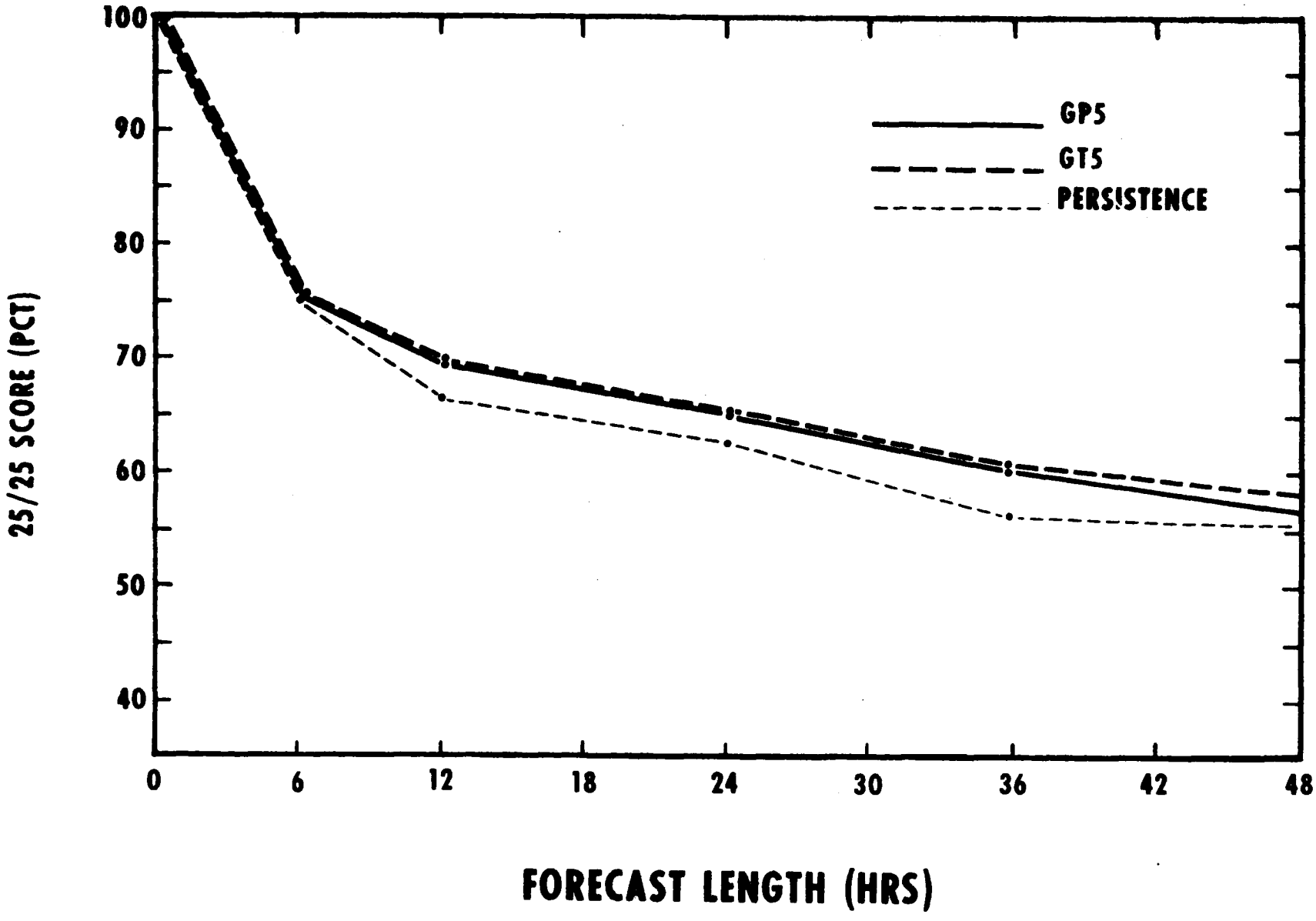

Figure 10. 25/25 score as a function of forecast length for the AFGWC production 5LAYER (GP5), the AFGWC test 5LAYER (GT5), and persistence in Case A (Table 1) for the fronthalf (FH) area, 14-day set.

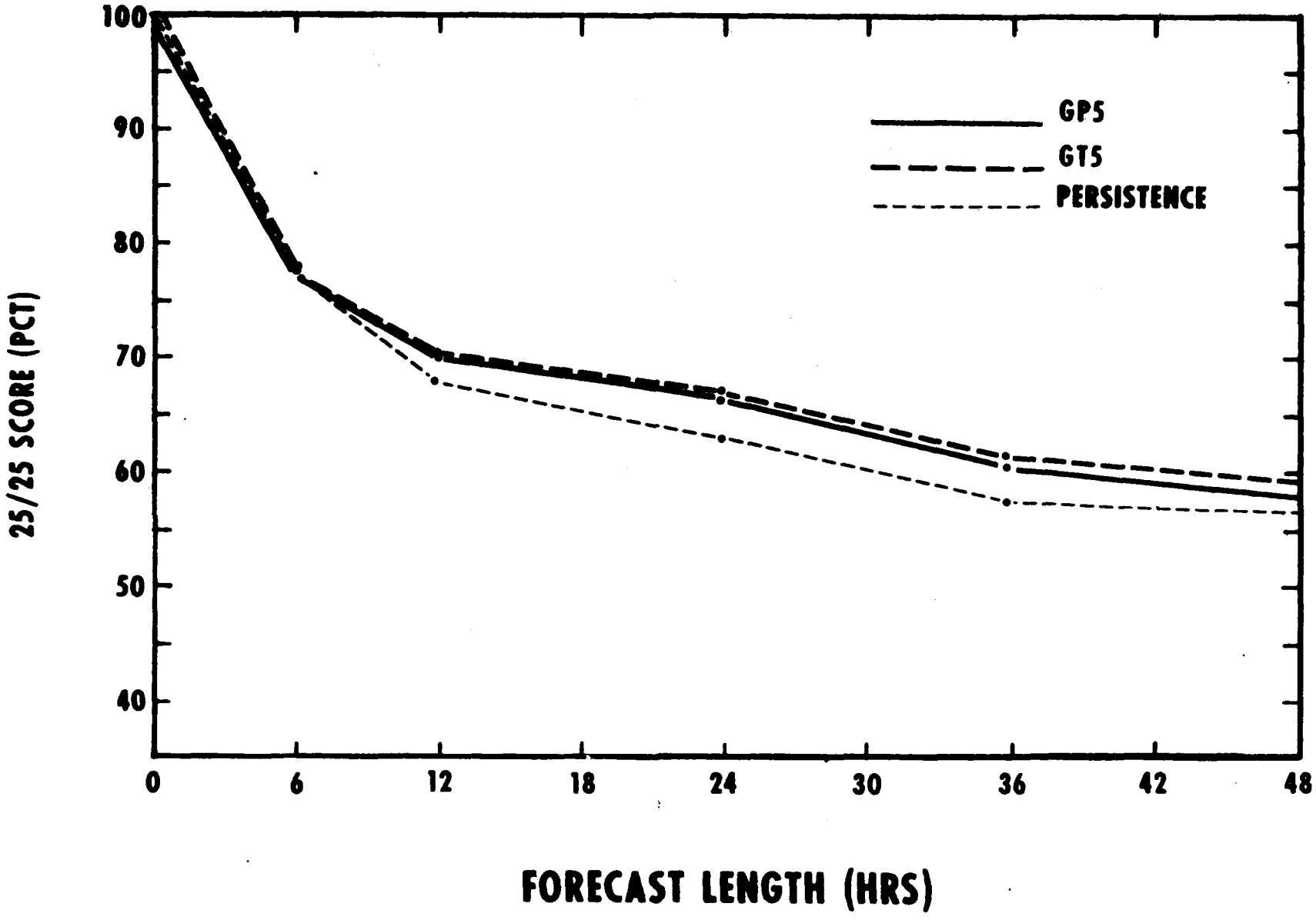

Figure 11. As in Figure 10 but for the latter 7-day set.

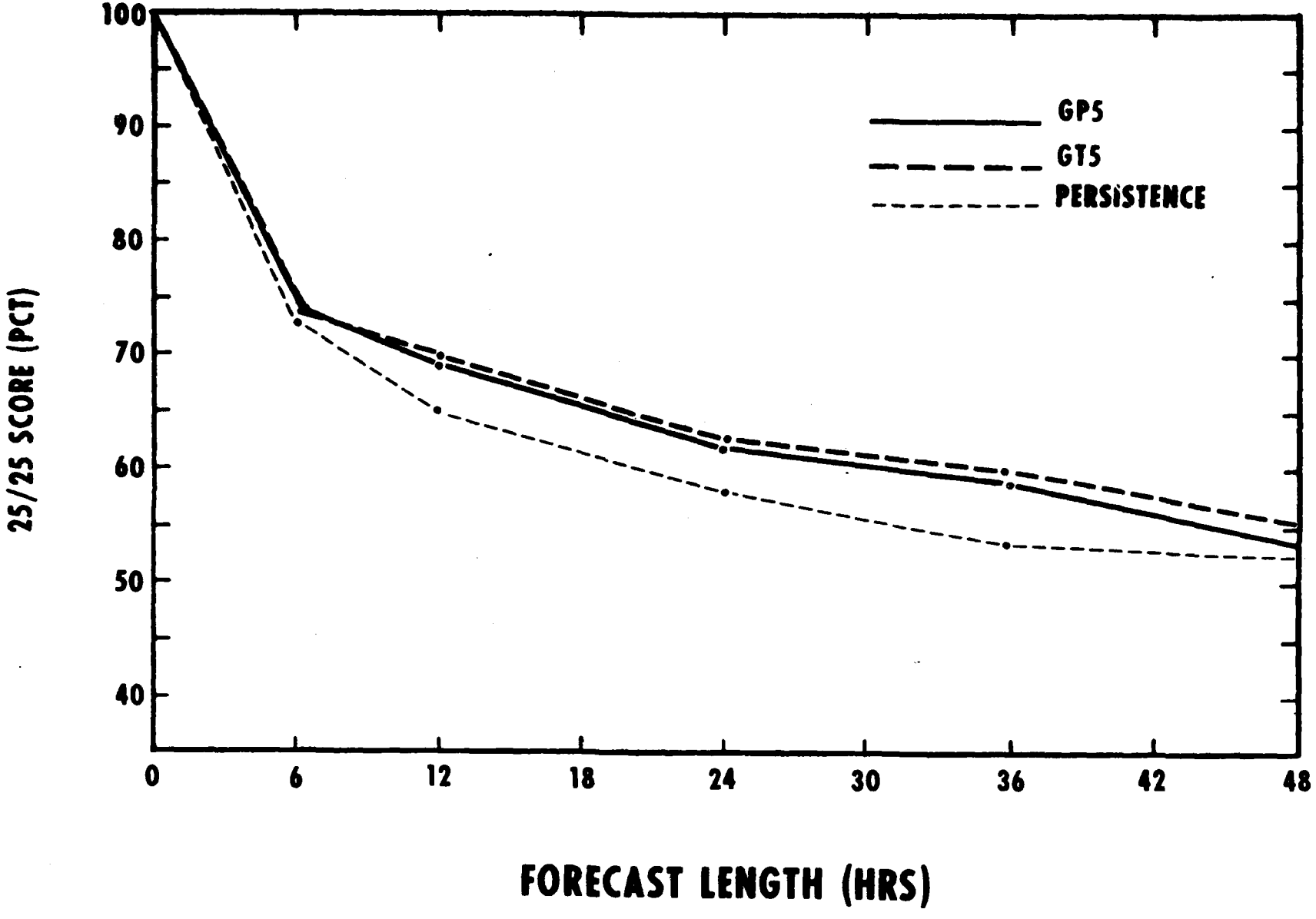

Figure 12. As in Figure 10 but for the fronthalf limited (FHL) area.

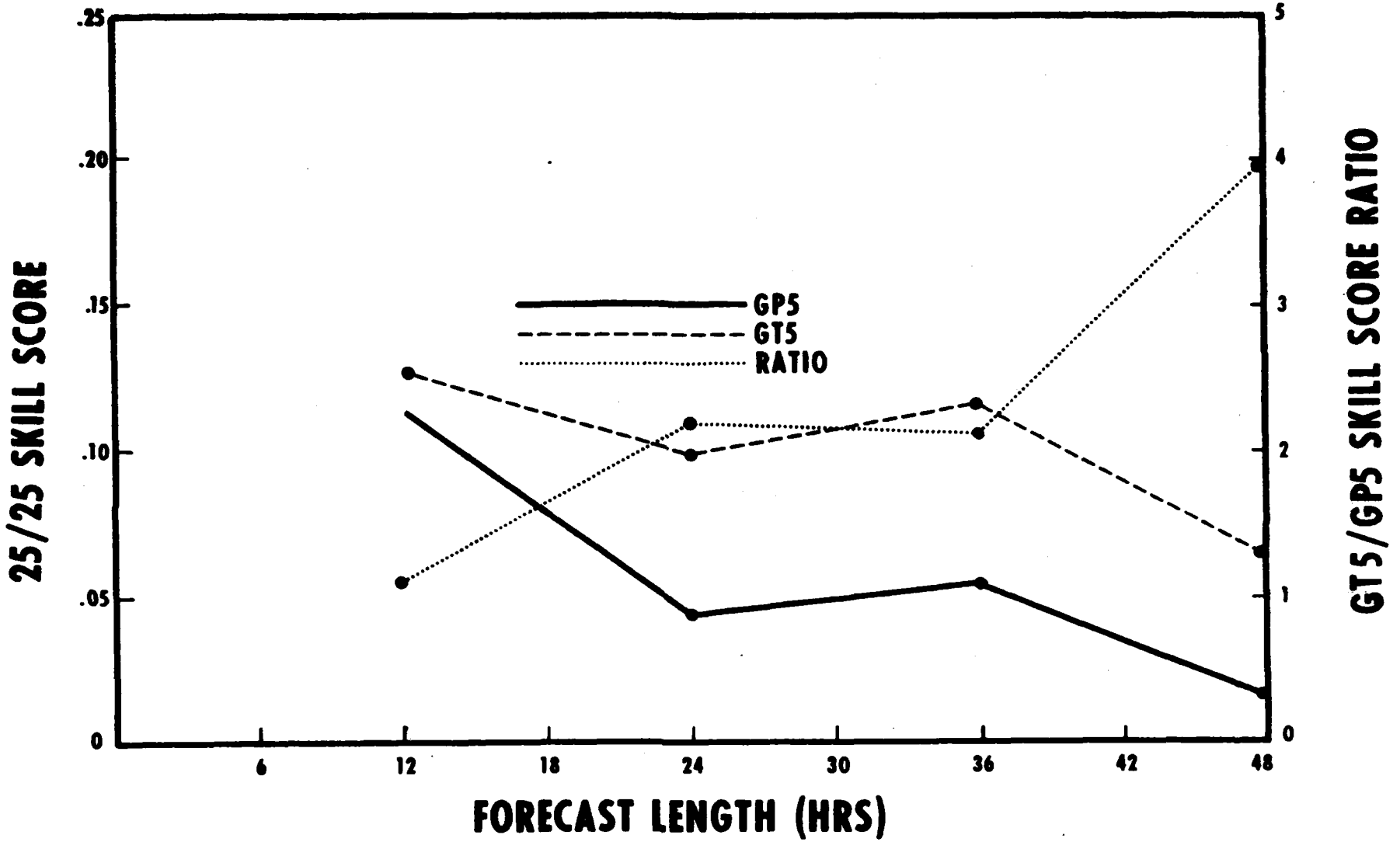

Figure 13. 25/25 skill score (using the data in Figure 7) as a function of forecast length for the AFGWC production 5LAYER (GP5) and the AFGWC test 5LAYER (GT5) Case A (Table 1) for the backhalf (BH) area, 14-day set. Also shown is the GT5 to GP5 skill-score ratio.

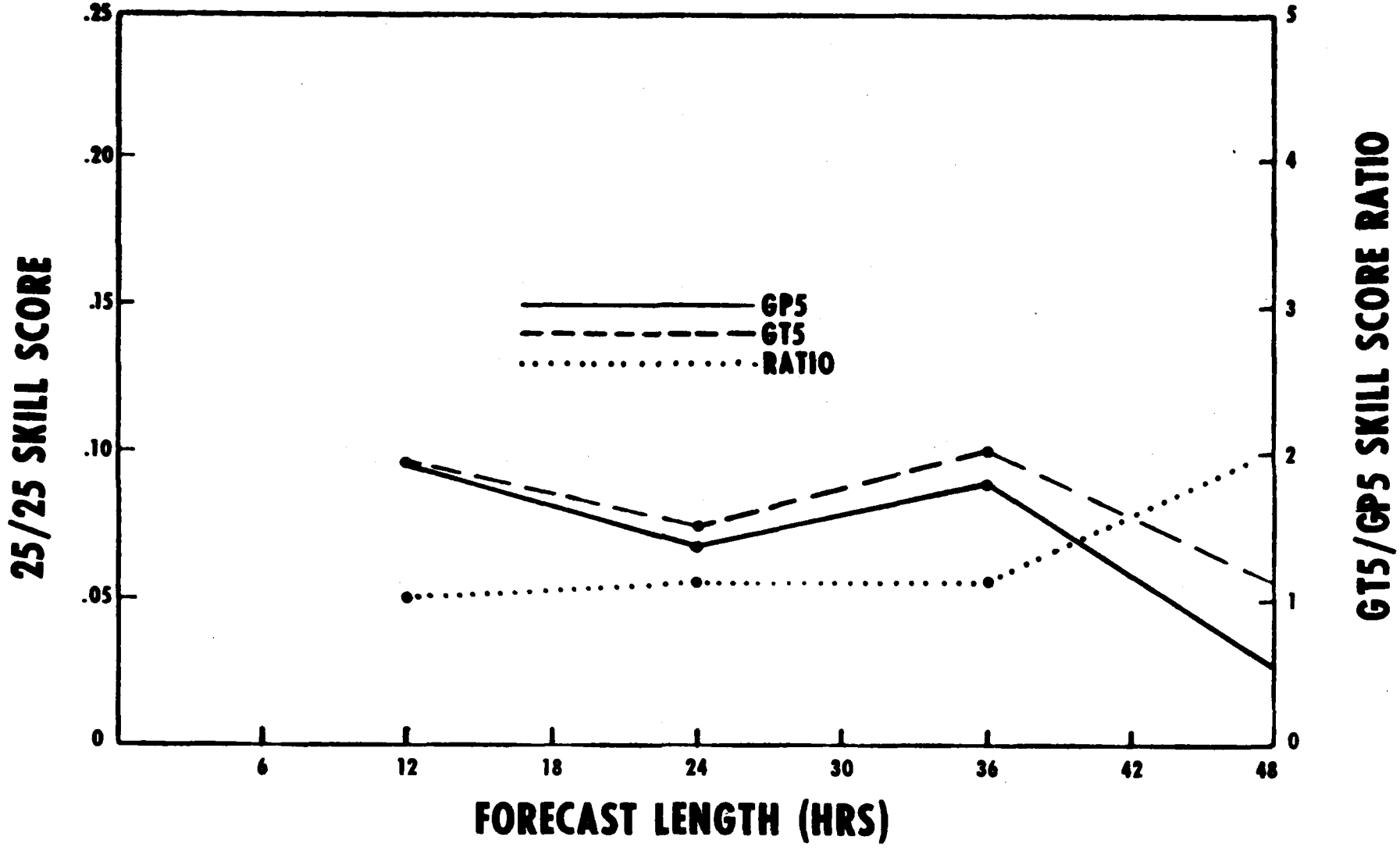

Figure 14. As in Figure 13 but for the fronthalf (FH) area using the data in Figure 10.

Table 2. Additional statistical information for Case A, the backhalf and fronthalf areas, contrasting persistence (PERS), AFGWC production (GP5), and test (GT5) 5LAYER cases.

CASE A (BACKHALF AREA)

FCST	RMSE			STDE			BIAS			LINEAR CORRELATION		
LENGTH	PERS	GP5	GT5	PERS	GP5	GT5	PERS	GP5	GT5	PERS	GP5	GT5
6	24.0	21.9	21.9	24.8	21.9	21.8	1.6	1.7	2.1	.755	.794	.797
12	30.1	26.7	26.4	30.1	26.7	26.4	.1	.0	2.1	.645	.702	.712
24	32.1	29.6	28.8	32.1	29.5	28.7	-.3	-1.7	1.6	.603	.651	.678
36	37.5	33.2	32.6	37.5	33.1	32.4	.0	-2.4	3.7	.450	.537	.575
48	37.8	35.4	35.0	37.8	35.3	34.7	.1	-3.2	4.3	.452	.503	.539

CASE A (FRONTHALF AREA)

FCST	RMSE			STDE			BIAS			LINEAR CORRELATION		
LENGTH	PERS	GP5	GT5	PERS	GP5	GT5	PERS	GP5	GT5	PERS	GP5	GT5
6	27.5	26.1	26.2	27.4	26.0	26.1	2.4	1.7	2.1	.684	.699	.700
12	32.6	29.4	29.5	32.5	29.4	29.4	2.2	1.0	2.5	.539	.603	.608
24	35.2	32.4	32.4	35.2	32.4	32.3	-1.0	-.8	2.3	.456	.539	.547
36	38.9	35.0	35.1	38.8	34.9	34.6	2.2	1.0	5.7	.343	.455	.474
48	39.8	38.0	37.6	39.8	38.0	37.2	.0	-.7	5.0	.303	.374	.404

Table 3. As in Table 2 but for the backhalf and fronthalf limited areas.

CASE A (BACKHALF LIMITED AREA)

FCST	RMSE			STDE			BIAS			LINEAR CORRELATION		
LENGTH	PERS	GP5	GT5	PERS	GP5	GT5	PERS	GP5	GT5	PERS	GP5	GT5
6	23.8	21.3	21.2	23.8	21.2	21.1	-1.3	.8	.9	.768	.802	.805
12	30.3	26.3	26.3	30.3	26.3	26.1	.0	.7	2.9	.620	.692	.704
24	33.9	30.4	29.7	33.9	30.4	29.6	-.2	-1.1	2.8	.536	.618	.651
36	38.3	33.0	32.7	38.3	33.0	32.4	-.5	-2.2	4.2	.393	.524	.564
48	39.2	36.2	35.9	39.2	36.1	35.6	.1	-3.1	4.6	.388	.471	.513

CASE A (FRONTHALF LIMITED AREA)

FCST	RMSE			STDE			BIAS			LINEAR CORRELATION		
LENGTH	PERS	GP5	GT5	PERS	GP5	GT5	PERS	GP5	GT5	PERS	GP5	GT5
6	27.9	26.3	26.3	27.8	26.2	26.2	2.0	1.4	1.9	.648	.670	.675
12	32.4	28.7	28.6	32.4	28.7	28.6	.1	-.3	1.5	.506	.593	.607
24	36.8	33.3	33.0	36.8	33.3	32.8	.3	-.3	3.4	.363	.481	.507
36	39.5	35.0	34.6	39.5	35.0	34.3	.9	-.7	4.6	.271	.423	.468
48	40.2	38.8	38.1	40.2	38.7	37.8	.6	-2.0	4.7	.232	.307	.361

While reduction in GT5 versus GP5 RMSE and STDE are fairly consistent in Tables 2 and 3 after 12 hours, the magnitude of the reductions is rather small. With the exception of the FH area, the remaining three areas in Tables 2 and 3 show an average reduction in GT5 versus GP5 STDE of about 0.7 percent for the 24-hour period and beyond. Relative to a typical 24- to 48-hour GP5 STDE value of around 34 percent, this 0.7 percent absolute average STDE reduction represents a percentage STDE improvement of about 2 percent. The average reduction in GT5 versus GP5 RMSE was somewhat less, being on the order of 0.5 percent for the BH, BHL, and FHL areas beyond 24 hours. This absolute RMSE reduction represents a percentage improvement of about 1.5 percent. Thus in this study, the 14 percent reduction in 7LHFM versus 6LDPE RMSVE values has generally translated into an order of magnitude smaller percentage reduction in GT5 versus GP5 RMSE values. Although the GT5 error reductions here are small, they appear statistically significant. Although no formal tests of statistical significance were performed on the error samples, we recall that a 0.7 percent STDE reduction is on the order of the 1-2 percent reduction that we anticipated in the estimates given in Section 3.1.1.

The RMSE, STDE, and bias statistics in Table 2 and 3 are analytically related according to

$$(5) \quad (\text{RMSE})^2 = (\text{STDE})^2 + (\text{bias})^2.$$

Equation (5) shows thatif the bias error is significant, then a significant portion of the total RMSE is attributable to bias errors. This fact is useful to numerical modelers, because it is often quite possible to find and remove the source of a systematic bias error in model forecasts and thereby reduce the total RMSE. On the other hand, it is usually much more difficult to discover the model source or sources contributing to the STDE.

In this context, we shall examine the GT5 bias errors in Table 2 and 3 in order to evaluate the possibility of further GT5 versus GP5 RMSE reductions. If the 7LHFM winds were routinely used in 5LAYER, it is likely that a substantial portion of the GT5 bias error in Tables 2 and 3 could be eliminated by appropriate model adjustments. In the current GP5 model, adjustments have been made which have reduced the bias error in most verified regions to less than 2.5 percent at 36 hours or less.

We see in Table 2 and 3 that the GT5 bias error at 36 hours is as high as 5.7 percent in the FH area and at 36 hours is never less than 3 percent in any area. To determine the cloudiness range in which most of the GT5 bias error is present, we show in Figures 15-16 and Figures 17-18 the 24- and 48-hour forecast cloud amount frequency of occurrence curves for the FH and BH regions respectively. In these figures, seven discrete cloud amount categories were utilized. To construct the figures, a given forecast or verifying cloud amount, which we recall may fall in the range 0-100 percent, is simply assigned to the closest of the seven discrete category values. The final number of occurrences in each category is divided by the entire sample total, T, and then multiplied by 100 to yield the percent frequency of occurrence.

In Figures 15-18, the dominant feature is the large positive GT5 bias in the "overcast" category of 95 percent. Clearly, this large overcast bias continues to grow as the forecast length increases, which largely accounts for the overall growth of the GT5 bias error in forecast time in Tables 2 and 3. This tendency in the GT5 forecasts to increase the extent of overcast cloud is an apparent response to the 7LHFM forecast vertical motion. Since the primary cloud generating mechanism in 5LAYER is upward displacements in the calculated three-dimensional parcel trajectories, the tendency toward increasing cloud in GT5 forecasts is most likely a response to more extensive and intense areas of upward motion in the 7LHFM versus the 6LDPE. This might be expected from the fact that the moist 7LHFM model, unlike the 6LDPE, includes latent heating effects. These tend to enhance the vertical motion mechanisms that depend on heating. We did not specifically compare 6LDPE and 7LHFM input vertical motion fields in this study and thus we could not further pursue this hypothesis.

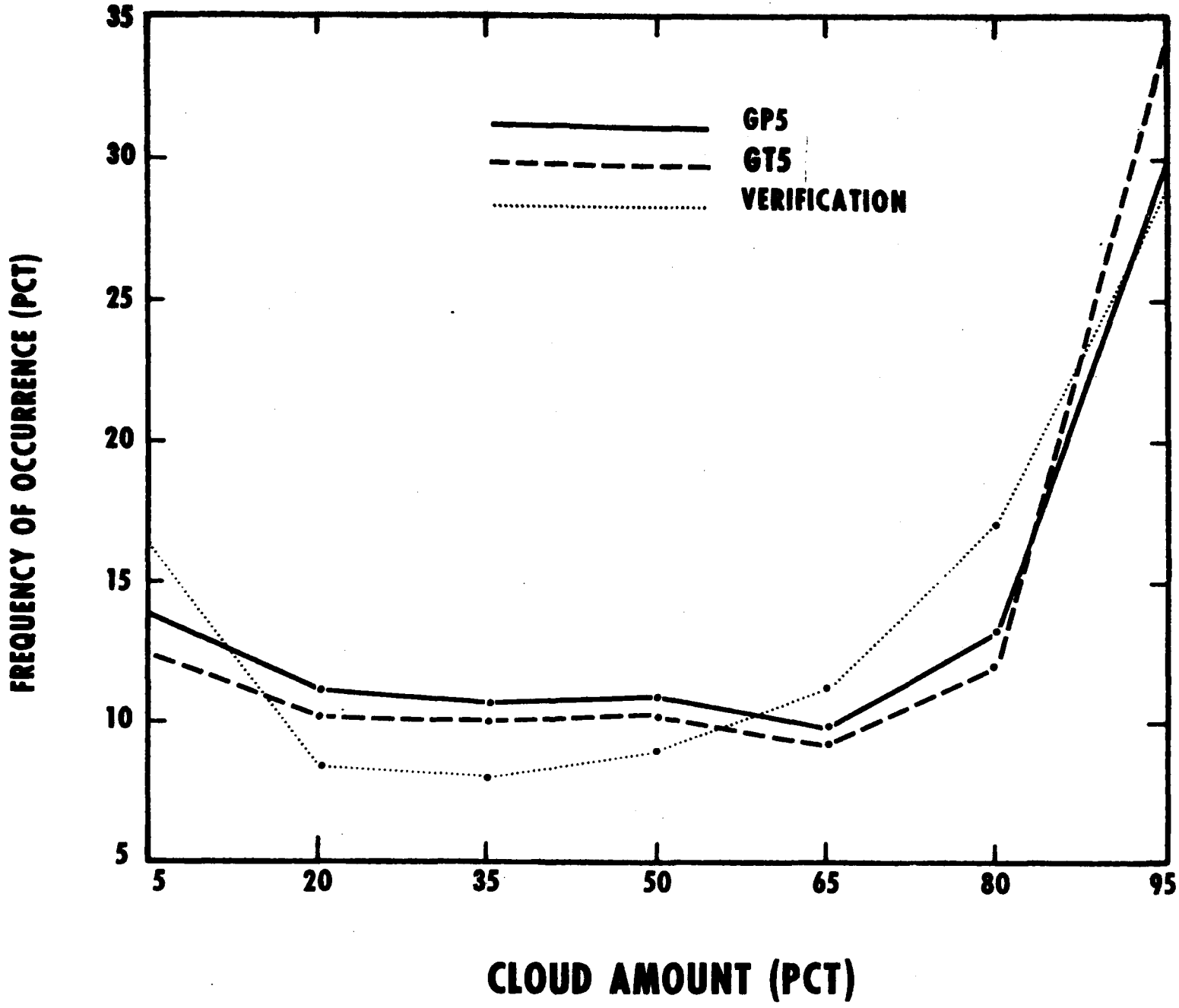

Figure 15. Total cloud frequency distribution for the AFGWC production 5LAYER (GP5) and the AFGWC test 5LAYER (GT5) 24-hour forecasts and verifying analysis in Case A (Table 1) for the fronthalf (FH) area, 14-day set.

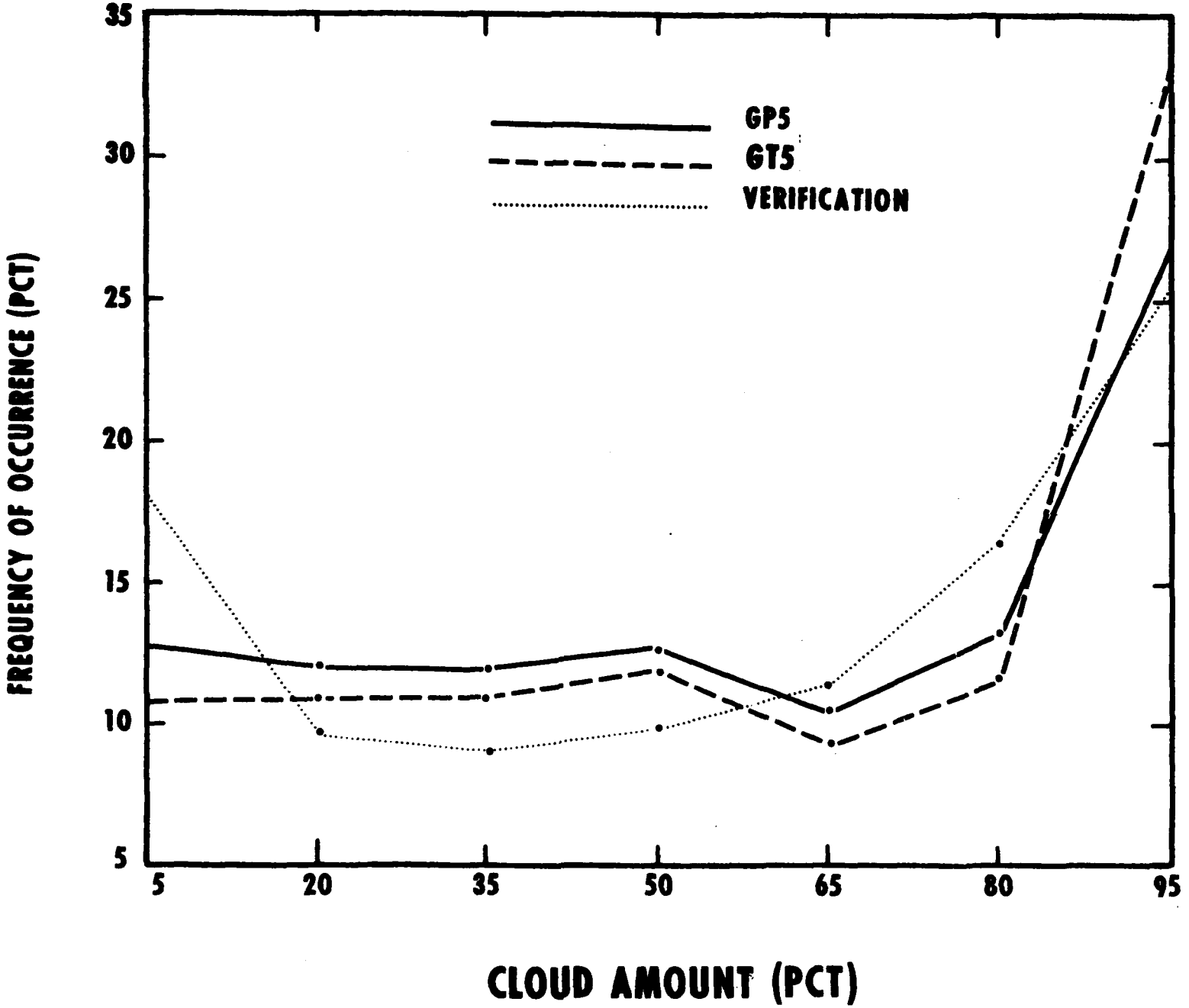

Figure 16. AS in Figure 15 but for 48 hours.

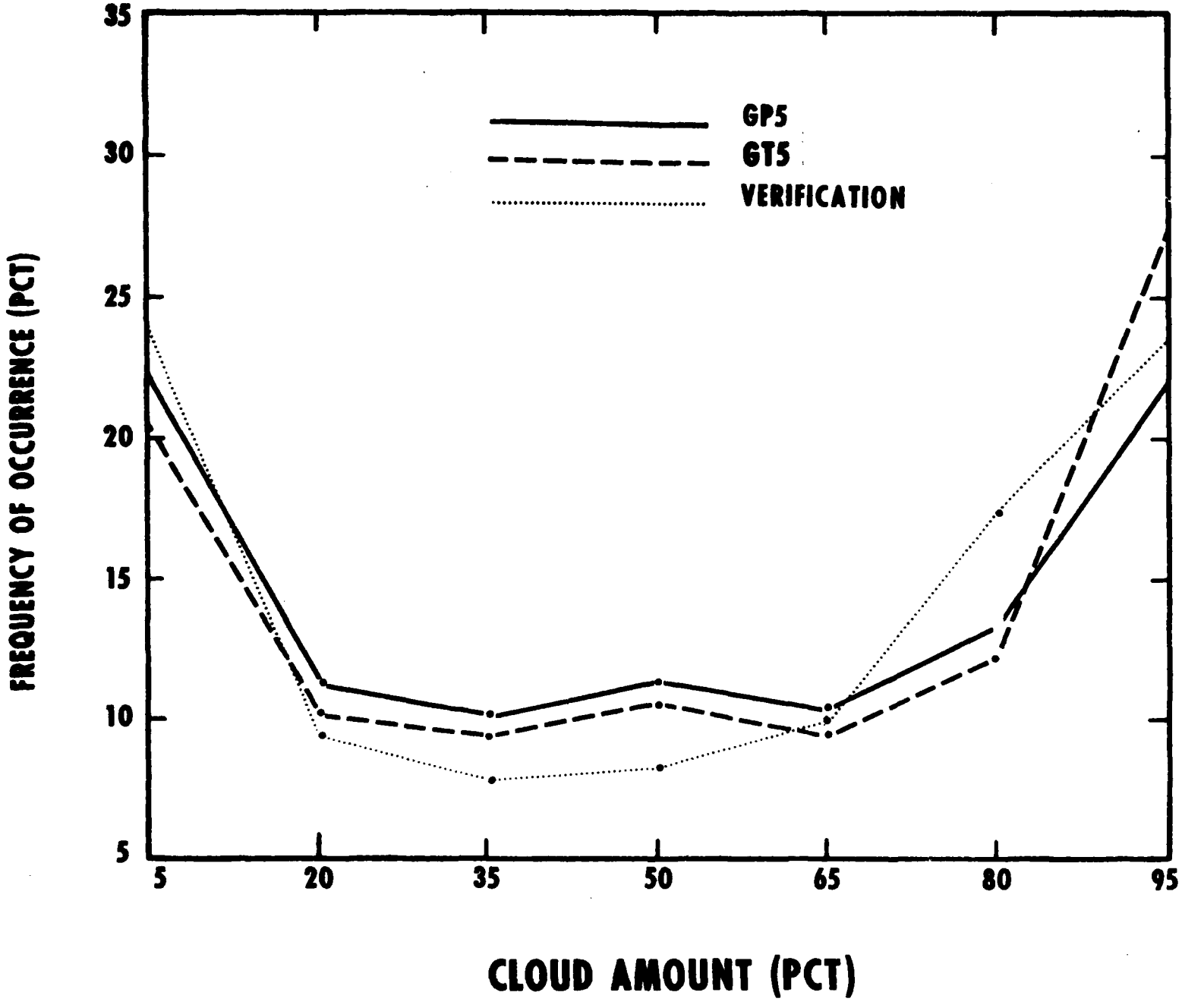

Figure 17. As in Figure 15 but for the backhalf (BH) area.

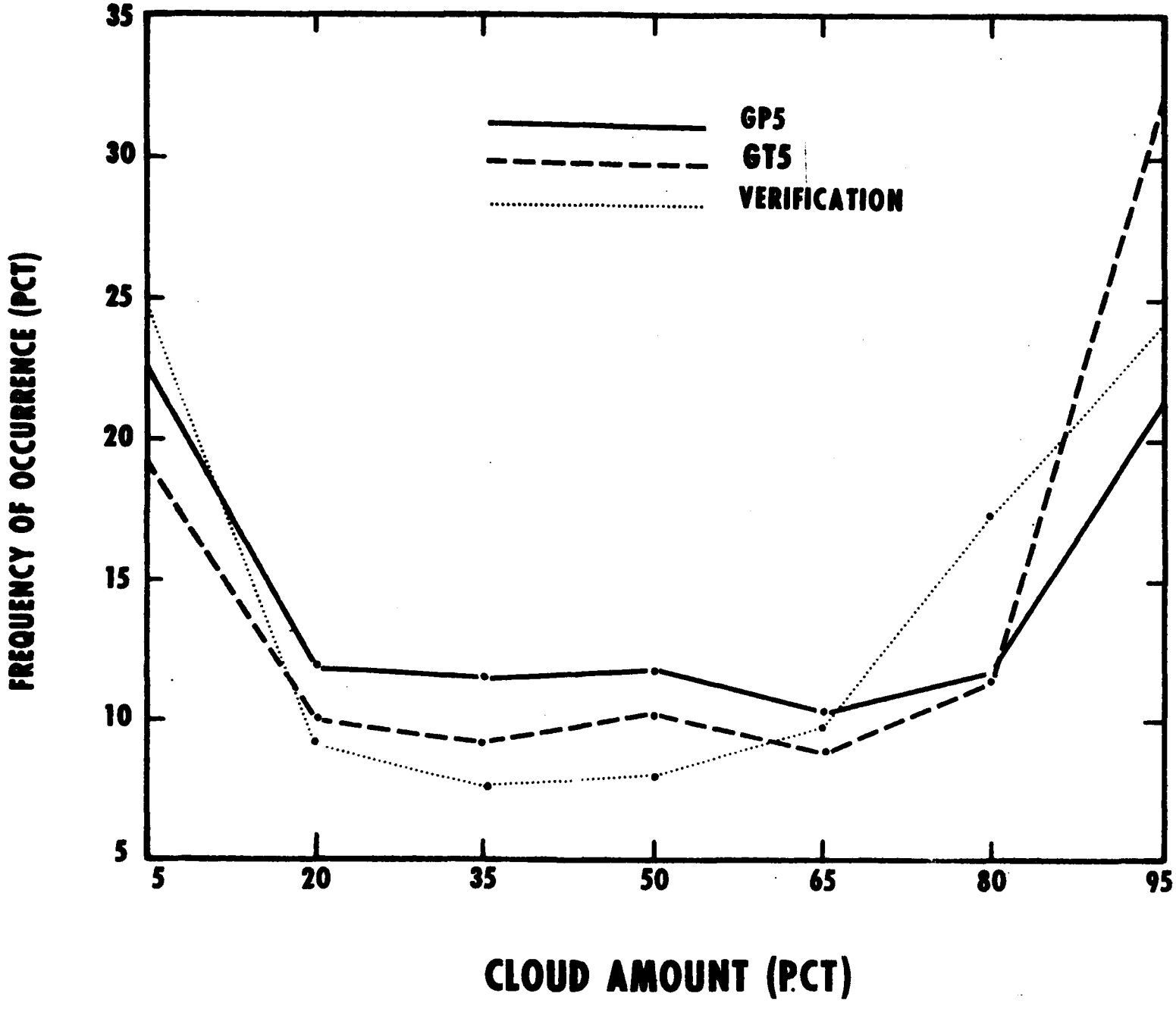

Figure 18. As in Figure 15 but for the backhalf (BH) area and for 48 hours.

3.1.3 Case B-C Results

In the Case A comparisons described in Section 3.1.2, we assumed that the 7LHFM and 6LDPE 00Z databases were available concurrently for input into the 03Z 5LAYER. In this section, we assume that the 0-hour basetime of the 7LHFM database is either 6 hours older (Case B comparisons) or 12 hours older (Case C comparisons) than the 0-hr basetime of the 6LDPE database that is used in the current production 5LAYER. The details of the various 7LHFM and 6LDPE databases used in 5LAYER for the Case B and C comparisons are given in Table 1. The motivation for the Case B and C comparisons was given toward the end of Section 3.1.1, in which we showed that the reduction in the RMSVE of the 7LHFM versus 6LDPE wind forecasts could be viewed as a 7LHFM 12-hour forecast extension relative to the 6LDPE. We want to determine here whether this 7LHFM versus 6LDPE 12-hour forecast extension will translate also into a GT5 versus GP5 12-hr forecast extension.

The 25/25 scores for the GP5, GT5, and persistence forecasts are given as a function of forecast length in Figures 19 and 20 for the FH and BH regions, respectively, for Case B in Table 1 and in Figures 21 and 22 for the FH and BH regions, respectively, for Case C in Table 1. In the following discussion, it is useful to compare Figures 19 and 21 (BH region) and Figures 20 and 22 (FH region) with Figure 7 (BH region, Case A) and Figure 10 (FH region, Case A).

Figure 19 and Figure 20 show that the superior accuracy of GT5 versus GP5 forecasts found in Case A continues also in Case B, although as expected, the extent of the superiority is reduced. Whereas in Case A the GT5 versus GP5 absolute 25/25 score improvement was about 3 percent and 1.5 percent in the BH and FH regions, respectively, for forecasts beyond 9 hours, the corresponding Case B improvement in Figures 19 and 20 averages only about 0.5 percent and 0.3 percent in the BH and FH regions, respectively. The superiority of GT5 versus GP5 forecasts in Case B is supported also by the statistics compared in Table 4. Aside from the poorer GT5 bias values, the GT5 RMSE, STDE, and linear correlation statistics are superior, albeit sometimes only slightly, than the corresponding GP5 statistics (with the single exception of the BH region 36-hour RMSE values). Comparing Table 4 with Table 2, we find in the BH region that the GT5 versus GP5 average STDE reduction of 0.1 percent over the 12- to 36-hour forecast range in Case A has actually increased to 0.4 percent in Case B. We can present no obvious reason for the latter unexpected increase. However, the important overall result here is that in Case B, GT5 total cloud forecasts are consistently more accurate than GP5 forecasts, despite GT5 7LHFM input being 6 hours older than GP5 6LDPE input.

As might be expected, the results are less straightforward in Case C. Figure 21 shows that the GT5 and GP5 25/25 scores over the BH region are essentially equivalent for all forecast periods shown. Table 5 shows that the GT5 RMSE and STDE values over the BH region are less than the GP5 values only for forecast periods less than about 24 hours. On the other hand, the GP5 and GT5 linear correlation values over the BH region, like the 25/25 scores, are essentially equivalent for all the forecast periods. The Case C results for the FH region more clearly favor the GT5 forecasts. Figure 22 and Table 5 show that the 25/25 score, RMSE, STDE and linear correlation values for the GT5 forecasts are essentially equivalent or slightly superior to the corresponding GP5 values for all forecast periods in the FH region. Overall then, we can generally conclude in Case C that GT5 total cloud forecast accuracy is essentially equivalent to GP5 total cloud forecast accuracy, with some slight degradation at 36 hours and (we anticipate) also at 48 hours. Equivalently, we may state that the 7LHFM versus 6LDPE 12-hour forecast extension roughly translates into a GT5 versus GP5 12-hour forecast extension.

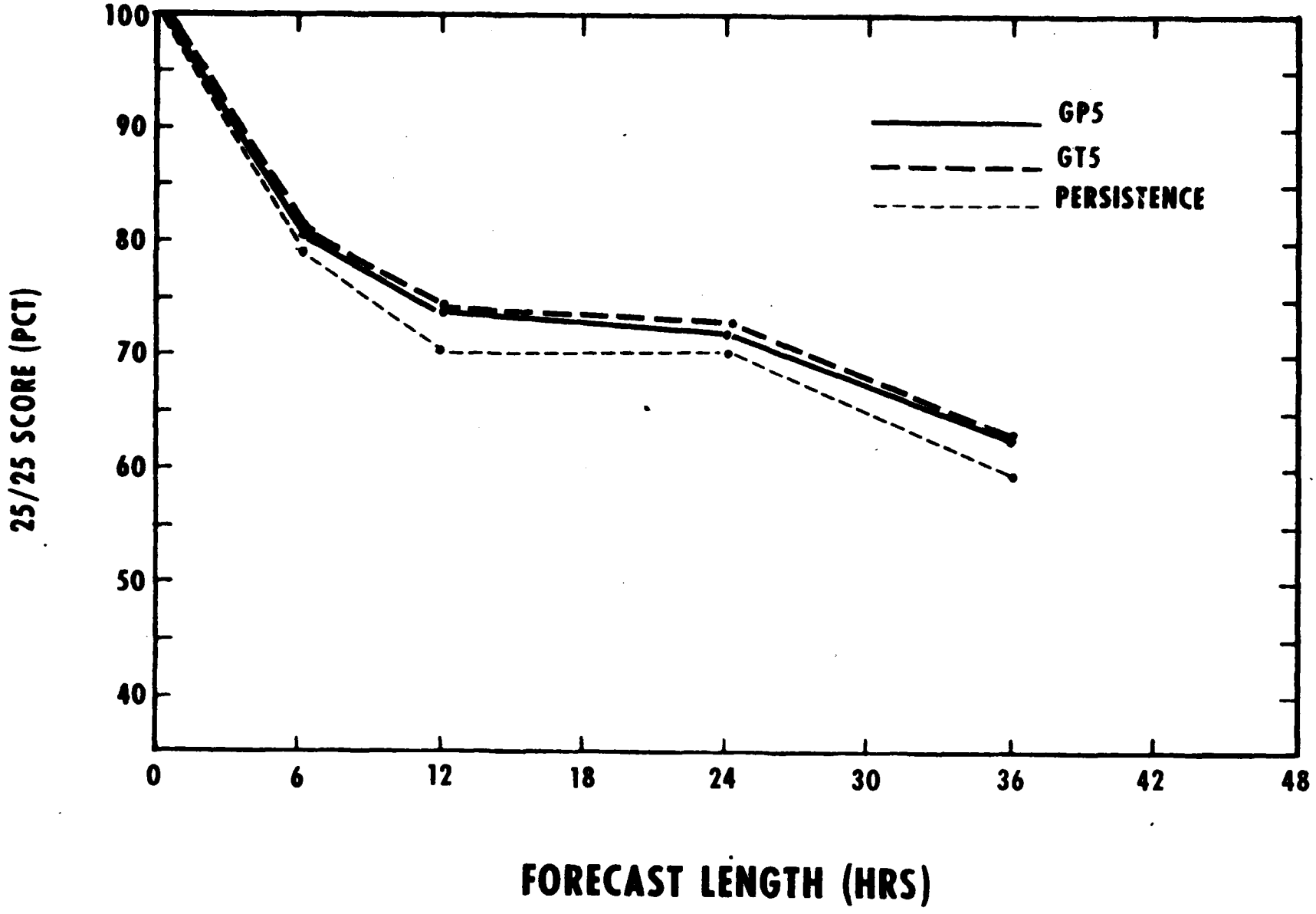

Figure 19. 25/25 score as a function of forecast length for the AFGWC production 5LAYER (GP5), the AFGWC test 5LAYER (GT5), and persistence in Case B (Table 1) for the backhalf (BH) area, 14-day set.

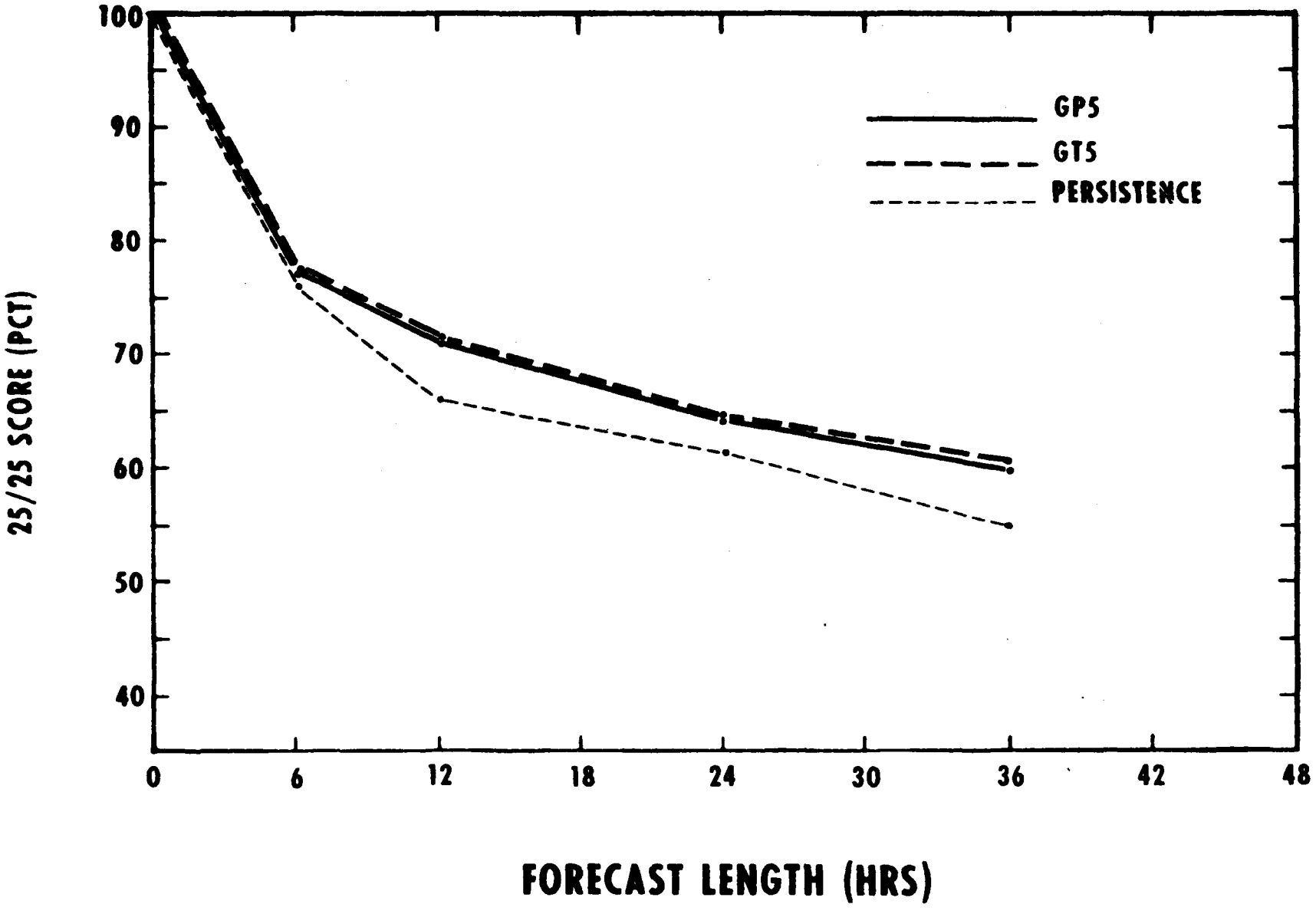

Figure 20. As in Figure 19 but for the fronthalf (FH) area.

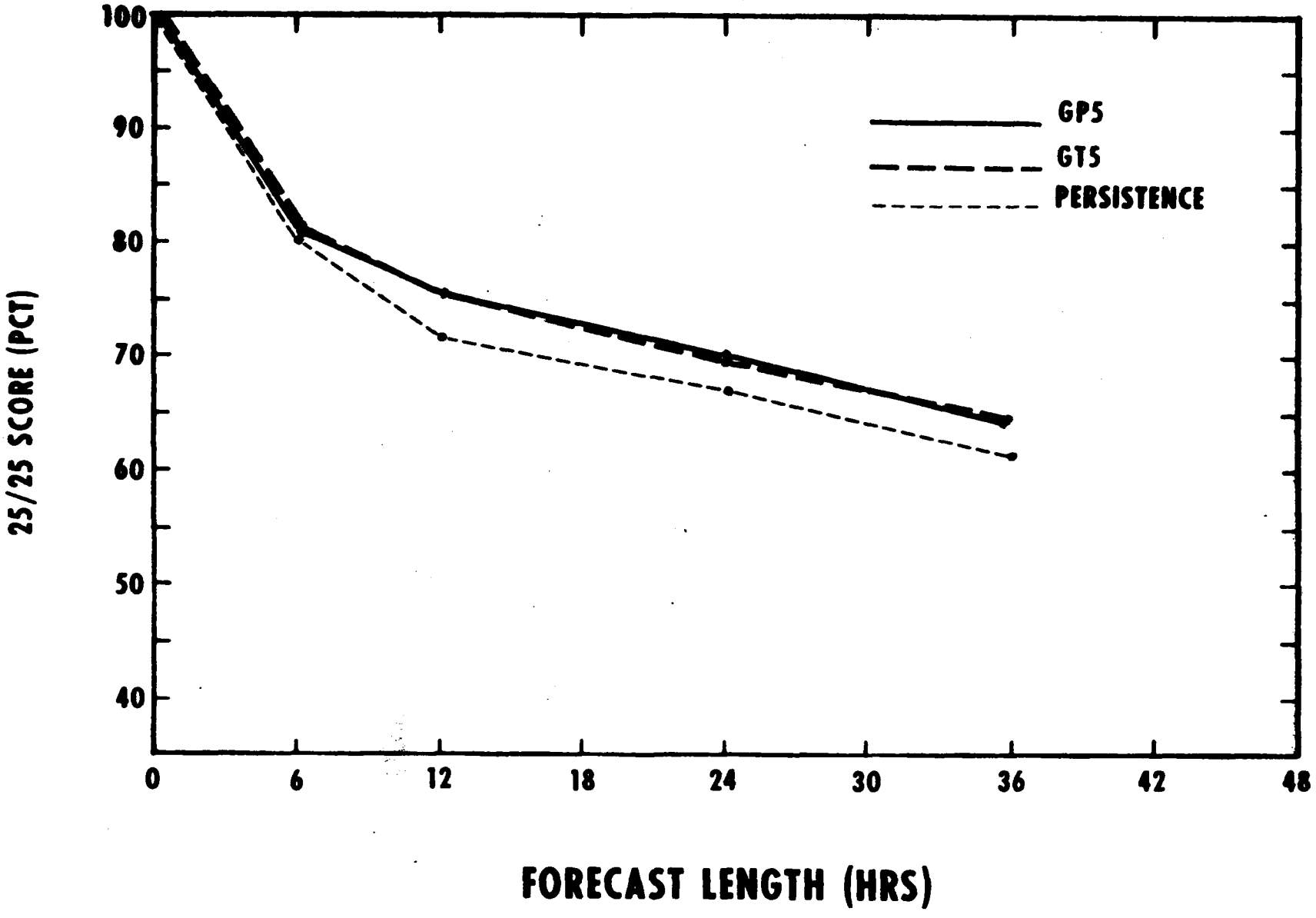

Figure 21. As in Figure 19 but for Case C (Table 1).

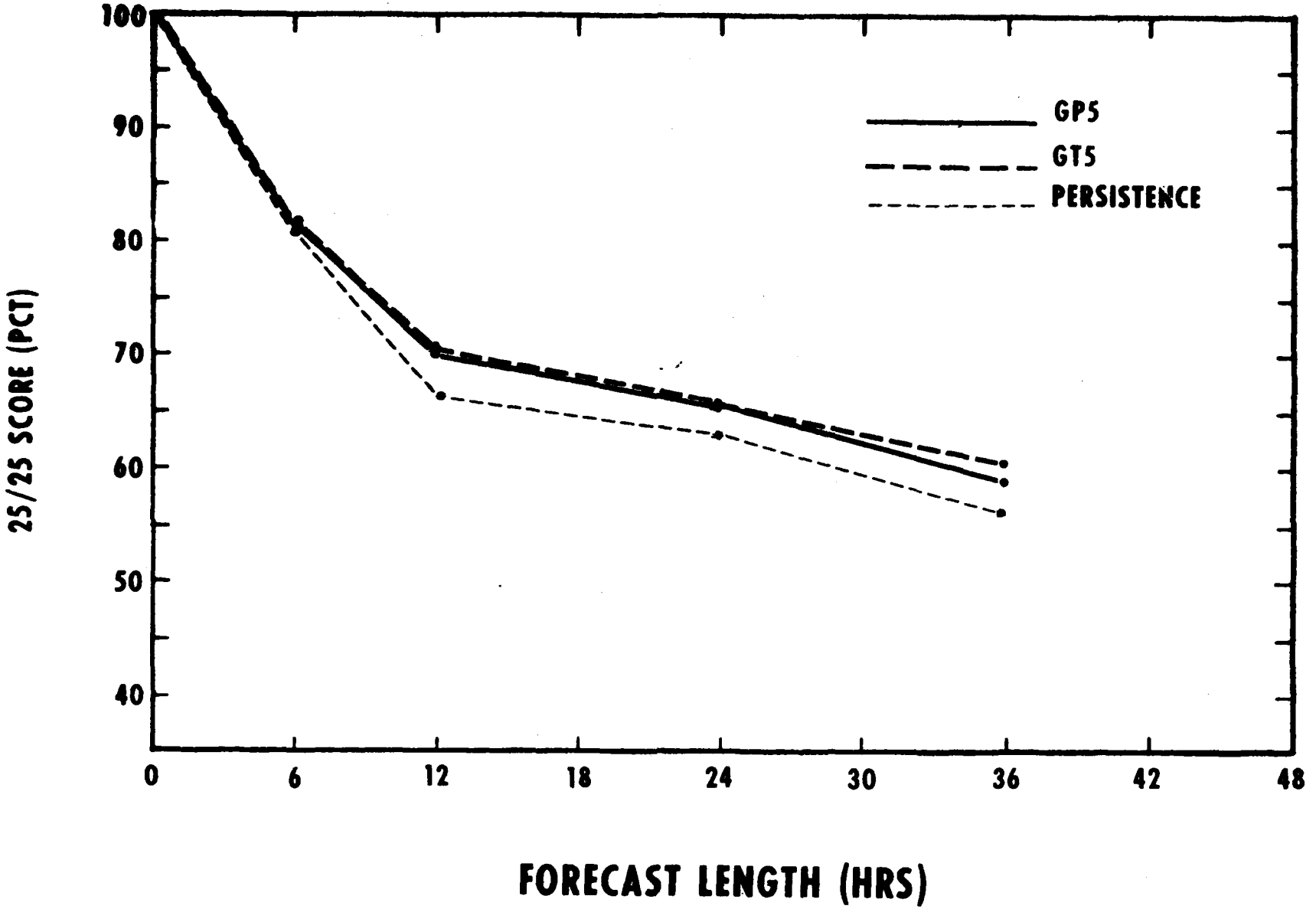

Figure 22. As in Figure 19 but for Case C (Table 1) and the fronthalf (FH) area.

Table 4. Additional statistical information for Case B, the backhalf and fronthalf areas, contrasting persistence (PERS), AFGWC production (GP5), and test (GT5) 5LAYER cases.

CASE B (BACKHALF AREA)

FCST		RMSE			STDE			BIAS		LINEAR CORRELATION		
LENGTH	PERS	GP5	GT5	PERS	GP5	GT5	PERS	GP5	GT5	PERS	GP5	GT5
6	24.6	22.5	22.4	24.6	22.5	22.4	-1.5	-.2	1.3	.754	.784	.785
12	30.1	26.4	26.4	30.0	26.4	26.2	2.1	1.0	3.4	.652	.720	.726
24	30.0	27.9	27.4	30.0	27.9	27.3	.0	-1.3	3.0	.628	.670	.696
36	37.4	33.6	34.0	37.3	33.5	33.4	2.1	-1.1	6.2	.462	.547	.569

CASE B (FRONTHALF AREA)

FCST		RMSE			STDE			BIAS		LINEAR CORRELATION		
LENGTH	PERS	GP5	GT5	PERS	GP5	GT5	PERS	GP5	GT5	PERS	GP5	GT5
6	27.3	25.1	24.9	27.3	25.1	24.9	-.2	.3	1.0	.690	.713	.718
12	32.5	28.5	28.2	32.5	28.5	28.2	-.4	-.2	1.0	.547	.614	.626
24	36.6	33.6	33.4	36.6	33.6	33.2	-.3	.3	3.3	.460	.534	.548
36	39.8	35.2	35.2	39.8	35.2	34.7	.7	.8	5.5	.325	.430	.457

Table 5. As in Table 4 but for Case C.

CASE C (BACKHALF AREA)

FCST		RMSE			STDE			BIAS		LINEAR CORRELATION		
LENGTH	PERS	GP5	GT5	PERS	GP5	GT5	PERS	GP5	GT5	PERS	GP5	GT5
6	23.9	22.4	22.4	23.7	22.2	22.2	3.7	3.1	3.2	.786	.803	.805
12	29.2	25.9	25.8	29.2	25.9	25.8	-.1	.1	.4	.663	.721	.727
24	32.7	29.3	29.8	32.7	29.3	29.7	-.1	.4	2.6	.573	.649	.648
36	36.4	32.2	33.2	36.4	32.2	33.0	.0	-.6	3.7	.480	.574	.570

CASE C (FRONTHALF AREA)

FCST		RMSE			STDE			BIAS		LINEAR CORRELATION		
LENGTH	PERS	GP5	GT5	PERS	GP5	GT5	PERS	GP5	GT5	PERS	GP5	GT5
6	24.0	22.9	22.8	24.0	22.9	22.8	-.5	-.6	.1	.743	.746	.749
12	32.7	29.0	28.8	32.5	28.9	28.8	-3.1	-2.4	-.4	.540	.614	.620
24	34.5	32.2	32.1	34.5	32.2	32.0	.0	-.3	3.0	.487	.549	.564
36	38.9	35.8	35.5	38.9	35.8	35.4	-2.2	-2.2	3.0	.344	.423	.449

3.2 Forecast Comparisons for Objective (b) (Cases D-F)

3.2.1 Preliminary Considerations

As pointed out in Section 2.3.3, Cases D-F in Table 1 represent a comparison of the total cloud forecast capability of two separate, independent analysis/forecast systems; namely, the AFGWC system (Tarbell and Hoke, 1979) and the NMC system (McPherson, 1980). We shall summarize here several crucial differences between the NMC and AFGWC systems in regard to moisture and cloud forecasts.

The NMC system does not include an analog to AFGWC's 3DNEPH/5LAYER cloud analysis/forecast subsystem. Rather, during the period of this test, NMC moisture field forecasts (RH, QPF, etc.) were obtained directly from the NMC 7-layer moist PE model. The main differences between NMC's 7LHFM PE forecast model and AFGWC's 6LDPE forecast model were given in Section 1. There are also important differences between the two systems in the data sources used to derive the initial moisture fields. At NMC, global upper-air mosture analyses are derived almost solely from conventional RAOB data. The one significant exception to this is in the North American region comprising the domain of NMC's LFM II regional model. In the land areas of the LFM II region, the NMC analysis system empirically converts surface-based cloud reports into relative humidity profiles. In ocean areas of the LFM II region, the NMC analysis system incorporates relative humidity profiles derived by manual, empirical methods that use visible and infrared satellite cloud imagery (Smigielski et. al, 1978). The crucial point here is that conventional cloud reports or satellite cloud imagery is used in the NMC moisture analysis only in one limited Northern Hemisphere area. Equally significant here is the fact that the Northern Hemisphere 7LHFM initial moisture fields south of about 20^{o}N were initialized with artificial, arbitrarily dry, relative humidity values apparently to minimize boundary problems.

In contrast to the moisture analysis procedures at NMC, the initial 5LAYER moisture fields in both hemispheres are derived at AFGWC almost solely on the basis of the global, objective, gridded cloud amounts provided by the 3DNEPH cloud analysis. The analyses produced by the 3DNEPH package rely primarily on visible and infrared satellite cloud imagery and conventional, surface-based cloud reports and only secondarily on upper-air RAOB moisture data. Briefly, the 5LAYER initial CPS moisture field is derived by compacting the high resolution (eight-mesh) 3DNEPH cloud analysis to the coarse (half-mesh) resolution of 5LAYER and then converting the compacted non-zero cloud amounts to CPS using the empirical curves of Figure 1. At those relatively few, strictly cloud-free grid points of the 3DNEPH, a different procedure is used to yield CPS values that instead reflect conventional upper-air RAOB moisture values (Friend and Mitchell, 1982). Overall then, the 5LAYER initial CPS moisture fields directly reflect the global cloud cover distribution. Owing to this difference in the extent to which NMC and AFGWC use conventional cloud reports and satellite cloud imagery in their initial moisture analyses, the cloud forecast comparisons in Case D will serve to define the value of initial cloud data as well as the value of using an advanced prediction model.

3.2.2 Case D Results

The 25/25 scores for the GP5, NP7, and persistence forecasts labeled Case D in Table 1 are given as a function of forecast length in Figures 23, 24, and 25 for the BH region (14-day set), BH region (first 7-day set), and BHL region (14-day set) respectively. The correspnding Case D results for the FH and FHL regions are given in Figures 26, 27, and 28. The NP7 and persistence data is plotted at 6 hourly intervals because of its availability, versus Case A, Figures 7-12 which have only 12 hourly forecast data available after the initial period.

Figures 23-28 show that the GP5 25/25 scores are substantially higher than the NP7 25/25 scores for forecast periods less than 24 hours. This result is a consequence of the large initial difference between the 0-hour GP5 and NP7 total cloud fields. This latter difference can be viewed as showing that the initial 0-hour NP7 moisture analysis (after conversion to CPS and then to total cloud by the methods of Section 2.2.1) does not reliably reflect the hemispheric cloud cover as analyzed by the compacted 3DNEPH cloud analysis (which provides the 0-hr GP5 initial total cloud). As is apparent in Figures 25 and 28, this initial difference is still large, though significantly reduced, when we verify only over the FHL and BHL areas, in which we have eliminated the arbitrarily dry subtropical areas of the 7LHFM initial moisture fields. We note in the BHL and FHL results of Figures 25 and 28 that the 0-hour disparity between GP5 and NP7 initial cloud fields is larger in the FHL region than in the BHL region, despite the use by NMC of satellite cloud imagery and surface-based cloud reports to augment the 0-hour 7LHFM initial moisture fields in the FHL area.

We observe in Figures 23 through 28 that for forecast periods of 24 hours and beyond, the GP5 and NP7 25/25 scores quickly converge, owing to the more rapid drop-off with time of the GP5 curve versus the NP7 curve. Hence, for forecast periods beyond approximately 24-30 hours, the NP7 forecasts become competitive with the GP5 forecasts. In particular, in the BHL region of Figure 25, the NP7 25/25 score actually surpasses that of the GP5 forecasts for forecast lengths of 24- to 48-hours. The superiority of NP7 forecasts over GP5 forecasts in Figure 25 is substantial for forecast lengths of 30-48 hours, where on the average we observe a doubling of the spread between model and persistence forecast curves. Equivalently, we may conclude that the skill score of NP7 forecasts is on the order of twice that of GP5 forecasts beyond 30 hours in Figure 25. The NP7 forecasts are less competitive in the FHL region in Figure 28, in which the NP7 25/25 score never exceeds that of the GP5 forecasts.

Figures 23 through 28 provide an excellent example of the importance of satellite and conventional cloud observations to short-range cloud forecasting. Despite the use of an advanced moist prediction model, the skill of the short-range cloud forecasts (0-24 hours) depends heavily on establishing a close link between an initial cloud analysis and the corresponding forecast model initial moisture analysis. After 24 hours however, we find in Figures 23-28 that the apparently superior dynamics of the 7LHFM model largely overcome the disadvantage of the inferior 7LHFM initial moisture analysis (inferior in a specific sense only, that is, in its reflection of the initial cloud cover as depicted by the compacted 3DNEPH cloud analysis).

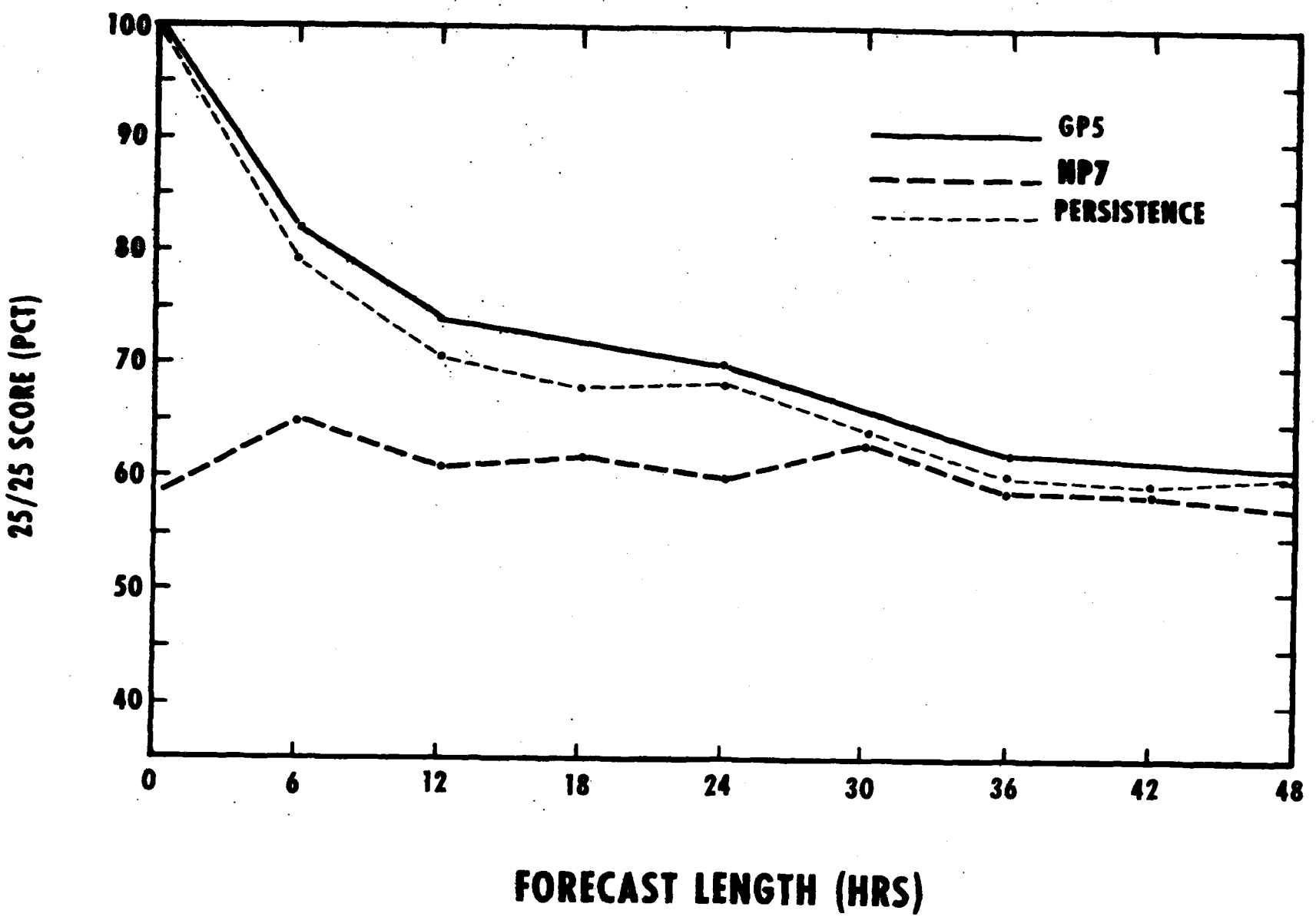

Figure 23. 25/25 score as a function of forecast length for the AFGWC production 5LAYER (GP5), the NMC production 7LHFM (NP7), and persistence in Case D (Table 1) for the backhalf (BH) area, 14-day set.

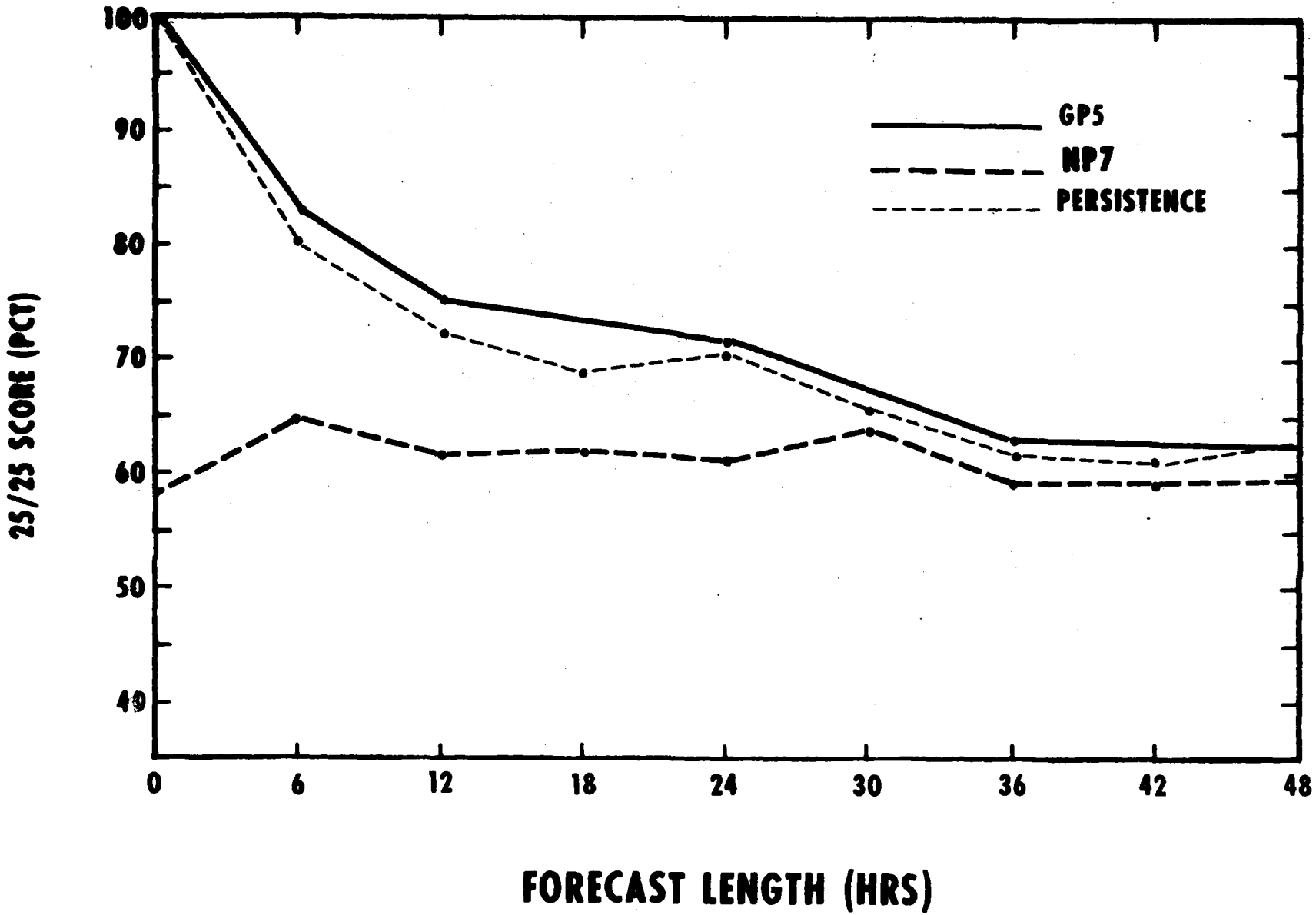

Figure 24. As in Figure 23 but for the first 7-day set.

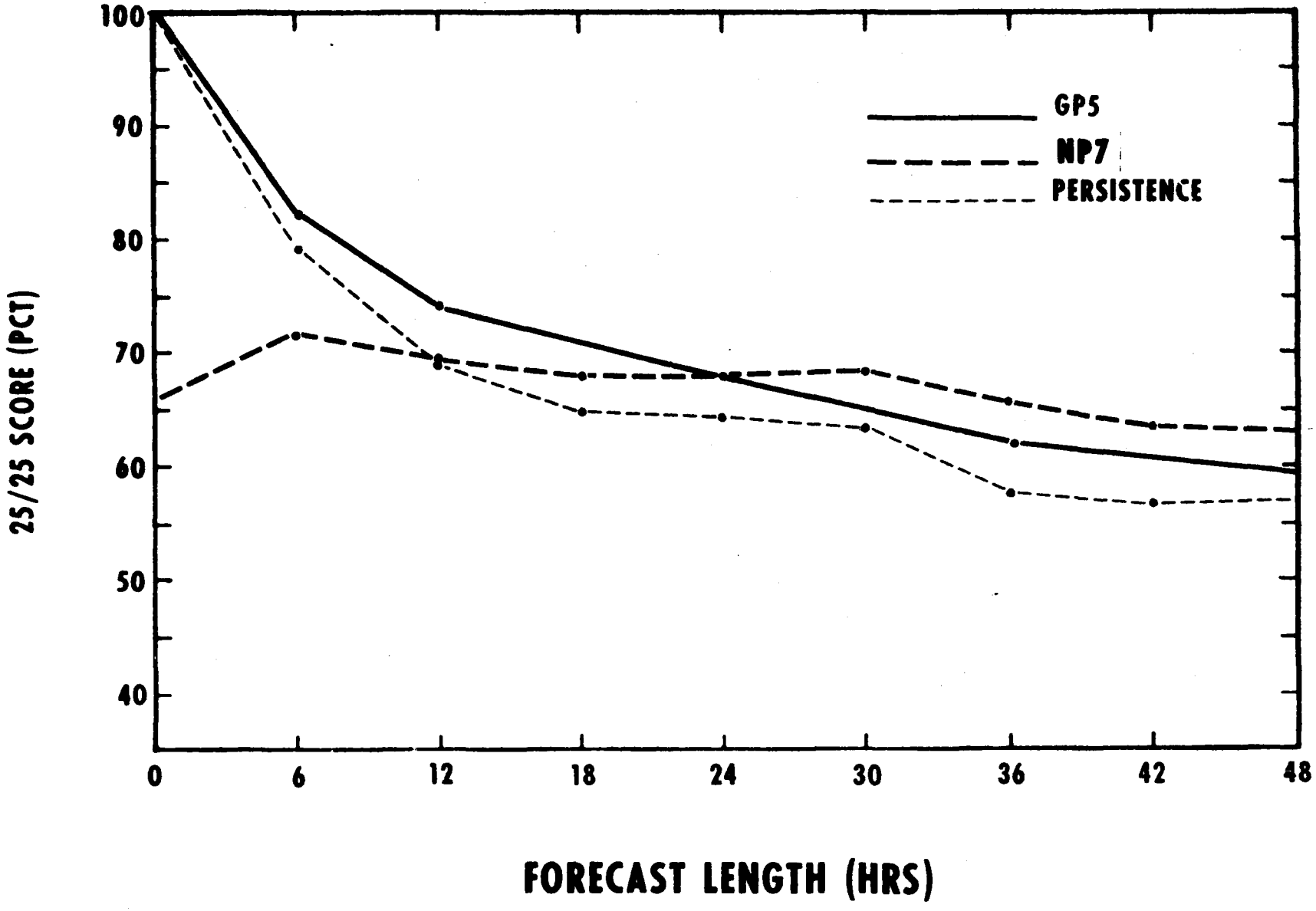

Figure 25. AS in Figure 23 but for the backhalf limited (BHL) area.

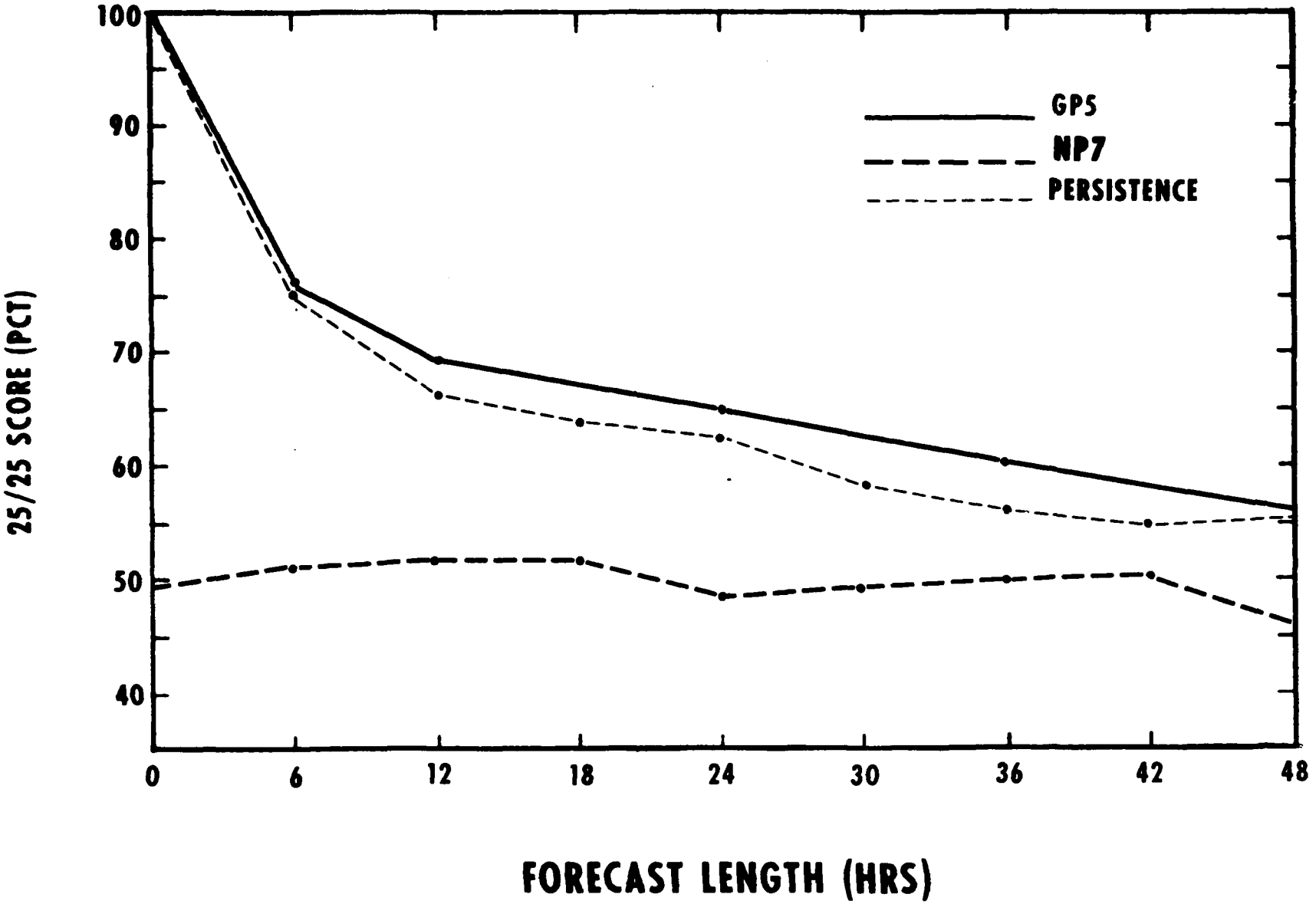

Figure 26. 25/25 score as a function of forecast length for the AFGWC production 5LAYER (GP5), the NMC production 7LHFM (NP7), and persistence in Case D (Table 1) for the fronthalf (FH) area, 14-day set.

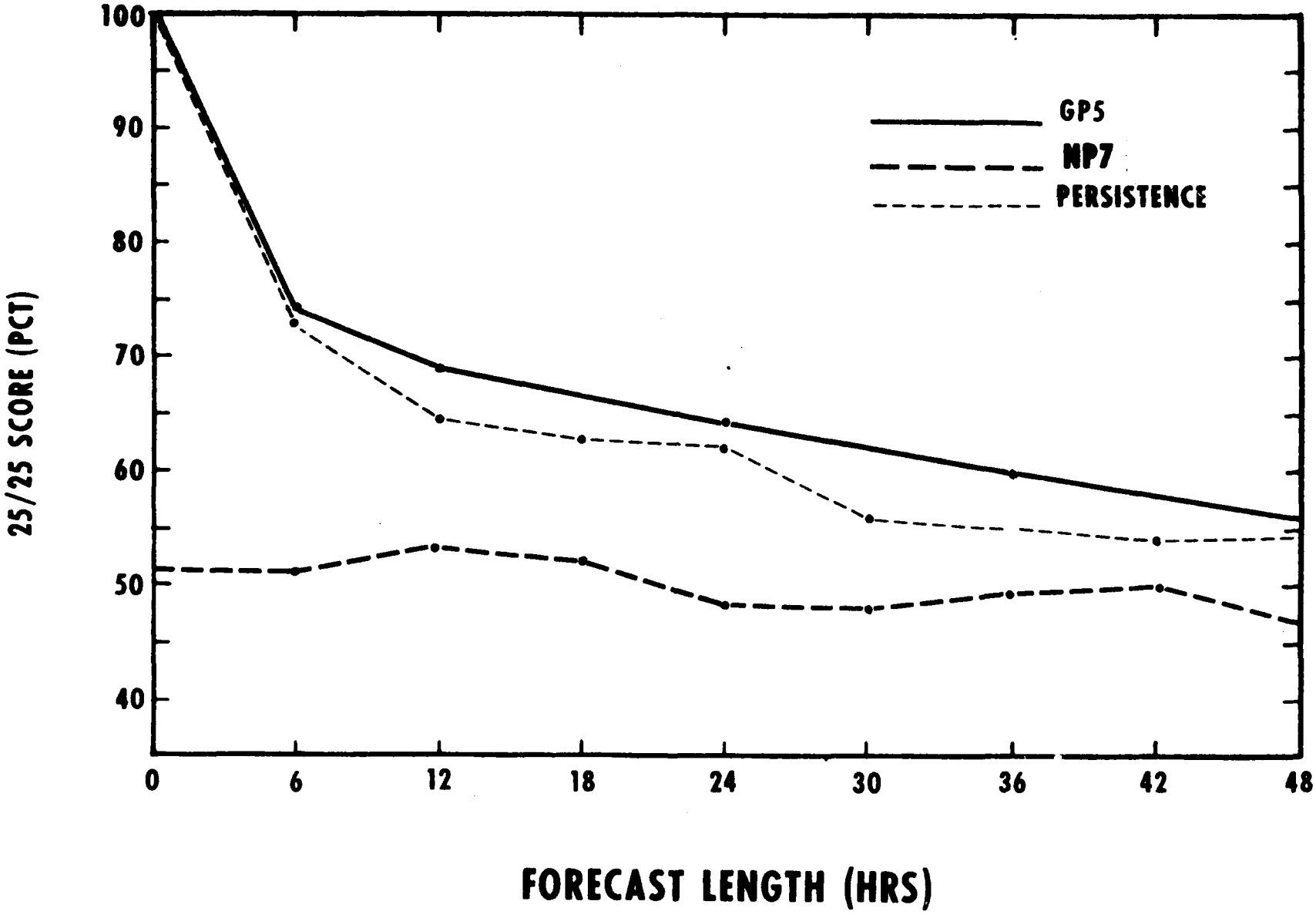

Figure 27. AS in Figure 26 but for the first 7-day set.

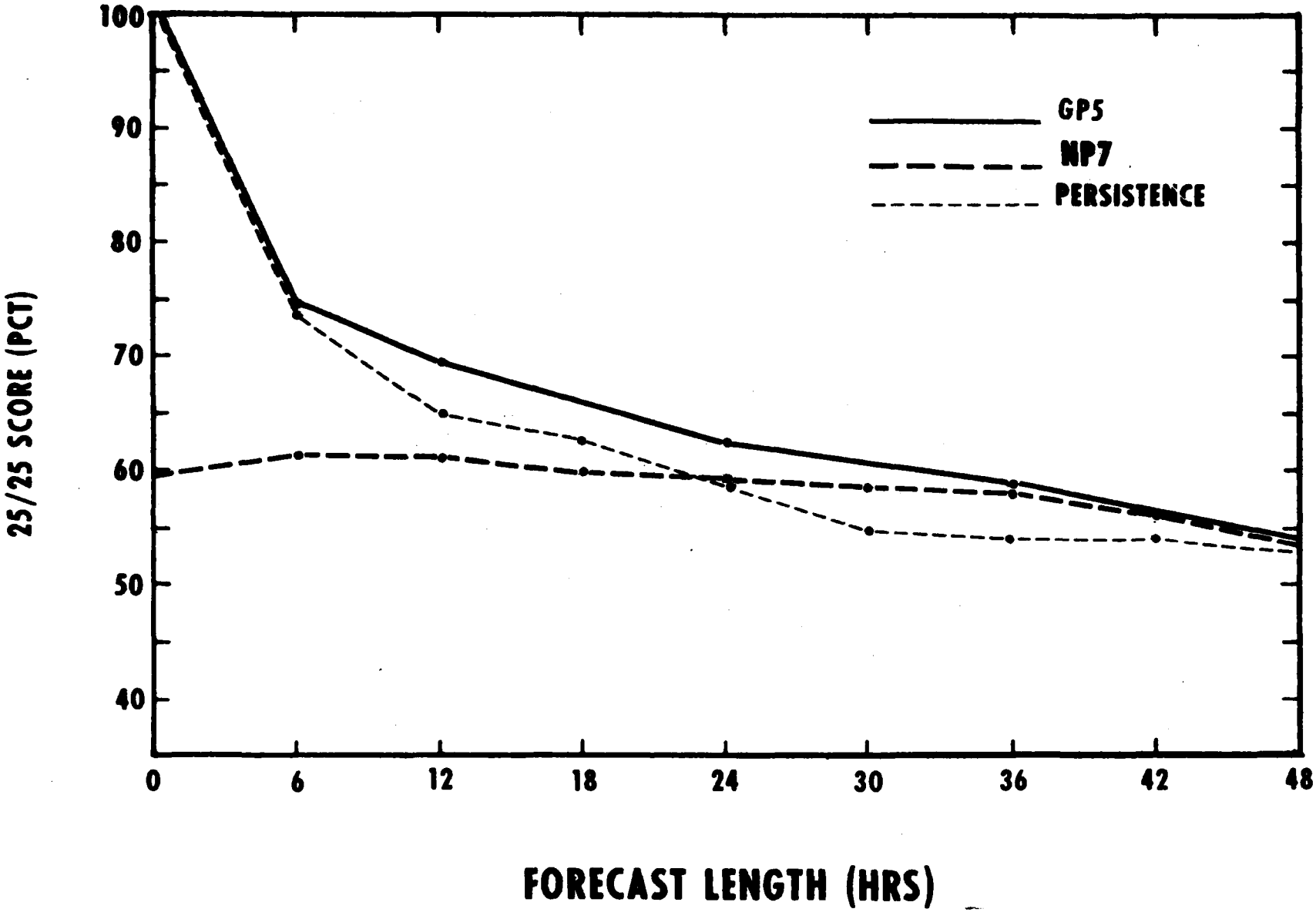

Figure 28. AS in Figure 26 but for the fronthalf limited (FHL) area.

The overall drop-off in time of the NP7 25/25 score curve is surprisingly small over the 48-hour forecast length of Figures 23-28. One might suspect from this small downward trend that the NP7 curves in Figures 23-28 reflect little more than the skill of a random forecast. This is not the case, however, as a purely random forecast, derived from a flat frequency distribution, only yields a 25/25 score of about 35 percent.

For completeness, we provide in Table 6 and 7 the Case D comparison results for the RMSE, STDE, linear correlation, and bias statistics. Aside from the bias, the trends and comparisons between the statistics in Table 6 and 7 are closely analogous to those shown for the 25/25 score in Figures 23-28 and will not be discussed further here. The bias results deserve further comment for the BHL and FHL regions in Table 7. (We recall that we have eliminated in these limited regions the subtropical areas in which the 7LHFM moisture fields suffer from an imposed dry bias.) Surprisingly, the NP7 forecasts in the BHL region show a positive bias (too much cloud) while those forecasts in the FHL region show a negative bias (too little cloud). One might have expected the opposite result based on the fact that the NMC 0-hour FHL area moisture analysis incorporates satellite and conventional cloud observations as an additional data source.

We shall consider the bias characteristics in the BHL and FHL regions in Case D further by examining the frequency of occurrence curves in Figures 29-32. Figure 29 shows wide disagreement, especially in overall shape, between the 0-hour initial frequency distribution curves of the NP7 and GP5 forecasts in the FHL area. In this context, the 0-hour GP5 curve is considered truth. Figure 30 for the BHL area on the other hand shows fair agreement at the clear and overcast ends and in overall shape between the 0-hour initial frequency distribution curves of the NP7 and GP5 forecasts. Thus, while the BHL area shows a larger 0-hour NP7 overall bias than does the FHL area in Table 7, the NP7 0-hour frequency distribution more closely reflects reality in the BHL area than in the FHL area. This also holds true when one examines the forecast frequency distributions, as for example, in Figures 31 and 32. The superiority of BHL versus FHL NP7 forecast frequency distributions probably accounts for the superior performance, relative to GP5, of the NP7 forecasts in the BHL versus the FHL area.

Table 6. Additional statistical information for Case D, the backhalf and fronthalf areas, contrasting persistence (PERS), AFGWC production (GP5), and NMC production 7LHFM (NP7) cloud forecast cases.

CASE D (BACKHALF LIMITED AREA)

FCST	RMSE			STDE			BIAS			LINEAR CORRELATION		
LENGTH	PERS	GP5	NP7	PERS	GP5	NP7	PERS	GP5	NP7	PERS	GP5	NP7
6	24.0	21.9	34.8	24.8	21.9	34.5	1.6	1.7	-4.9	.755	.794	.541
12	30.1	26.7	38.0	30.1	26.7	37.6	.1	.0	-5.6	.645	.702	.468
24	32.1	29.6	38.8	32.1	29.5	38.4	-.3	-1.7	-5.4	.603	.651	.461
36	37.5	33.2	39.4	37.5	33.1	38.7	.0	-2.4	-7.3	.450	.537	.443
48	37.8	35.4	40.3	37.8	35.3	39.8	.1	-3.2	-6.0	.452	.503	.421

CASE D (FRONTHALF LIMITED AREA)

FCST	RMSE			STDE			BIAS			LINEAR CORRELATION		
LENGTH	PERS	GP5	NP7	PERS	GP5	NP7	PERS	GP5	NP7	PERS	GP5	NP7
6	27.5	26.1	45.7	27.4	26.0	42.9	2.4	1.7	-15.9	.684	.699	.252
12	32.6	29.4	44.0	32.5	29.4	41.3	2.2	1.0	-15.0	.539	.603	.292
24	35.2	32.4	47.1	35.2	32.4	42.9	-1.0	-.8	-19.5	.456	.539	.249
36	38.9	35.0	45.3	38.8	34.9	42.9	2.2	1.0	-14.7	.343	.455	.267
48	39.8	38.0	48.2	39.8	38.0	44.5	.0	-.7	-18.6	.303	.374	.200

Table 7. As in Table 6 but for the backhalf and fronthalf limited areas.

CASE D (BACKHALF LIMITED AREA)

FCST	RMSE			STDE			BIAS			LINEAR CORRELATION		
LENGTH	PERS	GP5	NP7	PERS	GP5	NP7	PERS	GP5	NP7	PERS	GP5	NP7
6	23.8	21.3	28.3	23.8	21.2	27.9	-1.3	.8	4.9	.768	.802	.683
12	30.3	26.3	29.5	30.3	26.3	28.8	.0	.7	6.4	.620	.692	.664
24	34.1	30.4	30.7	34.1	30.4	30.0	-.2	-1.1	6.5	.533	.618	.654
36	38.3	33.0	31.9	38.3	33.0	31.8	-.5	-2.2	2.8	.393	.524	.609
48	39.2	36.2	34.3	39.2	36.1	34.1	.1	-3.1	3.8	.388	.471	.564

CASE D (FRONTHALF LIMITED AREA)

FCST	RMSE			STDE			BIAS			LINEAR CORRELATION		
LENGTH	PERS	GP5	NP7	PERS	GP5	NP7	PERS	GP5	NP7	PERS	GP5	NP7
6	27.9	26.3	33.8	27.8	26.2	33.8	2.0	1.4	-.8	.649	.670	.499
12	32.4	28.7	33.9	32.4	28.7	33.8	.1	-.3	-1.7	.506	.593	.489
24	36.8	33.3	35.7	36.8	33.3	35.5	.3	-.3	-3.7	.363	.481	.468
36	39.5	35.0	36.9	39.5	35.0	36.8	.9	-.7	-1.5	.271	.423	.439
48	40.2	38.8	39.6	40.2	38.7	39.4	.6	-2.0	-3.9	.232	.307	.359

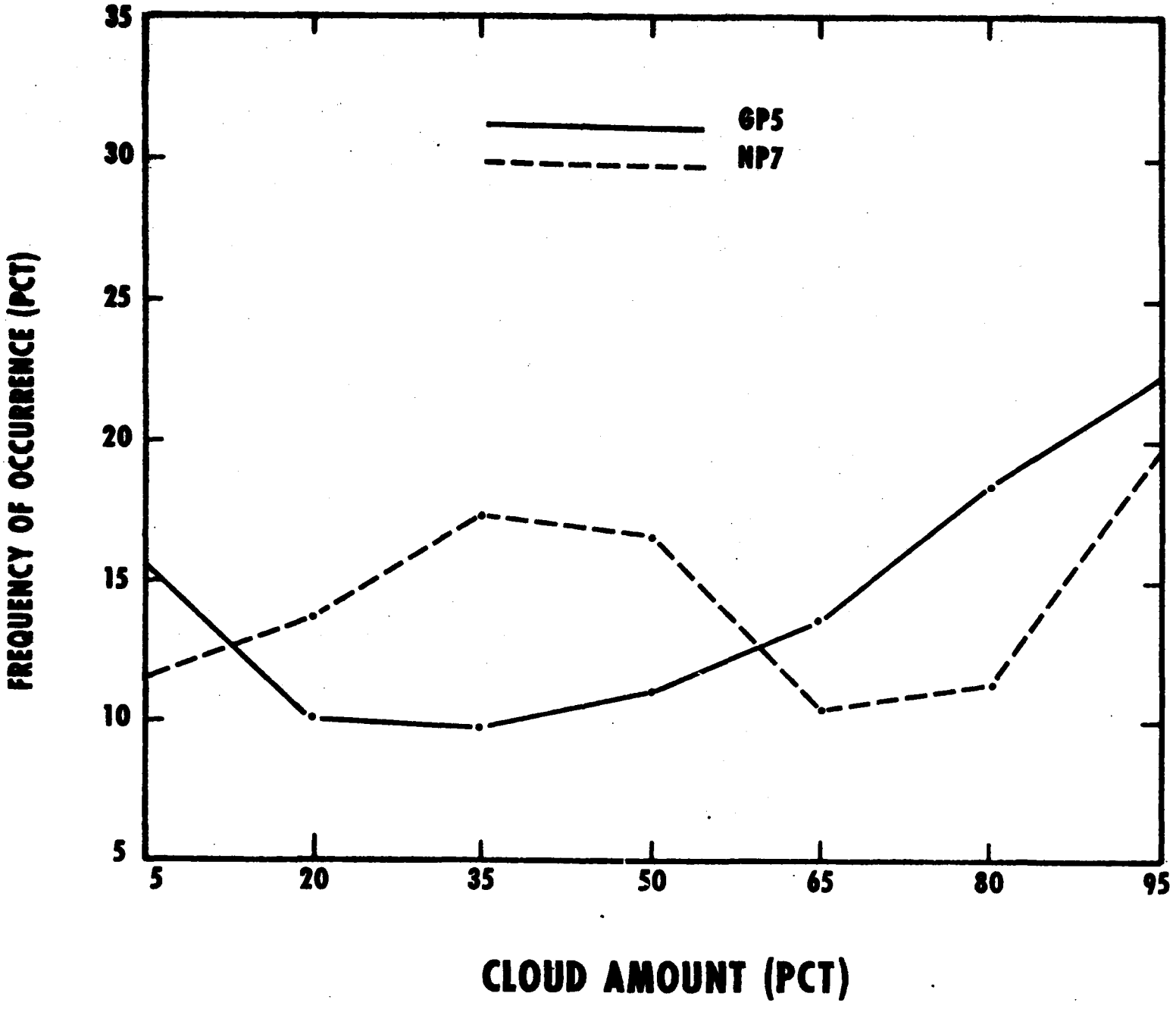

Figure 29. Total cloud frequency distribution for the AFGWC production 5LAYER (GP5) and the NMC production 7LHFM (NP7) 0-hour analyses in Case D (Table 1) for the fronthalf limited (FHL) area, 14-day set.

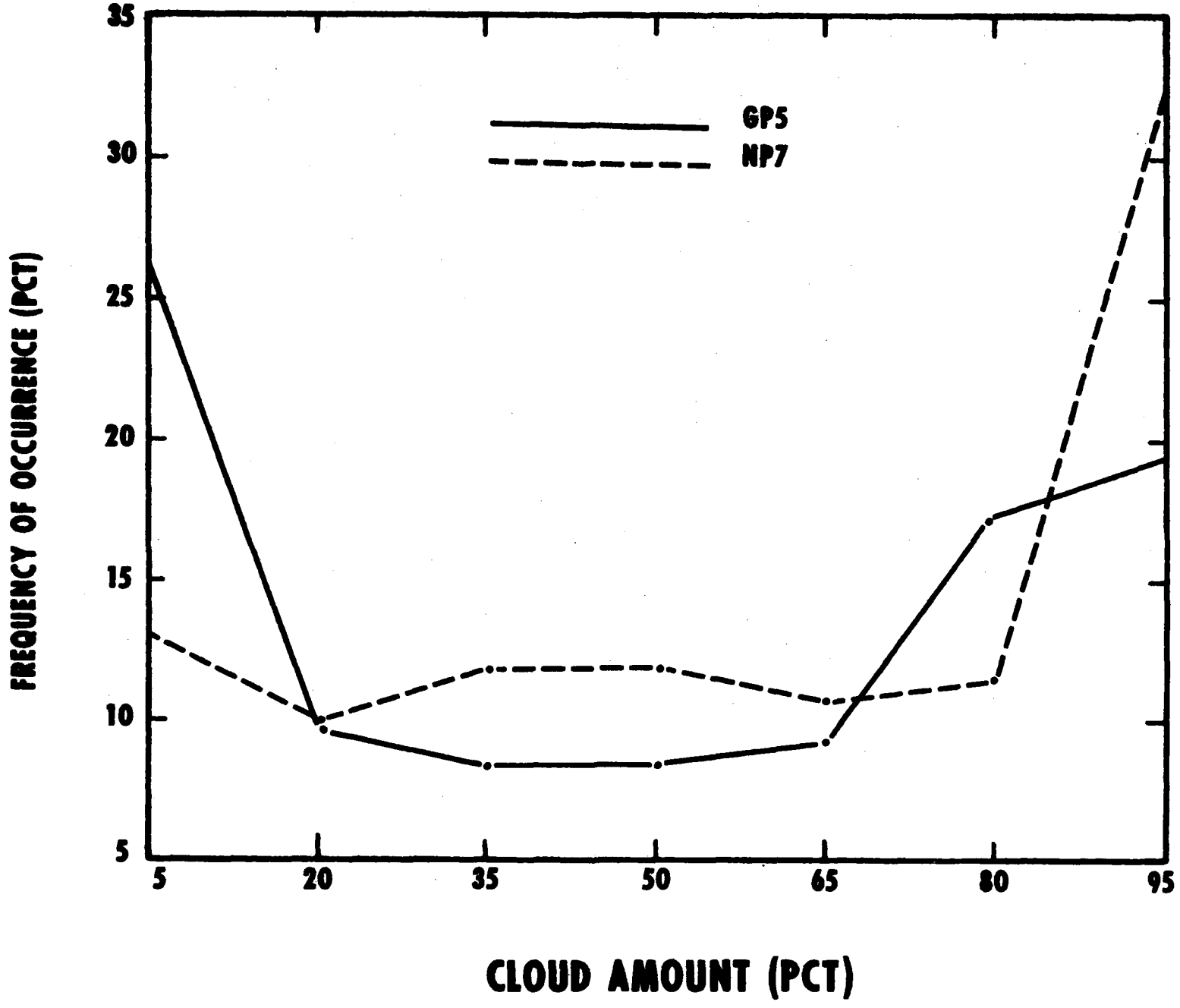

Figure 30. As in Figure 29 but for the backhalf limited (BHL) area.

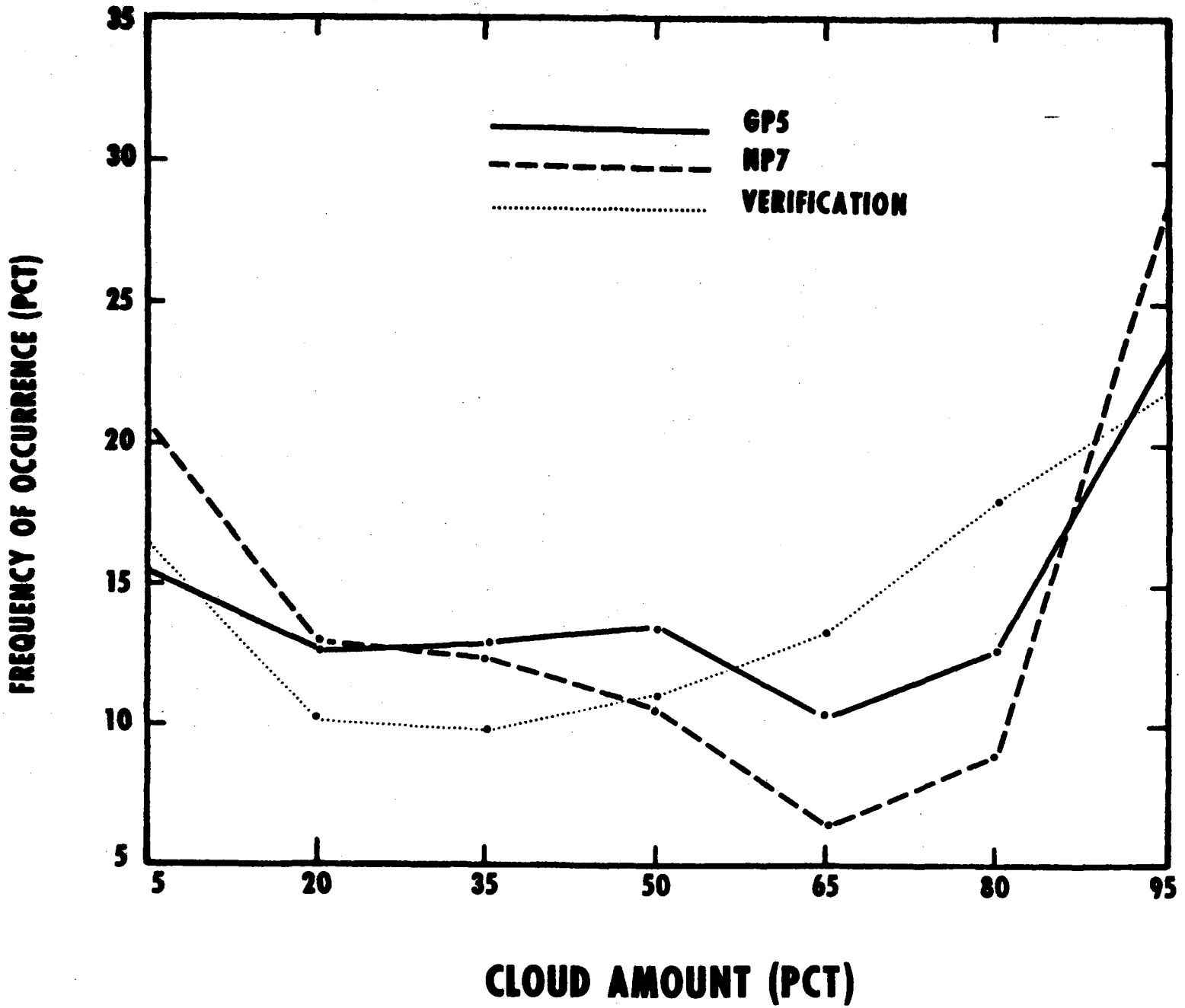

Figure 31. As in Figure 29 but for the 48-hour forecasts and verifying analysis.

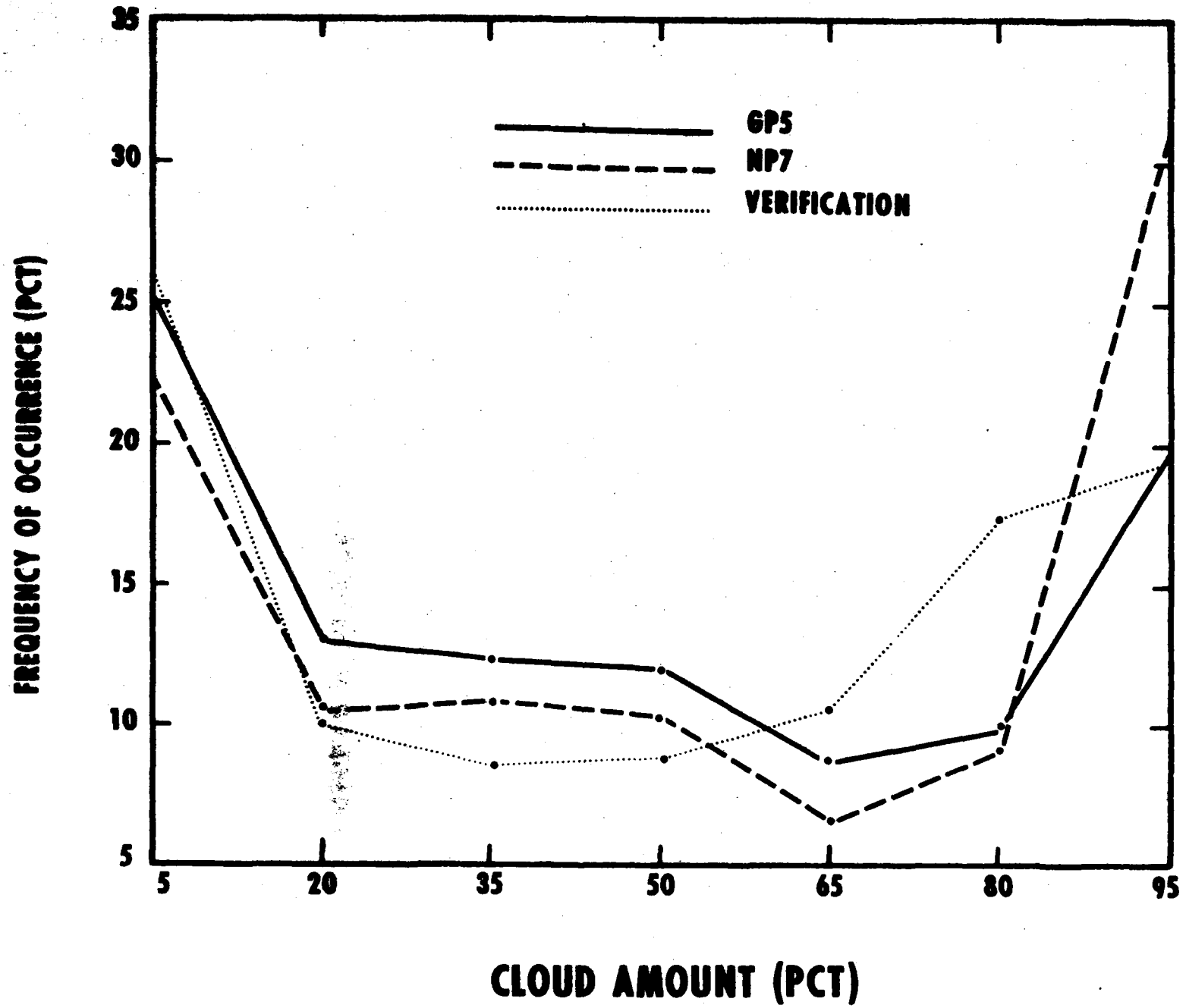

Figure 32. As in Figure 29 but for 48-hour forecasts and verifying analysis in the backhalf limited (BHL) area.

It is instructive in Case D to compare actual displays of GP5 and NP7 total cloud analysis and forecasts. Figures 33 and 34 provide shaded displays of GP5 and NP7 initial (0-hr) total cloud analyses derived from the Case D data set for the 10 Sep 1979 test day. In these figures, cloud-free regions are represented by white or blank areas and overcast regions are represented by heavily darkened areas. Increasing gradations of shading, then, denote larger cloud amounts. The artificially dry subtropical belt in the 7LHFM initial moisture fields is readily apparent in Figure 34. Even outstide the subtropics, there are obvious differences in the GP5 and NP7 analyses in Figure 33 and 34. In general, the NP7 cloud analysis is much smoother in appearance and it exhibits relatively gradual spatial transitions between clear and overcast areas. The GP5 cloud analysis, in contrast, is much less smooth and exhibits more spatial variability, sharper gradients between clear and overcast areas, and generally smaller, less organized overcast regimes. The smooth, continuous nature of the initial NP7 analysis in Figure 34 appears to be more appropriate as a representation of the continuous synoptic scale relative humidity distribution rather than as a representation of the highly discontinuous, synoptic and mesoscale cloud patterns routinely obtained in GP5 cloud analyses derived from the 3DNEPH.

The characteristics of the analysis displays in Figures 33 and 34 are largely persisted in the corresponding 24-hour GP5 and NP7 forecast displays in Figures 35 and 36. For completeness, the verifying GP5 analysis display is also provided in Figure 37. We see in Figure 36 that the dynamics of the 7LHFM has led to sharper cloud amount gradients, which are associated with an increase in strictly clear and strictly overcast areas. These sharper gradients, coupled with the more rapid and skillful movements of the major synoptic systems in Figure 36 versus Figure 35, contribute to the improvement in the NP7 versus GP5 forecast skill that was apparent at 24 hours and beyond in Figures 23-28.

3.2.3 Case E-F Results

Owing to the substantially worse overall performance of the NP7 versus GP5 forecasts in Case D (Figures 23-28 and Tables 6 and 7), the question of the impact of delayed 7LHFM databases in Cases E-F is largely immaterial. Clearly, a delay in the availability of the 7LHFM databases will further degrade the already poor NP7 performance documented in Case D. Therefore, the Case E and F comparisons in Table 1 will not be systematically pursued here.

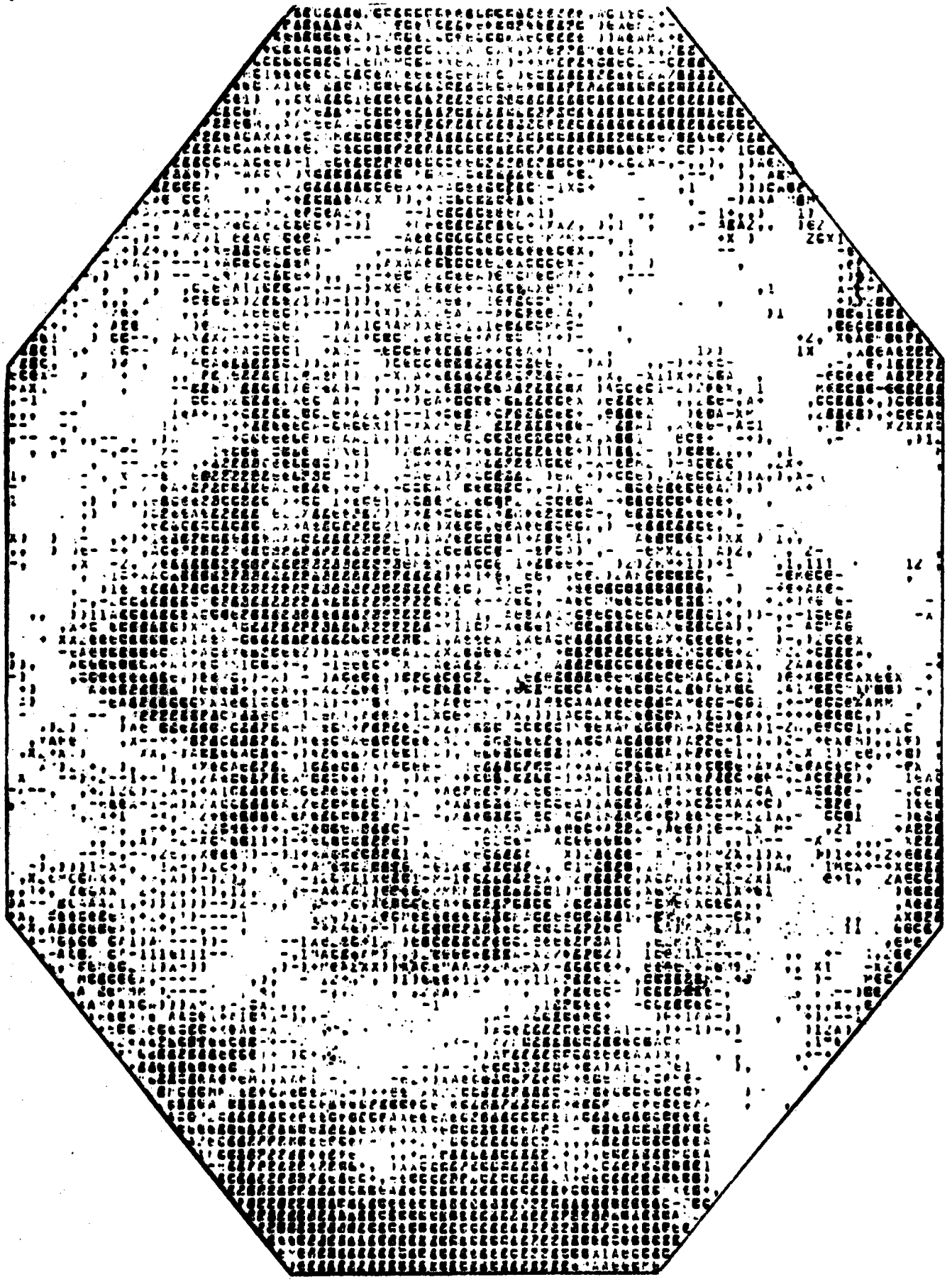

Figure 33. Shaded total cloud display of the AFGWC production 5LAYER (GP5) 0-hour analysis from the 03Z GP5 database on 10 September 1979. Blank areas are cloud-free and heavily darkened areas are overcast. All half-mesh (100nm) grid points are represented.

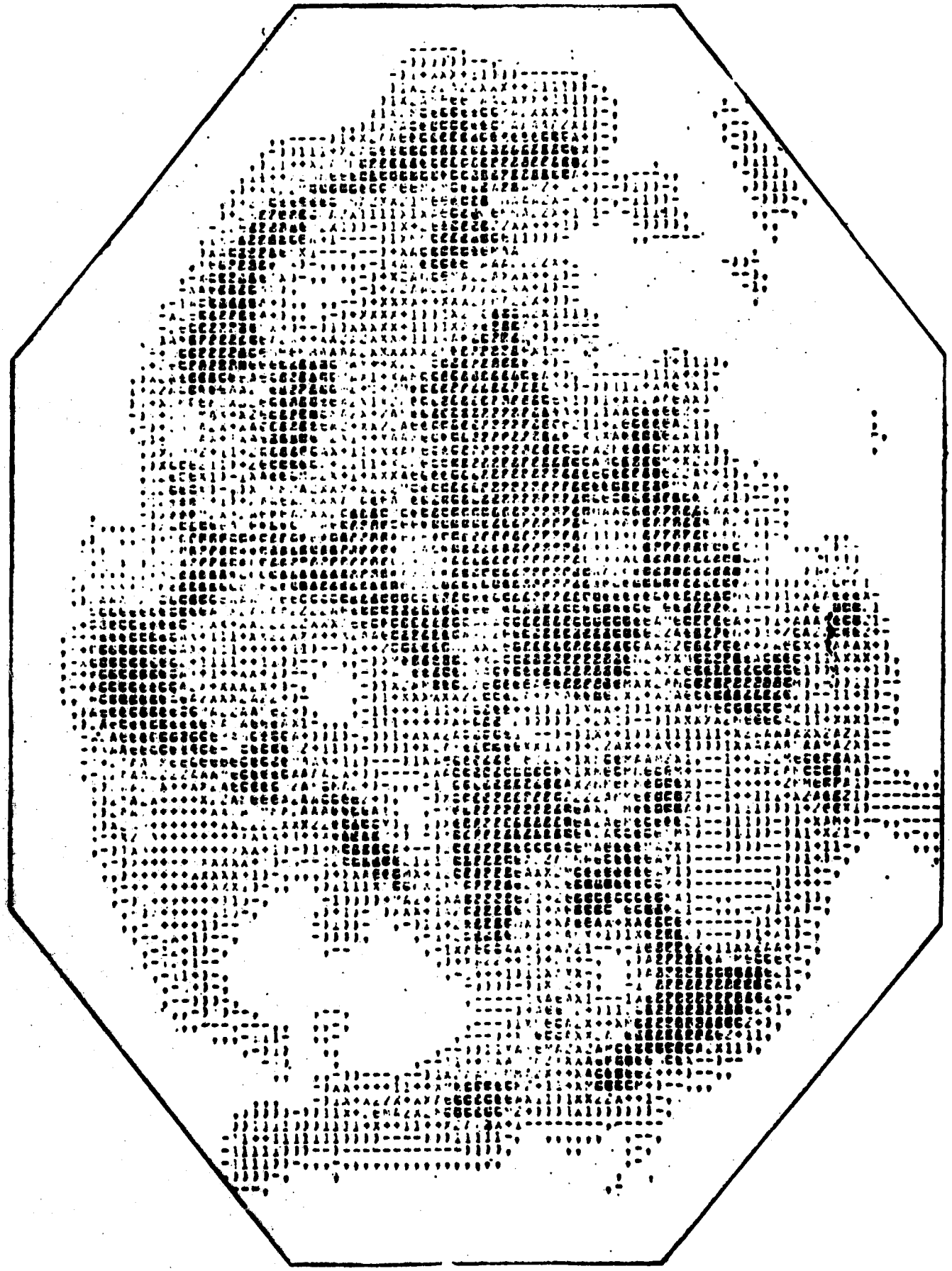

Figure 34. Shaded total cloud display of the NMC production 7LHFM (NP7) 3-hour forecast from the 00Z NP7 database on 10 September 1979. The forecast valid time agrees with that of the GP5 analysis in Figure 33. Otherwise as in Figure 33.

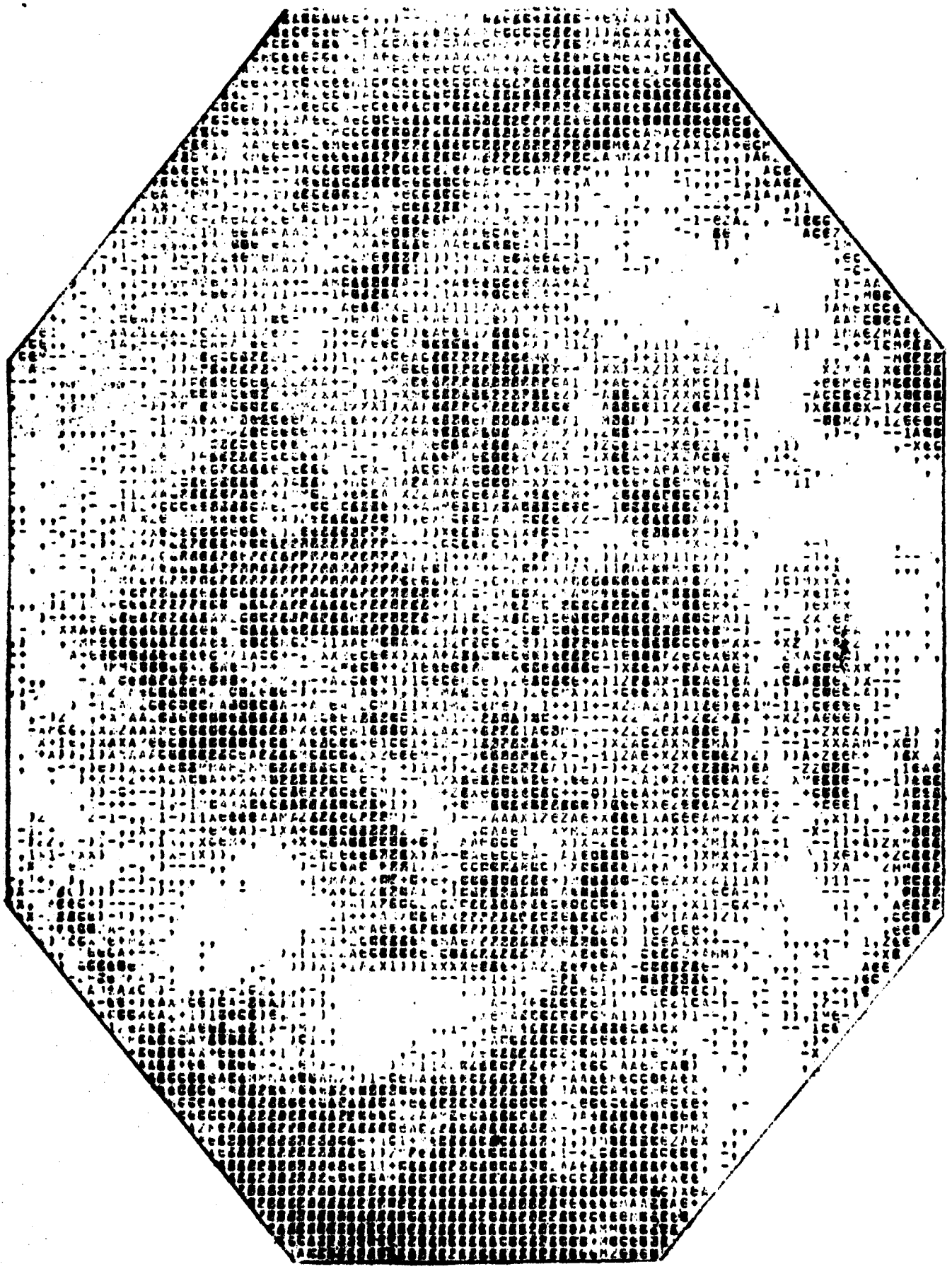

Figure 35. As in Figure 33 but for the 24-hour forecast.

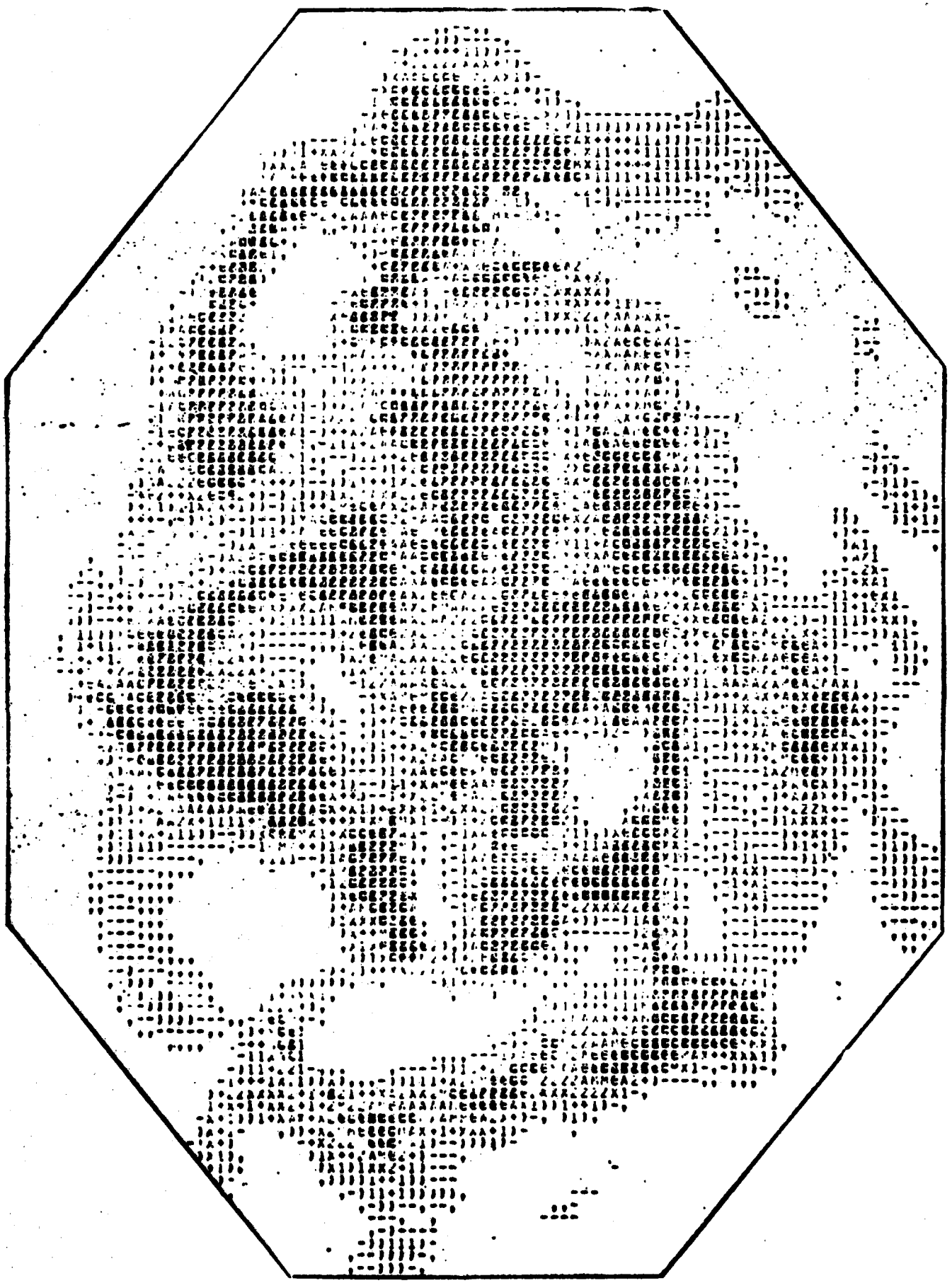

Figure 36. As in Figure 34 but for the 27-hour forecast. The forecast valid time agrees with that of the GP5 forecast in Figure 35.

Figure 37. As in Figure 33 but for the GP5 0-hour analysis from the 03Z GP5 database on 11 Sep 1979. This analysis represents the verifying field for the forecasts in Figures 35 and 36.

4 CONCLUSIONS AND RECOMMENDATIONS

4.1 Conclusions

The essence of the conclusions itemized below is embodied in Figure 38, which compares the forecast accuracy of persistence, the current production 5LAYER driven by 6LDPE winds (GP5), the test 5LAYER driven by 7LHFM winds (GT5), and the moist 7LHFM-derived cloud forecasts (NP7). We choose to depict the extra-tropical backhalf area results in this final composite figure because the GT5 and NP7 test forecasts provided their best results in this region.

(a) During the test period, the horizontal wind velocity forecasts from the 7LHFM model show an RMSVE reduction of approximately 14 percent when compared with the corresponding 6LDPE wind forecasts.

(b) The 7LHFM horizontal wind velocity forecasts of lengths up to TT + 12 hours exhibit essentially the same RMSVE accuracy as the corresponding 6LDPE forecasts of length TT hours during the test period.

(c) For forecast periods of 12 hours or greater, 5LAYER forecasts driven by 7LHFM winds show an absolute improvement in the 25/25 score of about 1.5 percent in the fronthalf area and about 3 percent in the backhalf area, relative to production 5LAYER forecasts driven by 6LDPE winds.

(d) For forecast periods of 24 hours or greater, 5LAYER forecasts driven by 7LHFM winds show a 25/25 skill score (computed relative to persistence) that is twice the 25/25 skill score of the production 5LAYER in the backhalf area. The corresponding skill score improvement in the fronthalf area was generally less.

(e) For forecast periods of 24 hours or greater, the 5LAYER forecasts driven by 7LHFM winds show an RMSE reduction of about 1.5 percent relative to the production 5LAYER forecasts. Thus, the 14 percent reduction in 7LHFM versus 6LDPE RMSVE values cited in (a) above generally translates into an order of magnitude smaller percent reduction in the RMSE values of the subsequent 5LAYER cloud forecasts.

(f) The 12-hour forecast extension exhibited in 7LHFM versus 6LDPE wind forecasts as cited in (b) above generally translates into an equivalent 12-hour forecast extension for 5LAYER driven by 7LHFM winds versus 5LAYER driven by 6LDPE winds.

(g) Owing to differences in the extent and method by which NMC and AFGWC use satellite and conventional cloud observations in deriving their respective initial moisture field analyses, there exists a large disparity between the initial cloud analyses obtained from the 7LHFM and production 5LAYER initial moisture fields. The 5LAYER initial cloud analyses agree more closely with satellite-observed cloud cover.

(h) As a consequence of the initial cloud analysis disparity cited in (g) above, the 0-24 hour cloud forecasts derived directly from the 7LHFM moisture forecasts show substantially less skill than the 0-24 hour production 5LAYER cloud forecasts, when both are verified against a compacted 3DNEPH analysis.

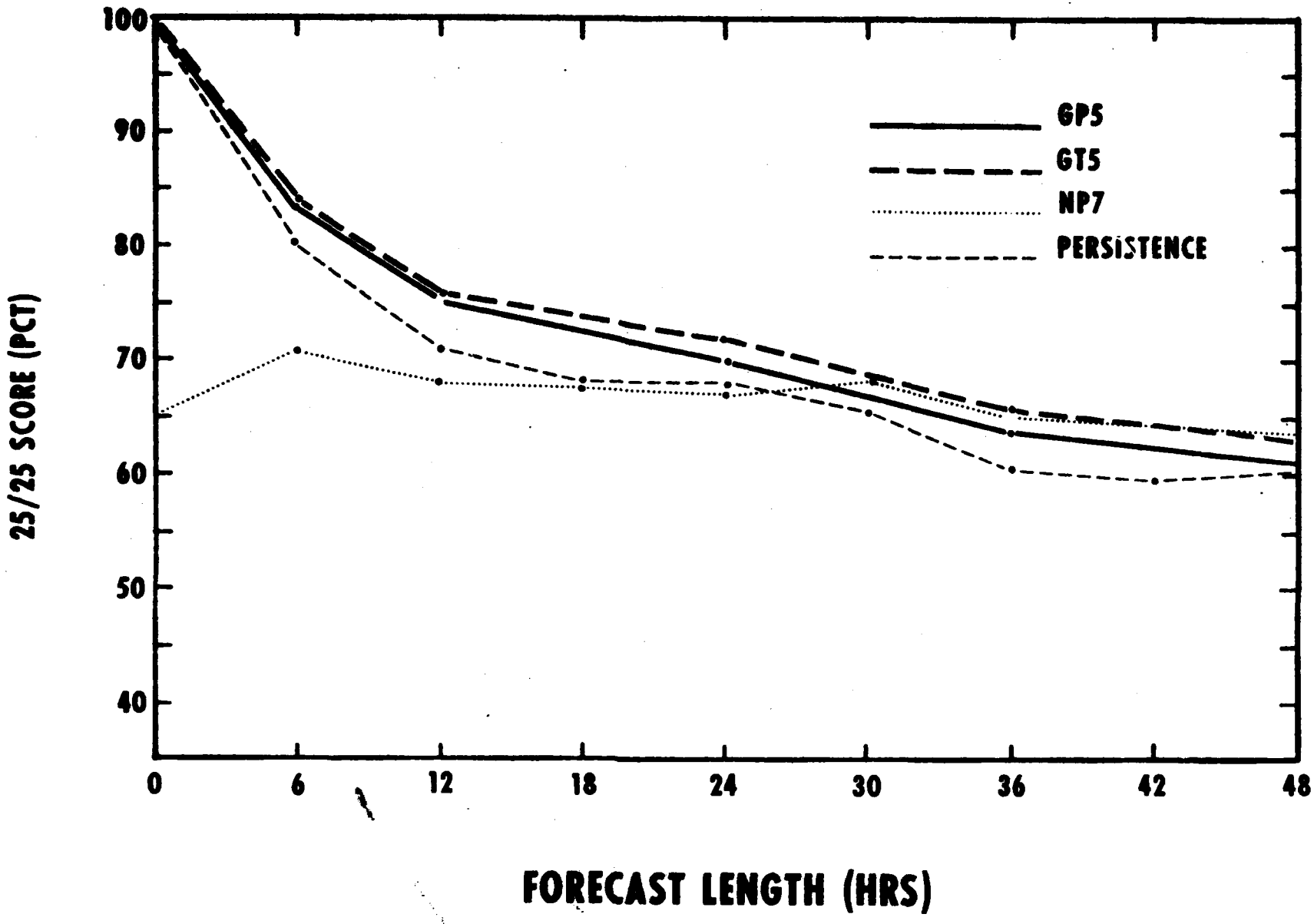

Figure 38. 25/25 score as a function for forecast lengths for the AFGWc production 5LAYER (GP5), the AFGWC test 5LAYER (GT5), the NMC production 7LHFM (NP7), and persistence for Cases A and D (Table 1) for the backhalf limited (BHL) area, 14-day set.

(i) Owing to apparently superior dynamics in the 7LHFM advanced prediction model, the disadvantage of having a 7LHFM initial moisture analysis that poorly reflects initial cloud cover is largely overcome for forecast periods beyond 24 hours. In the 24- to 48-hour forecast range, 7LHFM-derived cloud forecasts are competitive with, and in some cases superior to, the corresponding production 5LAYER forecasts. In particular, the 30- to 48-hour 7HFM-derived cloud forecasts exhibit a 25/25 skill score that is about twice that of the production 5LAYER forecasts in extratropical regions of the backhalf area.

4.2 Recommendation for Further Study

It is clear in Figure 38 that the best forecast accuracy over the entire range of 0-48 hours is achieved by the 5LAYER model driven by 7LHFM forecast winds. However, the slow drop-off of the NP7 skill curve in Figure 38 suggests that the greatest ultimate improvement in cloud forecast accuracy might be achieved by incorporating 3DNEPH cloud analyses into the derivation of the 7LHFM initial moisture fields. If we can thereby eliminate much of the initial disparity between the GP5 and NP7 curves in Figure 38, a significant improvement in cloud forecast accuracy may be realized. To pursue this possibility, we recommend that a follow-on models comparison test be performed in which NMC is provided with AFGWC 3DNEPH cloud analysis databases for incorporation into the initial moisture field of both the 7LHFM model and NMC's newly operational Global Spectral Model.

5. APPENDIX - GLOSSARY

This glossary is an alphabetical listing of the abbreviations and acronyms used in this Technical Note.

AFGWC - Air Force Global Weather Central

AWS - Air Weather Service

BH - Backhalf area of the 5LAYER forecast grid, primarily Europe and Asia

BHL - Backhalf area, but limited to points north of 30°N

CMC - Canadian Meteorological Center

CPS - Condensation Pressure Spread

DMSP - Defense Meteorological Satellite Program

ECMWF - European Center for Medium-range Weather Forecasting

FH - Fronthalf area of the 5LAYER forecast grid, primarily North America

FHL - Fronthalf area, but limited to points north of 30°N

FNOC - FLeet Numerical Oceanographic Center of US Navy (formerly FNWC)

GP5 - AFGWC Production 5LAYER

GT5 - AFGWC Test 5LAYER

HUFANL - Upper-air spectral (Hough function) analysis model

LCL - Lifting Condensation Level

LFM II - Limited-area Fine Mesh model, version 2

NESS - National Environmental Satellite Service

NMC - National Meteorological Center of US Dept of Commerce

NOAA - National Oceanic and Atmospheric Administration

NP7 - NMC Production 7LHFM

PE - Primitive Equation

QPF - Quantitative Precipitation Forecast

RAOB - Radiosonde Observation

RH - Relative Humidity

RMSE - Root Mean Square Error

RMSVE - Root Mean Square Vector Error

SAB - Scientific Advisory Board

STDE - Standard Deviation of the Error

TN - Technical Note

3DNEPH - Three-dimensional Nephanalysis cloud model at AFGWC

5LAYER - Five Layer hemispheric cloud forecast model at AFGWC

6LDPE - Six Layer Dry Primitive Equation model at AFGWC

6LVL - Six Level Quasi-geostrophic model (in use at AFGWC prior to 1975)

7LHFM - Seven Layer Hemispheric Fine Mesh model at NMC

6. REFERENCES

Friend, A. L., and K. E. Mitchell, 1982: The AFGWC automated cloud forecast models. (Technical Note in preparation), AFGWC, Air Weather Service (MAC), Offutt AFB, NE.

Fye, F. K., 1978: The AFGWC automated cloud analysis model. Technical Memorandum 78/002, AFGWC, Air Weather Service (MAC), Offutt AFB, NE, 97 pp.

Garrison, D. M., 1974: Cloud model properties. Aerospace Sciences Review, AWSRP 105-2, Air Weather Service (MAC), Scott AFB, IL, 29 pp.

Hoke, J. E., J. L. Hayes, and L. G. Renninger, 1979: Map projections and grid systems for meteorological applications. Technical Note 79/003, AFGWC, Air Weather Service (MAC), Offutt AFB, NE, 86 pp.

Irvine, W. S., 1981: Numerical cloud forecasting at AFGWC. (Unpublished manuscript).

McPherson, R. D., 1980: Evolution and present status of objective analysis/assimilation at NMC. Office Note 216, National Meteorological Center, National Weather Service (NOAA), Camp Springs, MD, 22 pp.

Shuman, F. G., and J. B. Hovermale, 1968: An operational six-layer primitive equation model. J. Appl. Meteor. 7, 525-547.

Smigielski, F., T. Burtt, F. Bittner, and S. Hirsch, 1978: Moisture bogus program. Technical Note 225, Synoptic Analysis Branch, National Environmental Satellite Service (NOAA), Camp Spring, MD 13 pp.

Tarbell, T. C., and J. E. Hoke, 1979: The AFGWC automated analysis/forecast model system. Technical Note 79/004, AFGWC, Air Weather Service (MAC), Offutt AFB NE, 52 pp.

END

FILMED

1-84

DTIC